Universidad de Concepción
Dirección de Postgrado
Facultad de Agronomía
Programa de Doctorado en Ciencias de la Agronomía

Secuestro de C del suelo en bosques de *Nothofagus obliqua* (Mirb.) Oerst. (Roble) con diferentes niveles de cobertura arbórea bajo manejo silvopastoril extensivo

Soil C sequestration in *Nothofagus obliqua* (Mirb.) Oerst. (Oak) forests with different levels of tree cover under extensive silvopastoral management

Tesis para optar al grado de Doctora en Ciencias de la Agronomía

CAMILA RAMOS CARRERAS
CHILLÁN-CHILE
2025

Profesor Guía: Erick Zagal Venegas
Dpto. de Suelos y Recursos Naturales
Facultad de Agronomía
Campus Chillán Universidad de Concepción

Esta tesis ha sido realizada en el Departamento de Suelos y Recursos Naturales de la Facultad Agronomía, Universidad de Concepción.

Profesor Guía

Dr. Erick Zagal Venegas
Facultad de Agronomía
Universidad de Concepción

Profesor Co-Guía

Dr. Francis Dube
Facultad de Ciencias Forestales
Universidad de Concepción

Comisión Evaluadora:

Dr. Leandro Paulino
Facultad de Agronomía
Universidad de Concepción

Dr. Juan Pablo Fuentes Espoz
Facultad de Ciencias Forestales y de la Conservación de la Naturaleza
Universidad de Chile

Director de Programa

Dra. Susana Ursina Fischer Ganzoni
Facultad de Agronomía
Universidad de Concepción

Camila Ramos Carreras, estudiante del Programa Doctorado en Ciencias de la Agronomía, Facultad de Agronomía, Universidad de Concepción, declara ser autor del presente trabajo titulado "**Secuestro de C del suelo en bosques de *Nothofagus obliqua* (Mirb.) Oerst. (Roble) con diferentes niveles de cobertura arbórea bajo manejo silvopastoril extensivo**". Se autoriza la reproducción total o parcial, con fines académicos, por cualquier medio o procedimiento, incluyendo la cita bibliográfica del documento.

AGRADECIMIENTOS

- Agradezco profundamente a mi tutor Erick Zagal por su generosidad al compartir su conocimiento y por su apoyo constante durante estos cuatro años.
- A mi co-tutor Francis Dube**,** por su guía y acompañamiento.
- A mi comisión de tesis**,** por sus valiosas recomendaciones y aportes que enriquecieron este camino.
- Al Programa de Doctorado en Ciencias de la Agronomía**,** por brindarme las herramientas necesarias para desarrollarme como investigadora.
- A la Agencia Nacional de Investigación y Desarrollo, por el fondo Doctorado Nacional (2022-21221453) que hizo posible mi formación en Chile.
- A mi familia, por su amor incondicional y por estar siempre presentes, incluso en la distancia.
- A Richard García, compañero de vida y también de este camino doctoral, con quien he compartido desafíos, aprendizajes y sueños.
- A Yadiana Ontivero, la persona que me habló de este programa y con quien compartí esta etapa llena de apoyo mutuo. Hoy es doctora y amiga, y junto a su esposo Michel, se convirtieron en mi familia en este camino.
- A mi familia chileno-cubana**,** los Perelli-Cuba**,** por acogernos como una parte de su familia.
- A mis amigos Sandra, José, Jean, Deliany, Omar, Luis, Ismaray, Yudelkis y sus familias por ser mi hogar lejos de casa.
- Al equipo del Laboratorio de Suelos de la Universidad de Concepción**,** especialmente a Carlos y Katherine, por su apoyo constante, su paciencia y amistad.

ÍNDICE GENERAL

ÍNDICE DE TABLAS

ÍNDICE DE ILUSTRACIONES

RESUMEN

La agroforestería representa una estrategia eficaz para reducir la deforestación, favorecer la rehabilitación/regeneración de ecosistemas degradados y mejorar la sostenibilidad del uso del suelo. Este estudio evaluó cómo distintos niveles de cobertura arbórea, la calidad de la hojarasca y la profundidad del suelo influyen en la capacidad de secuestro y estabilización de carbono (C) y nitrógeno (N) en Andisoles de bosques de Roble (*Nothofagus obliqua)* sometidos a manejo silvopastoril extensivo en Ranchillo Alto (37°04′52″ S, 71°39′14″ W), Región de Ñuble, Chile. Se analizaron tres sistemas silvopastoriles: abierto (Op, 85-95% de la radiación solar total sobre el dosel arbóreo), semiabierto (SOp, 65-75%) y semicerrado (SC, 45-55%) y un control sin manejo (Ctr), considerando cuatro profundidades de suelo (0–10, 10–20, 20–30 y 30–60 cm). Se realizaron análisis físicos, químicos y biológicos, fraccionamiento de materia orgánica (MOS) y determinación de C y no oxidable (Cnox). Las concentraciones más altas de C se registraron en los primeros 10 cm (13,9, 11,8, 11,5 y 8,5% para Op > SC > SOp y Ctr, respectivamente). A pesar de su mayor degradación, Op presentó los valores más altos de C, N y Cnox, probablemente por aportes pirogénicos históricos. Además, todos los sistemas silvopastoriles mostraron incrementos en la Materia Orgánica asociada a la Matriz Mineral (MAOM, por sus siglas en inglés) y stocks de C respecto al control sin manejo silvopastoril.

Complementariamente, se evaluó el efecto de la calidad de la hojarasca sobre la estabilización de C mediante incubaciones de 120 días, usando hojarasca de alta (GQ C/N ≈ 27) y baja calidad (LQ C/N ≈ 105) bajo los tres sistemas silvopastoriles (Op, SOp y SC) y dos profundidades de suelo (0–30 y 30–60 cm). La hojarasca LQ mejoró la transferencia y estabilización directa de POM→MAOM, mientras que la hojarasca GQ prolongó la residencia en fase lábil, favoreciendo las pérdidas de carbono respiratorio antes de la asociación mineral. La FTIR mostró que la Materia Orgánica Particulada (POM, por sus siglas en inglés) estaba enriquecida con señales alifáticas y la MAOM con grupos carbonilo oxidados. La apertura del dosel moduló los efectos de la calidad del sustrato.

En conjunto, estos resultados, y bajo las condiciones de este estudio, muestran que el manejo silvopastoril, la calidad de la hojarasca y la estructura del dosel regulan la captura y estabilización de C en Andisoles, aportando evidencia clave para la restauración de suelos degradados y mitigación del cambio climático.

ABSTRACT

Agroforestry represents an effective strategy to reduce deforestation, promote ecosystem rehabilitation/regeneration, and improve sustainable land use. This study evaluated how different levels of canopy cover, litter quality, and soil depth influence the capacity for carbon (C) and nitrogen (N) sequestration and stabilization in Andisols of roble (*Nothofagus obliqua)* forests under extensive silvopastoral management in Ranchillo Alto (37°04′52″ S, 71°39′14″ W), Ñuble Region, Chile. Three silvopastoral systems open (Op, 85-95% of total solar radiation above tree canopy), semi-open (Sop, 65-75%), and semi-closed (SC, 45-55%) and an unmanaged control (Ctr) were analyzed across four soil depths (0–10, 10–20, 20–30, and 30–60 cm). Physical, chemical, and biological analyses were performed, along with soil organic matter (SOM) fractionation and non-oxidizable carbon (Cnox) determination. The highest C concentrations were recorded in the upper 10 cm (13.9, 11.8, 11.5, and 8.5% for Op > SC > SOp and Ctr, respectively). Despite higher degradation, the Op system showed the highest C, N, and Cnox values, likely due to historical pyrogenic carbon inputs. In addition, all silvopastoral systems showed increases in Mineral-Associated Organic Matter (MAOM) and C stocks compared to the unmanaged control.

Complementarily, the effect of litter quality on C stabilization was assessed through a 120-day incubation, using high-quality (GQ C/N ≈ 27) and low-quality (LQ C/N ≈ 105) litter under the three silvopastoral systems (Op, SOp y SC) and two soil depths (0–30 and 30–60 cm). LQ litter enhanced direct Particulate Organic Matter (POM)→MAOM transfer and stabilization, whereas GQ litter prolonged residence in the labile phase, favoring respiratory carbon losses prior to mineral association. FTIR revealed aliphatic signatures enriched in POM and oxidized carbonyl groups in MAOM. Canopy openness modulated substrate quality effects.

Overall, these findings, under the conditions of this study, demonstrate that silvopastoral management, litter quality, and canopy structure, regulate carbon sequestration and stabilization in Andisols, providing key evidence for degraded soil restoration and climate change mitigation strategies.

I. INTRODUCCIÓN GENERAL

La degradación de los suelos constituye una de las problemáticas ambientales más graves y extendidas a nivel global, afectando directamente la resiliencia de los ecosistemas, la seguridad alimentaria y la capacidad de mitigación del cambio climático (Georgiou et al. 2022). Los suelos almacenan entre 1.500 y 2.400 Pg de carbono orgánico (CO) en el primer metro de profundidad, lo que representa el mayor reservorio terrestre de carbono (C) (Smith et al. 2020; Georgiou et al. 2022). Este C cumple funciones ecológicas esenciales al sustentar la fertilidad edáfica, favorecer la retención y circulación de agua, estabilizar la estructura del suelo y alimentar redes microbianas que regulan múltiples procesos biogeoquímicos (Timmusk y de-Bashan 2022). Sin embargo, durante las últimas décadas, la expansión agrícola intensiva, la deforestación, el sobrepastoreo y el cambio de uso del suelo han contribuido a la pérdida acelerada de materia orgánica y a la degradación estructural de extensas superficies (Don et al. 2011; Amoakwah et al. 2022).

En América Latina y el Caribe, cerca del 75 % de los suelos presentan algún grado de degradación, con impactos ecológicos y económicos considerables (Guerra et al. 2020; FAO 2022). En Chile, el panorama es especialmente alarmante, aproximadamente el 49 % del territorio nacional presenta algún nivel de erosión, y en algunas zonas entre las Regiones de Coquimbo y Los Lagos esta cifra supera el 56 % según CIREN (2010). Estudios recientes estiman que más de 47 millones de hectáreas equivalentes a cerca del 63 % de la superficie nacional están afectadas por procesos de degradación y desertificación (Huaico Malhue 2018; SAG 2021). Las causas principales incluyen sobrepastoreo, expansión urbana, uso agrícola sin medidas de conservación, deforestación y prácticas de manejo que reducen la cobertura vegetal protectora (Lebuy et al. 2022). La pérdida de cobertura de bosques nativos ha sido particularmente severa, más del 44 % han sido talados, afectando más de ocho millones de hectáreas, y géneros como *Nothofagus* han reducido su cobertura en más del 70 %, principalmente por la sustitución por pasturas para ganadería, plantaciones

forestales y expansión agrícola (Miranda et al. 2017; Del Pozo et al. 2024). Este proceso ha alterado profundamente la dinámica de entrada de materia orgánica al suelo, reduciendo los aportes de hojarasca y raíces e interrumpiendo ciclos de nutrientes y ha acelerado la erosión (Qu et al. 2024).

La restauración de suelos degradados constituye, por tanto, una prioridad tanto ecológica como productiva (FAO 2022). En este contexto, los sistemas agroforestales y silvopastoriles emergen como estrategias de manejo integradas que combinan la presencia de árboles con actividades agrícolas o pecuarias, generando beneficios múltiples (Ortiz et al. 2023; López-Sampson y Andrade 2024). Se ha demostrado que estos sistemas reducen significativamente la erosión, mejoran la estructura y fertilidad del suelo, protegen la biodiversidad y favorecen la captura de C tanto en la biomasa como en el suelo (Aynekulu et al. 2020; De Macêdo Carvalho et al. 2024). Además, pueden contribuir de manera efectiva a la mitigación del cambio climático al aumentar el secuestro de CO_2 del suelo en tasas estimadas entre 1,8 y 6,1 Mg C ha^{-1} $año^{-1}$, dependiendo de las especies vegetales, manejo y condiciones edafoclimáticas (Nair et al. 2010; FAO 2022; Gomes et al. 2025).

La materia orgánica del suelo (MOS) es el componente clave que vincula estos procesos ecológicos y productivos. Se trata de una mezcla compleja de compuestos orgánicos derivados de residuos vegetales, microbianos y transformaciones biogeoquímicas (Lehmann y Kleber 2015). Su presencia determina en gran medida la capacidad de los suelos para retener agua, estabilizar su estructura, almacenar nutrientes y secuestrar C a largo plazo (Cotrufo et al. 2013; Lavallee et al. 2020). La SOM no es homogénea: diferentes fracciones presentan tiempos de residencia, funciones y sensibilidades distintas. Una de las aproximaciones operativas más aceptadas para estudiar su dinámica es su separación física en materia orgánica particulada (POM, por sus siglas en inglés) y materia orgánica asociada a minerales (MAOM, por sus siglas en inglés) (Lavallee et al. 2020). La POM proviene principalmente de la fragmentación de hojarasca y raíces con escaso procesamiento microbiano y tiempos de residencia cortos, mientras que la MAOM está constituida por compuestos más finos, en su mayoría microbianos o microbiano-derivados

(exoenzimas), protegidos físicamente mediante enlaces organo-minerales o encapsulamiento dentro de microagregados, y posee tiempos de residencia que pueden extenderse por décadas o siglos (Sokol et al. 2022; Cotrufo y Lavallee 2022). Durante gran parte del siglo XX, la estabilidad de la SOM se interpretó principalmente a través de la hipótesis de recalcitrancia química, según la cual ciertos compuestos vegetales como lignina, cutina o moléculas con alto C/N se consideraban intrínsecamente resistentes a la descomposición microbiana y responsables de la persistencia del C en el suelo (Cotrufo et al. 2013; Cotrufo y Lavallee 2022; Buckeridge et al. 2022). Sin embargo, evidencia acumulada durante las últimas dos décadas ha desafiado este paradigma, mostrando que la persistencia de C depende más de procesos microbianos y de su interacción con la matriz mineral que de la composición química original (Cotrufo et al. 2013; Sokol et al. 2019; Zhang et al. 2021; Cotrufo y Lavallee 2022; Yu et al. 2022). Este cambio conceptual comenzó a inferirse con el marco Microbial Efficiency Matrix Stabilization (MEMS) (Cotrufo et al. 2013), que plantea que la formación de C estable en el suelo se basa en dos mecanismos interconectados: la eficiencia con que los microorganismos transforman materia orgánica fresca en biomasa y necromasa, y la protección fisicoquímica de esta necromasa por la matriz mineral. En este marco, los residuos vegetales de alta calidad con bajo C/N y alto contenido de nutrientes pueden generar más C estable que residuos de baja calidad, al favorecer una mayor eficiencia microbiana de transformación (Sokol et al. 2019; Lavallee et al. 2020; Cotrufo y Lavallee 2022).

El modelo original del MEMS ha sido actualizado con versiones más flexibles como MEMS 2.0 y el modelo “de dos vías” (two-pathway), que reconocen que los compuestos orgánicos pueden reciclarse entre fracciones particuladas, disueltas y asociadas a minerales antes de estabilizarse (Zhang et al. 2021; Cotrufo y Lavallee 2022; Yu et al. 2022). Este enfoque dinámico ofrece una comprensión más realista de las trayectorias del C en suelos y permite vincular propiedades del sustrato, actividad microbiana y estabilización a largo plazo. No obstante, la mayor parte de los estudios empíricos se han realizado en gradientes climáticos amplios o ecosistemas

contrastantes, lo que deja vacíos importantes respecto de cómo estos mecanismos operan a escalas locales, bajo distintas coberturas de dosel y profundidades de suelo. La aplicación de metodologías estandarizadas ha sido clave para operacionalizar estos conceptos. El fraccionamiento físico operativo propuesto por Lavallee et al. (2020) ha permitido separar SOM en POM y MAOM de forma reproducible y comparativa entre estudios. Paralelamente, técnicas espectroscópicas como la transformada de Fourier en el infrarrojo (FTIR), especialmente en su modalidad de reflectancia difusa (DRIFT), se han consolidado como herramientas no destructivas y eficientes para caracterizar cambios moleculares en la SOM. Bandas características como 2920/2850 cm^{-1} (C–H alifáticos) y 1620 cm^{-1} (C=C aromáticos) permiten seguir la transformación de compuestos vegetales hacia productos microbianos y posteriormente hacia formas estabilizadas asociadas a minerales (Margenot et al. 2023; Thabit et al. 2024).

Un elemento funcional central en este marco es la eficiencia microbiana de uso de carbono (CUE), definida como la fracción de C asimilado que se destina a la biosíntesis microbiana en relación con la fracción emitida como CO_2 (Cotrufo et al. 2013; Tao et al. 2023). Una CUE elevada implica una mayor proporción de C retenido en el sistema, aumentando la probabilidad de que se estabilice en MAOM (Wang et al. 2021; Tao et al. 2023b). La estimación de CUE→MAOM, basada en balances de C entre flujos respiratorios y la acumulación en fracciones estabilizadas, puede presentarse como un proxy funcional de la eficiencia microbiana de uso de C, ofreciendo una alternativa operacional a las metodologías isotópicas tradicionales que utilizan trazadores isotópicos como ^{18}O o ^{13}C en CO_2 respirado para estimar CUE microbiana a nivel celular (Spohn et al. 2016). Este enfoque permite vincular directamente la actividad microbiana con la eficiencia de estabilización de C en MAOM, integrando procesos de transformación y destino final del C en el suelo (Manzoni y Cotrufo 2024). En este contexto y para comprender la compleja red de relaciones entre calidad del sustrato, actividad microbiana y formación de SOM estable, se utilizan herramientas estadísticas multivariadas como los modelos de ecuaciones estructurales (SEM), que permiten identificar rutas causales directas e indirectas (Fan et al. 2016; Geyer et al. 2019).

En ecosistemas forestales degradados, como amplias zonas de bosque nativo chileno, estos mecanismos adquieren especial relevancia. Los sistemas silvopastoriles pueden favorecer la entrada de material vegetal al suelo, aumentar el reciclaje de nutrientes y promover la formación de C estable en profundidad (Dube et al. 2013; Cardinael et al. 2017; Alfaro et al. 2018; Aryal et al. 2022; Ramos et al. 2025). Sin embargo, aún existe escasa información sobre cómo diferentes calidades de litera interactúan con la estructura del dosel y la profundidad edáfica para determinar la eficiencia microbiana, la distribución de carbono entre POM y MAOM y las trayectorias de estabilización. Comprender estos mecanismos no solo es fundamental para mejorar estrategias de restauración, sino también para fortalecer políticas públicas de manejo sostenible de suelos y mitigación del cambio climático.

1. Hipótesis

1.1 La variación en la cobertura arbórea, el manejo silvopastoril en bosques de N*othofagus obliqua* y la calidad del material vegetal ingresado al suelo determinan el secuestro de carbono orgánico de un suelo Andisol del Centro Sur de Chile, a diferentes profundidades.

2. Objetivos:

2.1 Objetivo general

2.1.1 Evaluar el efecto de la cobertura arbórea, el manejo silvopastoril y la composición/calidad del material vegetal sobre el almacenamiento de carbono orgánico del suelo en el reservorio estable de la materia orgánica (MAOM) a diferentes profundidades.

2.2 Objetivos específicos:

2.2.1 Evaluar el efecto de la agroforestería en la recuperación de suelos degradados en un bosque de roble (*Nothofagus obliqua*) y su capacidad para estabilizar el carbono (C) y el nitrógeno (N) del suelo.

2.2.2 Determinar cómo influye la calidad de la hojarasca en la formación de materia orgánica estable y la eficiencia de uso del C bajo diferentes aperturas del dosel y profundidades del suelo en un experimento controlado.

REFERENCIAS

1. Alfaro, M., Dube, F., & Zagal, E. (2018). Soil quality indicators in an Andisol under different tree covers in disturbed Nothofagus forests. *Chilean Journal of Agricultural Research*, *78*(1), 106-116. https://doi.org/10.4067/S0718-58392018000100106
2. Amoakwah, E., Lucas, S. T., Didenko, N. A., Rahman, M. A., & Islam, K. R. (2022). Impact of deforestation and temporal land-use change on soil organic carbon storage, quality, and lability. *PLOS ONE*, *17*(8), e0263205. https://doi.org/10.1371/journal.pone.0263205
3. Aryal, D. R., Morales-Ruiz, D. E., López-Cruz, S., Tondopó-Marroquín, C. N., Lara-Nucamendi, A., Jiménez-Trujillo, J. A., Pérez-Sánchez, E., Betanzos-Simon, J. E., Casasola-Coto, F., Martínez-Salinas, A., Sepúlveda-López, C. J., Ramírez-Díaz, R., La O Arias, M. A., Guevara-Hernández, F., Pinto-Ruiz, R., & Ibrahim, M. (2022). Silvopastoral systems and remnant forests enhance carbon storage in livestock-dominated landscapes in Mexico. *Scientific Reports*, *12*(1), 16769. https://doi.org/10.1038/s41598-022-21089-4
4. Aynekulu, E., Suber, M., Van Noordwijk, M., Arango, J., Roshetko, J. M., & Rosenstock, T. S. (2020). Carbon Storage Potential of Silvopastoral Systems of Colombia. *Land*, *9*(9), 309. https://doi.org/10.3390/land9090309
5. Buckeridge, K. M., Mason, K. E., Ostle, N., McNamara, N. P., Grant, H. K., & Whitaker, J. (2022). Microbial necromass carbon and nitrogen persistence are decoupled in agricultural grassland soils. *Communications Earth & Environment*, *3*(1), 1-10. https://doi.org/10.1038/s43247-022-00439-0
6. Cardinael, R., Chevallier, T., Cambou, A., Béral, C., Barthès, B. G., Dupraz, C., Durand, C., Kouakoua, E., & Chenu, C. (2017). Increased soil organic carbon stocks under agroforestry: A survey of six different sites in France. *Agriculture, Ecosystems & Environment*, *236*, 243-255. https://doi.org/10.1016/j.agee.2016.12.011
7. Centro de Información de Recursos Naturales (CIREN). (2010). *Determinación de la erosión actual y potencial de los suelos de Chile*. Ministerio de Agricultura,

Gobierno de Chile. https://www.ciren.cl/noticias/el-49-de-territorio-en-chile-presenta-algun-grado-de-erosion/

8. Cotrufo, M. F., & Lavallee, J. M. (2022). Chapter One - Soil organic matter formation, persistence, and functioning: A synthesis of current understanding to inform its conservation and regeneration. En D. L. Sparks (Ed.), *Advances in Agronomy* (Vol. 172, pp. 1-66). Academic Press. https://doi.org/10.1016/bs.agron.2021.11.002
9. Cotrufo, M. F., Wallenstein, M. D., Boot, C. M., Denef, K., & Paul, E. (2013). The M icrobial E fficiency- M atrix S tabilization (MEMS) framework integrates plant litter decomposition with soil organic matter stabilization: Do labile plant inputs form stable soil organic matter? *Global Change Biology*, *19*(4), 988-995. https://doi.org/10.1111/gcb.12113
10. De Macêdo Carvalho, C. B., De Mello, A. C. L., Da Cunha, M. V., De Oliveira Apolinário, V. X., Dubeux Júnior, J. C. B., Da Silva, V. J., Silva Medeiros, A., Izidro, J. L. P. S., & Bretas, I. L. (2024). Ecosystem services provided by silvopastoral systems: A review. *The Journal of Agricultural Science*, *162*(5), 417-432. https://doi.org/10.1017/S0021859624000595
11. Del Pozo, A., Catenacci-Aguilera, G., & Acosta-Gallo, B. (2024). Consequences of Land Use Changes on Native Forest and Agricultural Areas in Central-Southern Chile during the Last Fifty Years. *Land*, *13*(5), 610. https://doi.org/10.3390/land13050610
12. Don, A., Schumacher, J., & Freibauer, A. (2011). Impact of tropical land-use change on soil organic carbon stocks - a meta-analysis: SOIL ORGANIC CARBON AND LAND-USE CHANGE. *Global Change Biology*, *17*(4), 1658-1670. https://doi.org/10.1111/j.1365-2486.2010.02336.x
13. Dube, F., Thevathasan, N.V., Stolpe, N.B., Espinosa, M., Zagal, E., Gordon, A.M. y Sáez, K. 2013. Selected C fluxes in *Pinus ponderosa*-based silvopastoral systems, exotic plantations and natural pastures on volcanic soils in the Chilean Patagonia. Agroforestry Systems 87(3): 525-542. https://doi.org/10.1007/s10457-012-9574-9

14. Fan, Y., Chen, J., Shirkey, G., John, R., Wu, S. R., Park, H., & Shao, C. (2016). Applications of structural equation modeling (SEM) in ecological studies: An updated review. *Ecological Processes*, *5*(1), 19. https://doi.org/10.1186/s13717-016-0063-3
15. FAO. (2022). The State of the World's Land and Water Resources for Food and Agriculture 2021 – Systems at breaking point. FAO ; https://openknowledge.fao.org/handle/20.500.14283/cb9910en
16. Georgiou, K., Jackson, R. B., Vindušková, O., Abramoff, R. Z., Ahlström, A., Feng, W., Harden, J. W., Pellegrini, A. F. A., Polley, H. W., Soong, J. L., Riley, W. J., & Torn, M. S. (2022). Global stocks and capacity of mineral-associated soil organic carbon. *Nature Communications*, *13*(1), 3797. https://doi.org/10.1038/s41467-022-31540-9
17. Geyer, K. M., Dijkstra, P., Sinsabaugh, R., & Frey, S. D. (2019). Clarifying the interpretation of carbon use efficiency in soil through methods comparison. *Soil Biology and Biochemistry*, *128*, 79-88. https://doi.org/10.1016/j.soilbio.2018.09.036
18. Gomes, V. M., Miranda Júnior, M. S., Silva, L. J., Teixeira, M. V., Teixeira, G., Schossler, K., Freitas, D. A. F. D., & Oliveira, D. M. D. S. (2025). A Global Meta-Analysis of Soil Carbon Stock in Agroforestry Coffee Cultivation. *Agronomy*, *15*(2), 480. https://doi.org/10.3390/agronomy15020480
19. Guerra, C. A., Rosa, I. M. D., Valentini, E., Wolf, F., Filipponi, F., Karger, D. N., Nguyen Xuan, A., Mathieu, J., Lavelle, P., & Eisenhauer, N. (2020). Global vulnerability of soil ecosystems to erosion. *Landscape Ecology*, *35*(4), 823-842. https://doi.org/10.1007/s10980-020-00984-z
20. Huaico Malhue, A. (2018). Análisis de la evolución de las áreas ambientalmente degradadas en Chile. *Revista de la Facultad de Ciencias Forestales y de la Conservación de la Naturaleza*, *50*(4). https://www.scielo.cl/scielo.php?pid=S0718-34292018000400061&script=sci_arttext

21. Lavallee, J. M., Soong, J. L., & Cotrufo, M. F. (2020). Conceptualizing soil organic matter into particulate and mineral-associated forms to address global change in the 21st century. *Global Change Biology*, *26*(1), 261-273. https://doi.org/10.1111/gcb.14859
22. Lebuy, R., Mancilla-Ruiz, D., Manríquez, H., & De La Barrera, F. (2022). Degraded Landscapes in Hillside Systems with Agricultural Use: An Integrated Analysis to Establish Restoration Opportunities in Central Chile. *Land*, *12*(1), 5. https://doi.org/10.3390/land12010005
23. Lehmann, J., & Kleber, M. (2015). The contentious nature of soil organic matter. *Nature*, *528*(7580), 60-68. https://doi.org/10.1038/nature16069
24. López-Sampson, A., & Andrade, H. J. (2024). Agroforestry systems in Latin America. *Agroforestry Systems*, *98*(5), 1075-1078. https://doi.org/10.1007/s10457-024-01002-w
25. Manzoni, S., & Cotrufo, M. F. (2024). Mechanisms of soil organic carbon and nitrogen stabilization in mineral-associated organic matter – insights from modeling in phase space. *Biogeosciences*, *21*(18), 4077-4098. https://doi.org/10.5194/bg-21-4077-2024
26. Margenot, A. J., Parikh, S. J., & Calderón, F. J. (2023). Fourier-transform infrared spectroscopy for soil organic matter analysis. *Soil Science Society of America Journal*, *87*(6), 1503-1528. https://doi.org/10.1002/saj2.20583
27. Miranda, A., Altamirano, A., Cayuela, L., Lara, A., & González, M. (2017). Native forest loss in the Chilean biodiversity hotspot: Revealing the evidence. *Regional Environmental Change*, *17*(1), 285-297. https://doi.org/10.1007/s10113-016-1010-7
28. Ortiz, J., Dube, F., Neira, P., Hernández Valera, R. R., De Souza Campos, P. M., Panichini, M., Pérez-San Martín, A., Stolpe, N. B., Zagal, E., & Curaqueo, G. (2023). Comparative Study between Silvopastoral and Agroforest Systems on Soil Quality in a Disturbed Native Forest of South-Central Chile. *Agronomy*, *13*(11), 2683. https://doi.org/10.3390/agronomy13112683

29. Qu, X., Li, X., Bardgett, R. D., Kuzyakov, Y., Revillini, D., Sonne, C., Xia, C., Ruan, H., Liu, Y., Cao, F., Reich, P. B., & Delgado-Baquerizo, M. (2024). Deforestation impacts soil biodiversity and ecosystem services worldwide. *Proceedings of the National Academy of Sciences*, *121*(13), e2318475121. https://doi.org/10.1073/pnas.2318475121
30. Ramachandran Nair, P. K., Nair, V. D., Mohan Kumar, B., & Showalter, J. M. (2010). Carbon Sequestration in Agroforestry Systems. En *Advances in Agronomy* (Vol. 108, pp. 237-307). Elsevier. https://doi.org/10.1016/S0065-2113(10)08005-3
31. Ramos, C., Zagal, E., Timmusk, S., Dube, F., Paulino, L., Ortiz, J., Intriago-Ávila, J., & Fuentes, J. P. (2025). Soil Carbon Sequestration in *Nothofagus obliqua* Forests with Different Canopy Cover Levels Under Silvopastoral Management. *Agronomy*, *15*(4), 855. https://doi.org/10.3390/agronomy15040855
32. Servicio Agrícola y Ganadero (SAG). (2021). *Memoria SIRSD-S 2010–2021*. Gobierno de Chile, Ministerio de Agricultura. https://www.sag.gob.cl/sites/default/files/Memoria%20%20SIRSD-S%20%20SAG%202010-2021%20Final.pdf
33. Smith, P., Soussana, J., Angers, D., Schipper, L., Chenu, C., Rasse, D. P., Batjes, N. H., Van Egmond, F., McNeill, S., Kuhnert, M., Arias-Navarro, C., Olesen, J. E., Chirinda, N., Fornara, D., Wollenberg, E., Álvaro-Fuentes, J., Sanz-Cobena, A., & Klumpp, K. (2020). How to measure, report and verify soil carbon change to realize the potential of soil carbon sequestration for atmospheric greenhouse gas removal. *Global Change Biology*, *26*(1), 219-241. https://doi.org/10.1111/gcb.14815
34. Sokol, N. W., Sanderman, J., & Bradford, M. A. (2019). Pathways of mineral-associated soil organic matter formation: Integrating the role of plant carbon source, chemistry, and point of entry. *Global Change Biology*, *25*(1), 12-24. https://doi.org/10.1111/gcb.14482
35. Sokol, N. W., Whalen, E. D., Jilling, A., Kallenbach, C., Pett-Ridge, J., & Georgiou, K. (2022). Global distribution, formation and fate of mineral-

associated soil organic matter under a changing climate: A trait-based perspective. *Functional Ecology*, *36*(6), 1411-1429. https://doi.org/10.1111/1365-2435.14040

36. Spohn, M., Klaus, K., Wanek, W., & Richter, A. (2016). Microbial carbon use efficiency and biomass turnover times depending on soil depth – Implications for carbon cycling. *Soil Biology and Biochemistry*, *96*, 74-81. https://doi.org/10.1016/j.soilbio.2016.01.016
37. Tao, F., Huang, Y., Hungate, B. A., Manzoni, S., Frey, S. D., Schmidt, M. W. I., Reichstein, M., Carvalhais, N., Ciais, P., Jiang, L., Lehmann, J., Wang, Y.-P., Houlton, B. Z., Ahrens, B., Mishra, U., Hugelius, G., Hocking, T. D., Lu, X., Shi, Z., … Luo, Y. (2023a). Microbial carbon use efficiency promotes global soil carbon storage. *Nature*, *618*(7967), 981-985. https://doi.org/10.1038/s41586-023-06042-3
38. Tao, F., Huang, Y., Hungate, B. A., Manzoni, S., Frey, S. D., Schmidt, M. W. I., Reichstein, M., Carvalhais, N., Ciais, P., Jiang, L., Lehmann, J., Wang, Y.-P., Houlton, B. Z., Ahrens, B., Mishra, U., Hugelius, G., Hocking, T. D., Lu, X., Shi, Z., … Luo, Y. (2023b). Microbial carbon use efficiency promotes global soil carbon storage. *Nature*, *618*(7967), 981-985. https://doi.org/10.1038/s41586-023-06042-3
39. Thabit, F. N., Negim, O. I. A., AbdelRahman, M. A. E., Scopa, A., & Moursy, A. R. A. (2024). Using Various Models for Predicting Soil Organic Carbon Based on DRIFT-FTIR and Chemical Analysis. *Soil Systems*, *8*(1), 22. https://doi.org/10.3390/soilsystems8010022
40. Timmusk, S., & de-Bashan, L. E. (2022). Microbiome: A Tool for Plant Stress Management in Future Production Systems. *Stresses*, *2*(2), 210-212. https://doi.org/10.3390/stresses2020014
41. Wang, B., An, S., Liang, C., Liu, Y., & Kuzyakov, Y. (2021). Microbial necromass as the source of soil organic carbon in global ecosystems. *Soil Biology and Biochemistry*, *162*, 108422. https://doi.org/10.1016/j.soilbio.2021.108422

42. Yu, W., Huang, W., Weintraub-Leff, S. R., & Hall, S. J. (2022). Where and why do particulate organic matter (POM) and mineral-associated organic matter (MAOM) differ among diverse soils? *Soil Biology and Biochemistry*, *172*, 108756. https://doi.org/10.1016/j.soilbio.2022.108756
43. Zhang, Y., Lavallee, J. M., Robertson, A. D., Even, R., Ogle, S. M., Paustian, K., & Cotrufo, M. F. (2021). Simulating measurable ecosystem carbon and nitrogen dynamics with the mechanistically defined MEMS 2.0 model. *Biogeosciences*, *18*(10), 3147-3171. https://doi.org/10.5194/bg-18-3147-2021

II. CHAPTER I: SOIL CARBON SEQUESTRATION IN *NOTHOFAGUS OBLIQUA* FORESTS WITH DIFFERENT CANOPY COVER LEVELS UNDER SILVOPASTORAL MANAGEMENT

Camila Ramos [1], Erick Zagal [2] *, Salme Timmusk [3], Francis Dube [4], Leandro Paulino [2], Juan Ortiz [2], Jean Intriago [5] and Juan Pablo Fuentes [6]

[1]Doctoral Program in Agronomy Sciences, Faculty of Agronomy, Universidad de Concepción, Chillán 3812120, Chile
[2]Spectroscopy Laboratory (Vis-IR) and Sustainable Soil Management, Soils and Natural Resources Department, Faculty of Agronomy, University of Concepción, Chillán 3812120, Chile
[3]Department of Forest Mycology and Pathology, Uppsala BioCenter, P.O. Box 7026, SE-75007 Uppsala, Sweden
[4]Department of Silviculture, Faculty of Forest Sciences, University of Concepción, Victoria 631, Concepción 4030000, Chile
[5]Soils and Natural Resources Department, Faculty of Agronomy, University of Concepción, Chillán 3812120, Chile
[6]Master Program in Agronomic Sciences, Faculty of Agronomy, Universidad de Concepción, Chillán 3812120, Chile
[7]Department of Silviculture and Nature Conservation, Faculty of Forest Sciences and Nature Conservation, University of Chile, Santiago 8820808, Chile
*Author to whom correspondence should be addressed.

Agronomy ***2025****, 15(4), 855;* ***https://doi.org/10.3390/agronomy15040855***

Submission received: 5 March 2025 / Revised: 25 March 2025 / Accepted: 26 March 2025 / Published: 29 March 2025

Abstract

Agroforestry contributes to slowing deforestation, favoring ecosystem regeneration and improving land use sustainability. This study evaluated the impact of silvopastoral systems on soil recovery and their capacity to sequester and stabilize carbon © and nitrogen (N) in degraded soils of a native *Nothofagus obliqua* forest in Ranchillo Alto (37°04′52″ S, 71°39′14″ W), Ñuble Region, Chile. Three open (Op), semi-open (SOp), and semi-closed (SC) silvopastoral systems were analyzed and compared with a control (Ctr) without silvopastoral management across four soil depths (0–10, 10–20, 20–30, 30–60 cm). Physical, chemical, and biological analyses were performed, along with soil physical organic matter (SOM) fractionation. The highest C levels were found in the 0–10 cm depth (13.9, 11.8, 11.5, and 8.5% for Op > SC > SOp and Ctr, respectively). Despite its higher degradation, Op presented the highest levels of C, N,

and non-oxidizable C (Cnox), possibly due to pyrogenic carbon from old potato burns. Furthermore, the same trend was observed for mineral associated organic matter (MAOM) fraction and C stocks in all silvopastoral systems compared to the control. These results underline the potential of silvopastoral practices to improve soil quality and increase long-term carbon sequestration, contributing to sustainable soil restoration strategies.

Keywords: agroforestry; C stocks; soil restoration; climate change; particulate organic matter; organic matter in mineral fraction; stable C

1. Introduction

In Chile, decades of overuse of natural resources have led to 37.8% of the national territory showing soil degradation, in moderate to severe conditions, concentrated mainly in the central part of the country [1,2]. This degradation is mainly caused by the felling of more than 44% of native forests, affecting more than 8 million hectares (Mha). The genus *Nothofagus* has been one of the most impacted, decreasing its original area by more than 70%. This reduction is mainly due to anthropogenic activities, including the expansion of urban areas, croplands, and forest plantations, although most of the surface has been cleared for the growth of pastures for livestock use, reaching up to 3 Mha [3].

Given this scenario of increasing soil and environmental degradation, various sustainable practices have been promoted in recent years to mitigate the impact of human activities. Among them, silvopastoral systems (SPSs) have played a fundamental role. According to several studies [4,5,6], the integration of trees in production systems reduces erosion, improves soil fertility and quality, protects biodiversity, and contributes to the mitigation of climate change through carbon © sequestration, being able to store between 1.8 and 6.1 Mg of soil organic carbon (SOC) per year [5,7].

Recent studies have highlighted the importance of including native forests and agroforestry systems in conservation and climate change mitigation policies [6,8]. Since 2019, the Intergovernmental Panel on Climate Change (IPCC) [9] has underlined the

crucial role of these systems in C capture and their potential to reduce greenhouse gas emissions, conserve biodiversity, and protect soil [10,11]. FAO [12] as well called for collaboration between the agricultural and forestry sectors to expand agroforestry practices, defining agroforestry as a key climate solution due to its capacity to store large amounts of soil organic matter (SOM), which helps the provision of multiple ecosystem services [13]. According to Voltr et al. [14], in agroecosystems with a marked presence of woody species, high amounts of SOM are produced, which translate into annual net increases in ecosystem C, of which around 60% of the C is in the form of SOC.

SOM can be defined as the complex mixture of different compounds from plants and soil microorganisms [15]. The physical separation of SOM by particle size operationally into particulate organic matter (POM) and matrix-associated organic matter (MAOM) minerals is an approach that helps to understand the distribution of SOM and responses to environmental change [16,17,18,19,20]. It is proposed that POM and MAOM have different formation pathways and mean residence times in soil. It is postulated that POM (labile fraction of C) comes from the fragmentation or depolymerization of plant litter, while MAOM (stable fraction of C) comes from the transformations or modifications carried out by soil microorganisms and/or their exoenzymes, which grant it different degrees of physicochemical protection [21].

Understanding the mechanisms of SOM formation and stabilization, as well as its sensitivity to disturbances and environmental changes, is fundamental for predicting its future dynamics [22]. Representing SOM pools based on the processes that regulate their formation, and stabilization is crucial for developing sustainable management strategies. In this context, SPSs stand out for their ability to restore degraded soils by facilitating the incorporation and recycling of nutrients through SOM contributions. However, knowledge about the implementation of these systems in degraded native forests, particularly at different soil depths, and their capacity to stabilize SOC in the long term remains limited. Therefore, the objective of this study was to evaluate the effect of agroforestry on the recovery of degraded soils in a native roble *(Nothofagus obliqua)* forest and its ability to capture and stabilize soil C and nitrogen (N).

2. Materials and Methods

2.1. Description of the Study Area

The study was conducted in Ranchillo Alto public property located in the foothills of the Ñuble region, Chile (37°04′52″ S, 71°39′14″ W; 1200–2000 m a.s.l.), covering approximately 635 ha (Figure 1). This property corresponds to a native forest that has undergone prolonged degradation mainly due to indiscriminate logging, overgrazing, and extraction of saw-quality timber and firewood (browsing, depredation). The foothills of the Ñuble region have a humid temperate Mediterranean climate with a marked winter season, and annual temperatures of 13.5 °C, but can exceed 25 °C in summer. The annual rainfall may exceed 3.000 mm in a normal year. Snowfall occurs mostly between May and September, reaching when there are low temperatures and frequent frosts. The soils are Andisols, “Santa Barbara” series (medial, amorphic, mesic Typic Haploxerands), and locally known as “trumaos” [23].

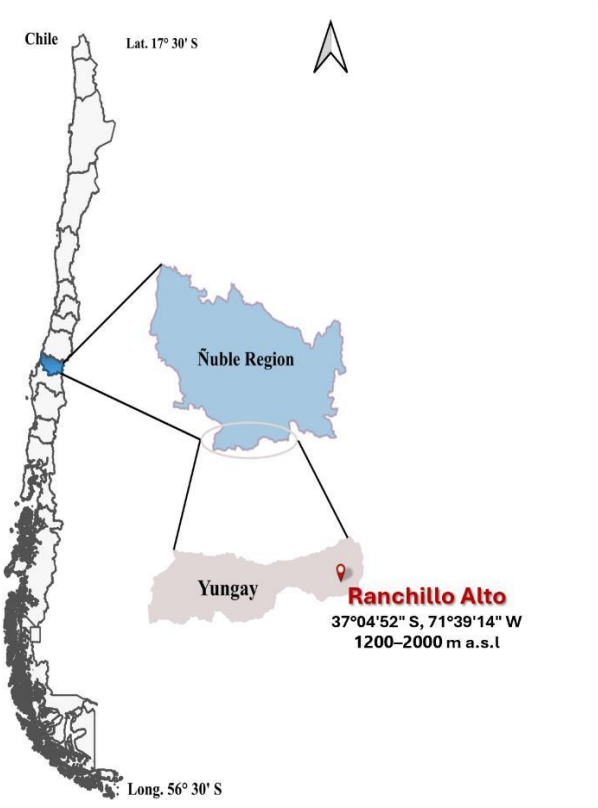

Figure 1. Location of the native forest study site (Ranchillo Alto) in south-central Chile.

2.2. Conditioning of Experimental Treatments

In order to restore the ecosystem value of the forest, experimental treatments of silvopastoral systems (SPSs) were implemented in the northern and southern sectors of the property in 2016. This study was carried out in the period 2023–2024 and focused on three SPSs located in the southern sector, which cover approximately 10 ha. These SPSs represent different levels of open canopy, defined according to the degree of previous disturbance of the forest. The sites were classified as open (Op) +++, semi-open (SOp) ++, and semi-closed (SC) +. In addition, a control of degraded native forest without silvopastoral intervention (Ctr) was included (Table 1).

Table 1. General information for each tree covers conditions in the silvopastoral systems located in the southern sector of Ranchillo Alto.

Open Canopy	Location	NPr Surface (ha)	Tree Density (ha^{-1})	Forest Species	Percentage of Light	Degradation	Soil Sampling
Ctr	37°4′50″ S, 72°26′30″ W 1250 m.a.s.l	3×.33	-	Roble (*Nothofagus obliqua*)	-	'	4 depths (0–10, 10–20, 20–30 and 30–60 cm)
Op	37°14′51″ S, 72°26′30″ O 1250 m.a.s.l	3× 1.33	60	Roble (*Nothofagus obliqua*)	85–95%	' ' '	4 depths (0–10, 10–20, 20–30 and 30–60 cm)
SOp	37°14′50″ S, 72°26′30″ W 1250 m.a.s.l	3× 1.33	134	Roble (*Nothofagus obliqua*)	65–75%	' '	4 depths (0–10, 10–20, 20–30 and 30–60 cm)
SC	37°14′49″ S, 72°26′30″ W 1250 m.a.s.l	3× 1.33	258	Roble (*Nothofagus obliqua*)	45–55%	'	4 depths (0–10, 10–20, 20–30 and 30–60 cm)

NP: number of plots. The '+' signs indicate the degree of degradation: + low degradation, ++ medium degradation, +++ high degradation. Source: modified from Ortiz et al. [23].

The SPSs located in the southern sector already had the three canopy conditions defined for this study previously established in 2016 [24], so, in 2023 we validated mean percentages of solar radiation at ground level as well as leaf area indices and determined that no modifications in tree density were necessary as these levels had not changed over time. To quantify and compare the percentages of cover for each treatment and their evolution over time, the results were corroborated with a second

series of hemispheric photos (15–20 random points in each plot) taken with a Solariscope SOL 300B (Behling, Germany) [25].

The woody component in the three silvopastoral systems (SPSs) is represented by roble (*Nothofagus obliqua*). In the study area, current land use is primarily based on controlled grazing practices. In 2016, during its establishment, a mixture of 12 species of grasses and legumes was sown, with the objective of improving the quality of feed for livestock, while maintaining the vegetation cover and favoring the regeneration of the ecosystem, since the previous degradation had strongly reduced the availability of grazing. High-quality feed contributes to improved availability and animal nutrition. Additionally, it is more palatable food, considering that livestock tends to consume selectively. The herbaceous component included oats (*Avena sativa* L.), vetch (*Fabaceae purpurea* L.), clover (*Trifolium incarnatum* L., T. *subterraneum* L. and *T. vesiculosum* L.), *Lolium multiflorum* var. Westerwoldicum, *Phalaris aquatica* L., *Lolium perenne* L., and *Dactylis glomerata* L., in addition to the regrowth of radal *(Lomatia hirsuta*).

Currently, due to the conditions of the forest in the foothills, as well as the low temperatures and the presence of snow in winter, more resistant species have prevailed, notably quilla (*Chusquea quila*), radal, and *Festuca arundinacea* L. The latter is present in all three silvopastoral systems, especially in Op and SOp, and to a lesser extent in SC, which is related to the degree of solar radiation available, as it requires sun for optimal development.

Likewise, in the Op system there is a marked presence of radal, a pioneer species indicative of forest degradation, which rapidly colonizes open areas after a disturbance. Its abundance in Op, the most degraded site, is associated with the clearing carried out for potato (*Solanum tuberosum* L.) cultivation more than 50 years ago, where stubble burning was also practiced. These activities have caused changes in soil properties and carbon dynamics.

It is important to highlight that the silvopastoral systems were established within a native forest with the aim of restoring soil quality and the ecosystem value of the forest. As

part of this strategy, livestock stocking rates have been carefully managed and kept low, preventing further disturbances since the initial sowing.

From a statistical perspective, efforts were made to minimize variability in cultural practices among the sites, ensuring that the main source of variation was canopy openness, defined according to the previous level of degradation. Other practices, such as species sowing, were carried out uniformly across all sites to prevent them from becoming a confounding factor in the analysis. The experimental control allows us to attribute the observed differences in the results mainly to the initial degradation conditions and the effects of the silvopastoral treatment, enabling a more accurate assessment of the impact of these practices in relation to the study's objectives.

2.3. Soil Sampling

A completely randomized design with three replicates (plots) randomly distributed at each tree cover level treatment was used for soil sampling.

Soil samples were collected from each plot, consisting of five random sub-samples taken at different depths: 0–10 cm, 10–20 cm, 20–30 cm, and 30–60 cm, following the recommendations of Kögel-Knabner [23]. In addition, a sample of the shallow depth (0–30 cm) was taken in the field for chemical and physical analyses, which were not the main focus of this study and where we expected less variability in the first three depths. The other depths (0–10, 10–20, and 20–30) were included to evaluate differences that might be found in the first 30 cm of soil, particularly in biological analyses and labile and stable carbon forms.

The samples were placed in a thermal box with ice to be transported from the forest to the laboratory and stored at 4 °C. All samples were sieved through a 2 mm stainless steel sieve and then divided into 2 parts, one of which was air-dried for subsequent physical and chemical analyses, and the other of which was conditioned to 60% water-filled pore space (WFPS), ideal for biological analyses. Chemical and physical analyses were carried out in the Soil Laboratories for corresponding analyses and for biological ones in the Spectroscopy Laboratory (Vis-IR) and Sustainable Soil Management department of the Faculty of Agronomy of the University of Concepción.

2.4. Soil Analysis

2.4.1. Evaluation of Physical Parameters

For physical analyses, bulk density (BD) was determined using the cylinder method. A soil sample was collected in the field at the corresponding depth using a metal cylinder of known volume. The sample was then carefully extracted, avoiding compaction, and transported to the laboratory. In the laboratory, the sample was oven-dried at 105 °C for 24 h to remove all moisture. The dry weight of the soil was then measured, and BD was calculated as the ratio of dry soil mass to cylinder volume. Particle density (PD) was assessed by the pycnometer method and texture was analyzed by the Bouyoucos hydrometer method, all following the methodology described by Sandoval et al. [24].

2.4.2. Evaluation of Chemical Parameters

Chemical analyses of the soil, including $pH_{(WATER)}$, organic matter (OM), $N_{(AVAILABLE)}$, P, K, effective cation exchange capacity (ECEC), exchangeable Al, Ca, Mg, K, Na (Al_{EXCH}, Ca^{2+}_{EXCH}, Mg^{2+}_{EXCH}, K^{+}_{EXCH}, Na^{+}_{EXCH}), NH_4^+, NO_3^-; Al, K, Ca, and Mg saturation (Al_{SAT}, K^{+}_{SAT}, Ca^{2+}_{SAT} and Mg^{2+}_{SAT}) were performed according to the protocols of Sadzawka et al. [25].

2.4.3. Evaluation of Biological Parameters

Total enzymatic activity in soil was assessed by fluorescein diacetate (FDA) hydrolysis, a method that estimated the enzymatic activity of hydrolytic enzymes involved in OM degradation. For analysis, 1.0 g of moist soil was weighed into screw-capped test tubes (triplicates plus a blank). A total of 9.9 mL of sodium phosphate buffer was added to the samples and 10 mL to the blank, followed by 0.1 mL of fluorescein diacetate (FDA) only to the samples. After vortexing, the tubes were incubated at 25 °C for 1 h. After incubation, they were cooled in an ice bath. For colorimetry, 10 mL of acetone was added to each tube, vortexed, and filtered. The absorbance of the filtrate was measured at 490 nm against a reagent blank prepared with acetone and distilled water [26].

The activity of β-glucosidase, a key component of carbohydrate degradation in soil, was assessed using the method [27], based on the release of p-nitrophenol after

incubating the soil with p-nitrophenyl-β-D-glucopyranoside (25 mM) in MUB-HCl (pH 6) at 37 °C for 1 h. It was then cooled on ice, centrifuged at 6000 rpm for 5 min, and after the addition of 0.5 M $CaCl_2$ and THAM-NaOH buffer (pH 12), the absorbance at 400 nm was measured. Both the absorbance of β-glucosidase and FDA enzymatic activity were measured using a UV-visible spectrophotometer (AA3, BRAN + LUEBBE, Norderstedt, Germany).

For soil respiration, 20 g of moist soil conditioned at 60% WFPS per treatment (in triplicate) was weighed into a Falcon tube. These vials were sealed with specialized caps that allow gas (CO_2) extraction using a precision syringe, which was then injected into a gas analyzer (see below) to perform microbial respiration analysis. The vials with soils were kept in an incubation chamber at 22 °C for 14 days. This requires that the soil has been conditioned at 60% WPFS. Basal soil CO_2 emission was calculated at 3, 5, 7, 10, and 14 days of incubation. To perform the gas extraction process, homogenization of the Falcon's headspace was previously performed by extracting 1 mL of gas and injecting it again three times. The 1 mL gas sample was then injected into a unidirectional dual-wavelength non-dispersive infrared (NDIR) gas analyzer (LI-820, Li-COR Bioscience, Lincoln, NE, USA), using a modification as described by Craine et al. [28].

2.4.4. Soil Physical Fractionation

The physical fractionation of the soil was conducted following the method described by Lavallee et al. [21] to enhance understanding of soil C fraction dynamics. Briefly, soils were sieved to 2 mm, and 5 g of oven-dried soil at 105 °C was shaken with 15 mL of 0.5% sodium hexametaphosphate solution and five 1 mm glass beads for 18 h to disperse the soil. The dispersed soil was then rinsed through a 53 µm sieve, with the fraction passing through (<53 µm) collected as MAOM, while the remaining material was classified as POM.

2.4.5. Total Carbon, Oxidizable Carbon, Non-Oxidizable Carbon, and Carbon Stocks

Total carbon (TC) and total nitrogen were determined in each of the soil samples and their fractions using the dry combustion method based on the Dumas principle [29]. The different samples and their fractions were subjected to chemical oxidation with sodium dichromate dihydrate to determine the proportion of oxidizable carbon (Cox), following the Walkley–Black method [1,25]. Since there is no inorganic C in this volcanic soil, TC = total organic carbon (TOC). Non-oxidizable carbon (Cnox) was determined by the difference between TC and Cox (Cnox = TOC − Cox).

The carbon stock (C stock) for each soil layer was calculated by multiplying the OC concentration by the BD and the thickness of the sampled soil layer (cm). The formula used was as follows:

$$\text{C stock } (\text{Mg C ha}^{-1}) = \frac{\text{OC concentration } (\%)}{100} \times \text{BD } (\text{g cm}^{-3}) \times \text{depth (cm)} \times 10 \quad (1)$$

2.5. Statistical Analysis

To evaluate the effect of Op, SOp, SC, and Ctr canopy cover on the different chemical, physical, and biological analyses at the different depths (0–10; 10–20; 20–30; and 30–60 cm), a two-way ANOVA was performed, and for significant differences, Tukey post hoc analyses were performed, using the R program (RStudio 2024). A principal component analysis (PCA) was performed to identify patterns in the variability of the variates studied and to reduce the dimensionality of the data. This analysis allowed us to observe the distribution of the samples based on the treatments and soil depths, and to evaluate the relationship between the different soil variables studied. The PCA was performed using the R program (RStudio 2024), employing the prcomp function with previously centered and scaled data.

3. Results and Discussion

Our physical analyses of the soil revealed that BD and PD, as well as the texture, remained within the typical range for volcanic soils under the different site conditions (Table 2) [1].

Table 2. Physical properties of soil under different open canopy levels and depth.

Open Canopy/Depth	BD (g cm^3)	PD (g cm^3)	Sand (%)	Silt (%)	Clay (%)
Ctr (0–30)	0.66 ± 0.02 Aa	2.26 ± 0.00 Aa	34.63 ± 1.10 Aa	42.57 ± 0.40 Ab	22.79 ± 0.77 Aa
Ctr (30–60)	0.63 ± 0.02 Ab	2.24 ± 0.01 Ab	36.60 ± 4.09 Aa	46.13 ± 3.77 Aa	17.27 ± 0.40 Ab
Op (0–30)	0.61 ± 0.02 Aa	2.14 ± 0.02 ABb	37.17 ± 0.37 Aa	45.80 ± 0.37 Ab	17.03 ± 0.68 Ba
Op (30–60)	0.76 ± 0.08 Ab	2.21 ± 0.00 ABa	33.80 ± 2.36 Aa	48.87 ± 0.37 Aa	17.33 ± 1.41 Bb
SOp (0–30)	0.61 ± 0.03 Aa	2.09 ± 0.01 Bb	40.57 ± 1.23 Aa	43.90 ± 1.33 Ab	15.50 ± 0.99 Ba
SOp (30–60)	0.72 ± 0.06 Ab	2.12 ± 0.09 Ba	35.70 ± 1.04 Aa	50.03 ± 1.59 Aa	14.27 ± 0.37 Bb
SC (0–30)	0.60 ± 0.01 Aa	2.06 ± 0.01 Bb	39.77 ± 3.01 Aa	43.03 ± 0.82 Ab	17.20 ± 2.12 ABa
SC (30–60)	0.64 ± 0.06 Ab	2.20 ± 0.05 Ba	37.13 ± 2.53 Aa	45.07 ± 1.17 Aa	17.80 ± 2.47 ABb

n: 24 and $p < 0.05$ ± SD. Different capital letters mean significant differences between conditions, while lowercase letters indicate significant differences between depths. BD: bulk density, PD: particle density.

Individually, the BD showed representative values for Andisols ranging between 0.60 and 0.76 g/cm3. The density variation depended more on the soil depth than on the canopy opening, being more significant in the surface horizon ($p \leq 0.05$). These observations coincide with the results of Gomez et al. [30], who reported similar findings in Andisol soils from forests under silvopastoral management in Argentine Patagonia. In addition, the PD, like the BD, presented variations in terms of soil depth, giving significant differences ($p \leq 0.05$). The PD ranged from 2.06 to 2.21 g cm−3 with a mean value of 2.1 g cm−3, which is within representative ranges of volcanic soils rich in OM, according to Ortiz et al. [31] and Nissen et al. [32], who estimated ranges of 1.9 to 2.1 (0 to 15 cm) and 1.9 to 2.0 (0 to 20 cm) for PD in forest soils (0–15 cm).

The soil texture, like the rest of the physical variables, did not show differences in terms of canopy opening levels, but did show significant differences between soil depths for sand and silt ($p \leq 0.05$). The results found for texture coincide with those reported by Gomez et al. [30].

Chemical analyses of the soil generally showed results representative of Andisol soils (Table 3). The observed pH values are slightly acidic, fluctuating between 5.41 and 5.66, a typical characteristic of Andisol soils. The pH did not show significant differences ($p > 0.05$), although there was a trend in both depths, with the Op condition having the

lowest values, which could be attributed to a higher acidity favored by a high OM content [33].

Table 3.Chemical properties of soil under different open canopy levels and depth

Open Canopy /Depth	pH (Water)	OM [1] (%)	N [2] (mg kg^{-1})	P (mg kg^{-1})	K^+ (mg kg^{-1})	ECEC (cmol kg^{-1})	Al_{EXCH*} (cmol kg^{-1})	$Ca^{2+}{}_{EXCH*}$ (cmol kg^{-1})	$Mg^{2+}{}_{EXCH*}$ (cmol kg^{-1})
Ctr (0–30)	5.45 ± 0.05 Aa	14.51 ± 1.56 Ca	17.7 ± 0.30 Ba	1.88 ± 17.76 Aa	110.28 ± 0.04 Aa	3.96 ± 1.52 Aa	0.09 ± 0.01 ABa	3.01 ± 1.34 Aa	0.50 ± 0.14 Aa
Ctr (30–60)	5.66 ± 0.04 Aa	9.07 ± 1.44 Cb	8.30 ± 3.18 Bb	1.23 ± 8.03 Aa	37.60 ± 0.02 Ab	1.37 ± 0.72 Ab	0.03 ± 0.01 Abb	0.95 ± 0.59 Ab	0.22 ± 0.10 Ab
Op (0–30)	5.45 ± 0.05 Aa	22.07 ± 0.52 Aa	21.10 ± 0.05 ABa	0.67 ± 0.05 Aa	91.17 ± 0.05 Aa	2.14 ± 0.05 Aa	0.18 ± 0.05 Aa	1.43 ± 0.05 Aa	0.26 ± 0.05 Aa
Op (30–60)	5.41 ± 0.04 Aa	14.38 ± 0.27 Ab	14.40 ± 0.04 ABb	0.53 ± 0.04 Aa	45.27 ± 0.04 Ab	0.86 ± 0.04 Ab	0.07 ± 0.04 Ab	0.49 ± 0.04 Ab	0.14 ± 0.04 Ab
SOp (0–30)	5.62 ± 0.21 Aa	17.49 ± 1.44 BCa	20.57 ± 0.09 ABa	0.73 ± 19.36 Aa	62.57 ± 0.05 Aa	2.36 ± 1.57 Aa	0.07 ± 0.04 Ba	1.83 ± 1.43 Aa	0.27 ± 0.12 Aa
SOp (30–60)	5.63 ± 0.08 Aa	10.52 ± 1.73 BCb	10.83 ± 0.09 ABb	0.67 ± 22.66 Aa	46.60 ± 0.06 Ab	1.20 ± 0.56 Ab	0.01 ± 0.00 Bb	0.83 ± 0.48 Ab	0.16 ± 0.02 Ab
SC (0–30)	5.50 ± 0.18 Aa	18.37 ± 1.48 Ba	26.97 ± 0.14 Aa	0.90 ± 21.32 Aa	90.50 ± 0.05 Aa	3.43 ± 1.52 Aa	0.14 ± 0.09 ABa	2.62 ± 1.43 Aa	0.39 ± 0.13 Aa
SC (30–60)	5.44 ± 0.12 Aa	12.67 ± 1.39 Bb	17.30 ± 0.05 Ab	0.57 ± 38.09 Aa	81.87 ± 0.06 Ab	1.92 ± 0.84 Ab	0.09 ± 0.05 ABb	1.29 ± 0.69 Ab	0.25 ± 0.08 Ab

n: 24 and $p < 0.05$ ± SD. Different capital letters mean significant differences between conditions, while lowercase letters indicate significant differences between depths. $_{EXCH*}$: exchangeable. [1] OM is obtained by multiplying %C by 1.724 [2]. Available mineral N.

OM showed a decrease with depth in all treatments, an expected pattern given that OM is mostly concentrated in the surface horizon due to the accumulation of leaf litter and roots. In the surface horizon (0–30 cm), the Op system presents the highest OM value (22.07%), followed by SC, SOp, and Ctr respectively, reflecting the direct contribution of OM in the silvopastoral treatments compared to the control. The OM values are relatively higher than those reported in other studies [30]; this is mainly due to the location of the forest in the foothills, where low temperatures throughout the year slow down the decomposition processes of soil microorganisms [34].

Available N decreased with depth in all treatments, which is consistent with that presented in OM. In silvopastoral systems, nitrogen levels were considerably higher than in the Ctr, especially in the surface horizon ($p \leq 0.05$). These results suggest that SPSs favor microbial activity and nitrogen mineralization, which increases the

availability of this nutrient for plants. This is consistent with previous studies, indicating that this type of practice can improve nitrogen retention and availability in soils, mainly due to the incorporation of organic waste from animals in these systems, which provides an additional source of nitrogen [35]. On the other hand, legumes planted in 2016 in SPSs failed to persist due to forest conditions. However, despite their visible disappearance, the initial establishment of these plants may have influenced soil fertility, contributing to higher long-term nitrogen availability in these systems. In contrast, the Ctr, which did not receive legume seeding, lacks this additional source of nitrogen, which could explain the observed differences in nutrient dynamics between the sites [36].

Phosphorus (P) presented low values in all treatments, which is a common characteristic of Andisols due to the high phosphate adsorption capacity of the short-range-order (SRO) minerals present in volcanic soils in Chile. These minerals are important for retaining nutrients in the soil, limiting the availability of the nutrient for plants [37]. In addition, there was a tendency for Op and SOp systems to have the lowest P values, which could be related to the prominent presence of radal in these two conditions. Radal, as a species of the Proteaceae family, has a remarkable ability to compete and adapt to phosphorus-poor soils, which allows it to be particularly efficient in the absorption of this nutrient. This efficiency, however, can reduce the availability of P for other plant species, thus contributing to a reduction in the concentration of this nutrient in the soil [38].

ECEC values were highest at the 0–30 cm depth ($p \leq 0.05$). At this depth, ECEC showed a tendency to decrease with increasing canopy disturbance (+). This capacity is directly related to mineralogical composition, particularly the higher clay content, and furthermore, to the values observed for K, Ca, and Mg, as the ECEC favors the accumulation of amorphous minerals, which contribute significantly to the cation retention capacity [39]. The chemical properties of the soil, specifically the cations K, Ca, and Mg, have remained constant over time [31], without significant changes. This suggests that the ecosystem is recycling nutrients efficiently. Other chemical properties, such as the exchangeable cations $NH_4^+{}_{EXCH}$, $K^+{}_{EXCH}$, $Na^+{}_{EXCH}$, as well as the

anion NO_3^- and the saturation percentages of Al_{SAT}, K^+_{SAT}, Ca^{2+}_{SAT}, and Mg^{2+}_{SAT}, are presented in **Table A1**.

FDA activity is a measure of overall enzymatic activity in soil, used as an indicator of total microbial activity. **Figure 2** shows the results of microbial biomass activity as a function of open canopy and soil depth. FDA hydrolysis analyses reveal significant differences both between different soil depths ($p \leq 0.05$) and between different canopy openness conditions ($p \leq 0.05$).

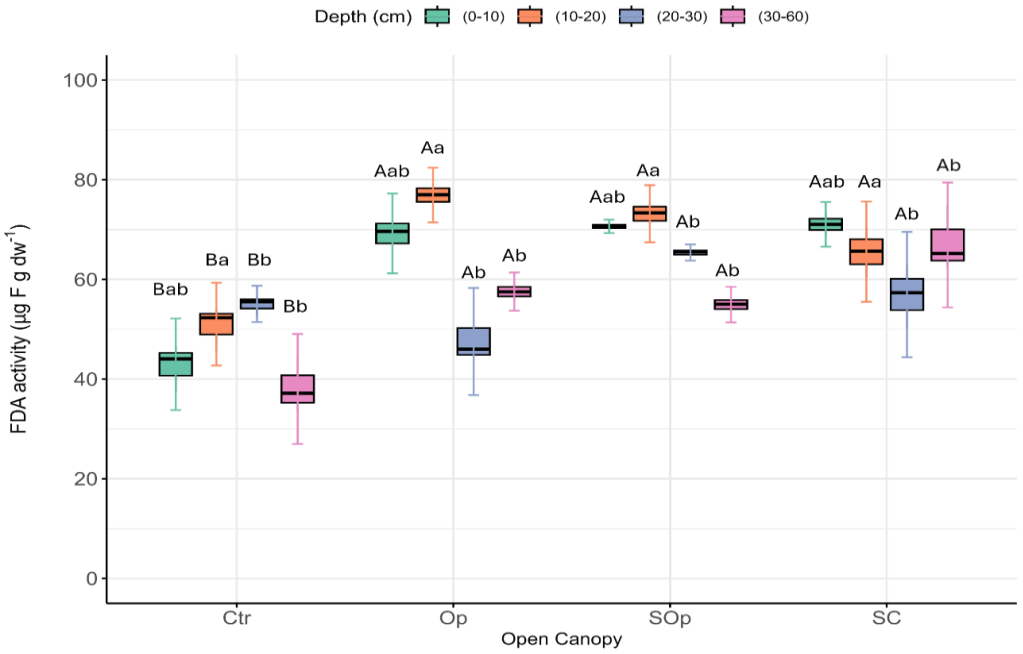

Figure 2. Microbial biomass activity determined by FDA hydrolysis as a function of open canopy (Ctr: control; Op: open; SOp: semi-open; SC: semi-closed) and soil depth (0–10; 10–20; 20–30; and 30–60 cm).Uppercase letters indicate significant differences between open canopy conditions, while lowercase letters indicate significant differences between soil depths. Differences were considered significant according to Tukey's test ($p < 0.05$). The box-and-whisker plot shows the distribution of the data in the box and the whiskers show the deviation. The line shows the mean of the data.

It is observed that FDA activity decreases as soil depth increases, regardless of the type of management. This is related to the fact that soil microorganisms, which are responsible for the hydrolysis of FDA, are more concentrated in the surface layers of the soil, where there is greater availability of OM and nutrients. On the other hand, significant differences are observed between the plots with silvopasture compared to

the control, which may suggest that including SPSs helps soils recover their microbial functional capacity after having been degraded.

The results obtained for the FDA in this study are consistent with those of previous research carried out at the site by Ortiz et al. [8]. However, they are higher than those reported by Reyes et al. [40], who evaluated the biological activities of the soil in a relict forest in south-central Chile within a mixed forest community. Their results are very similar to those of the Ctr, while SPSs present higher values. This indicates that these systems promote greater biological activity in the soil, possibly due to the combination of plant species and management practices that favor the availability of OM and microbial diversity.

Like FDA activity, soil respiration showed significant differences between conditions and soil depths ($p \leq 0.05$) (**Figure 3**). The accumulated CO_2 fluxes, measured in a closed system for 14 days, were higher at shallow depths (0–10 cm) compared to the other depths for the four treatments. The SOp and SC conditions were those that showed the greatest increase in CO_2 emissions. This relationship could be influenced by variations in litter contributions, since a higher tree density leads to a greater incorporation of OM into the soil and a greater metabolic activity of microorganisms. In addition, closed systems limit the incidence of sunlight, which helps to preserve the humidity and temperature conditions in the litter, favoring the subsequent proliferation of fungi and bacteria.

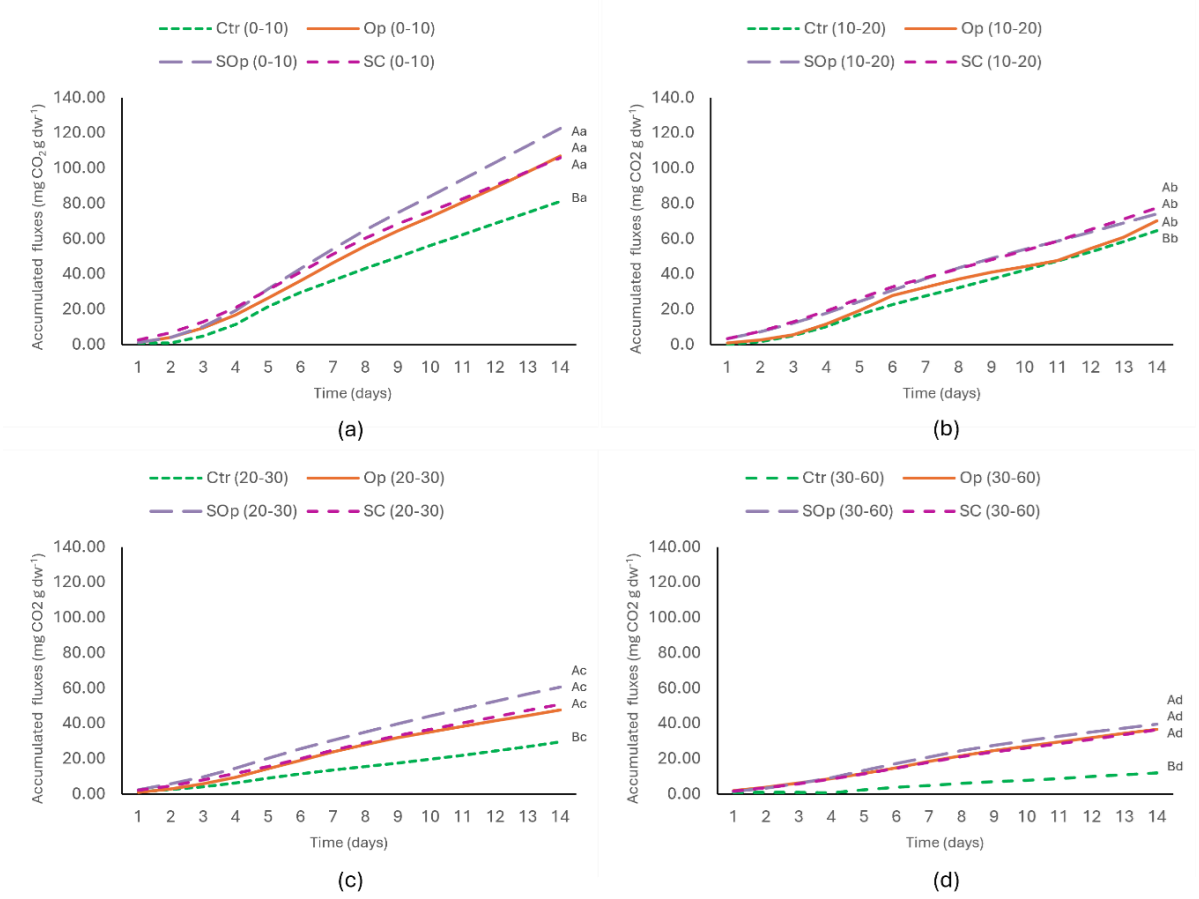

Figure 3. Cumulative soil respiration fluxes over a 14-day period. Each line represents a time series of CO2 measurements for different open canopy levels: (a) depth 0–10 cm; (b) depth 10–20 cm; (c) depth 20–30 cm; and (d) 30–60 cm.Analysis of variance (ANOVA) was used to determine significant differences. Uppercase letters indicate significant differences between open canopy levels (in each figure), while lowercase letters indicate significant differences between soil depths (between figures). Differences were considered significant at $p < 0.05$.

β-Glucosidase, unlike FDA activity and respiration, did not show significant differences between conditions ($p > 0.05$) (Figure 4). However, it was observed that Op > SC > Sop > Ctr showed a similar trend to the rest of the biological analyses. This is because this indicator is less sensitive to changes in soil conditions, since its activity is more related to specific processes of the C cycle, while FDA and respiration reflect a broader range of microbial metabolic activities and responses to environmental variations [40]. Regarding depth, it did show significant differences, finding greater β-Glucosidase activity in the surface horizons. Since β-Glucosidase is an important indicator of the

decomposition of SOM, especially of polysaccharides such as cellulose, this result could have been conditioned by the fact that in the superficial horizons (0–10 cm) there is the greatest availability of C-rich substrates, such as those from the decomposition of leaf litter, and as one goes deeper into the profile (30–60 cm), the contributions of fresh OM and oxygen conditions decrease, which limits enzymatic activity.

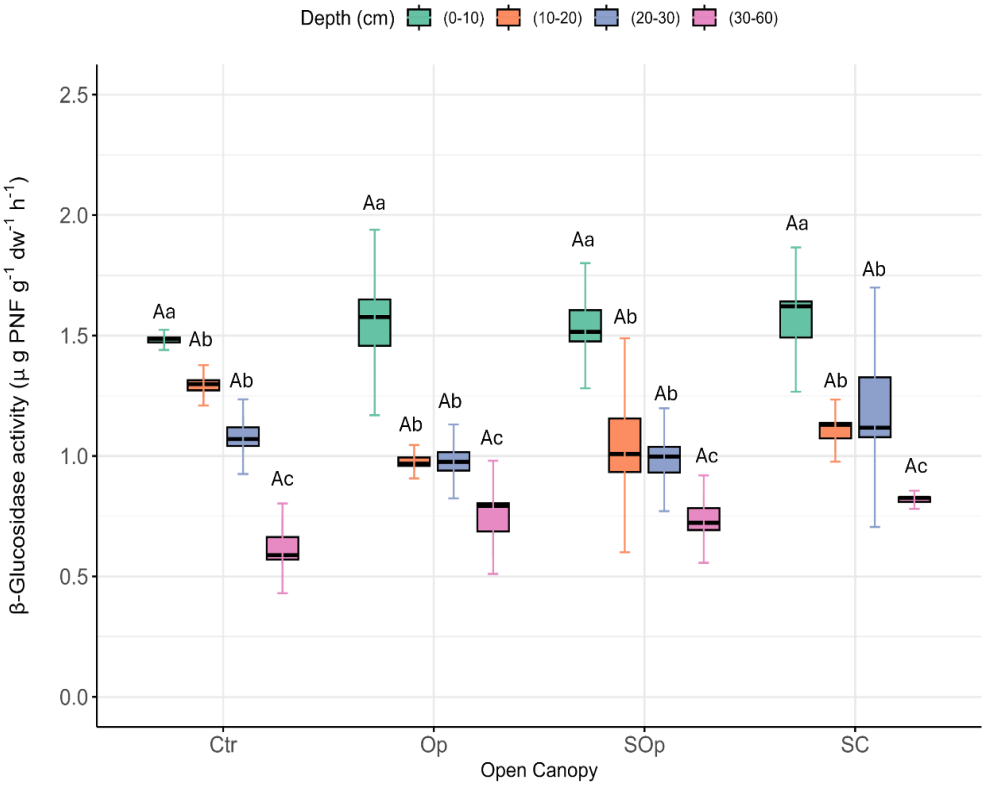

Figure 4. β-Glucosidase activity as a function of open canopy (Ctr: control; Op: open; SOp: semi-open; SC: semi-closed) and soil depth (0–10; 10–20; 20–30; and 30–60 cm). Uppercase letters indicate significant differences between open canopy levels, while lowercase letters indicate significant differences between soil depths. Differences were considered significant according to Tukey's test ($p < 0.05$). The box-and-whisker plot shows the distribution of the data in the box and the whiskers show the deviation. The line shows the mean of the data.

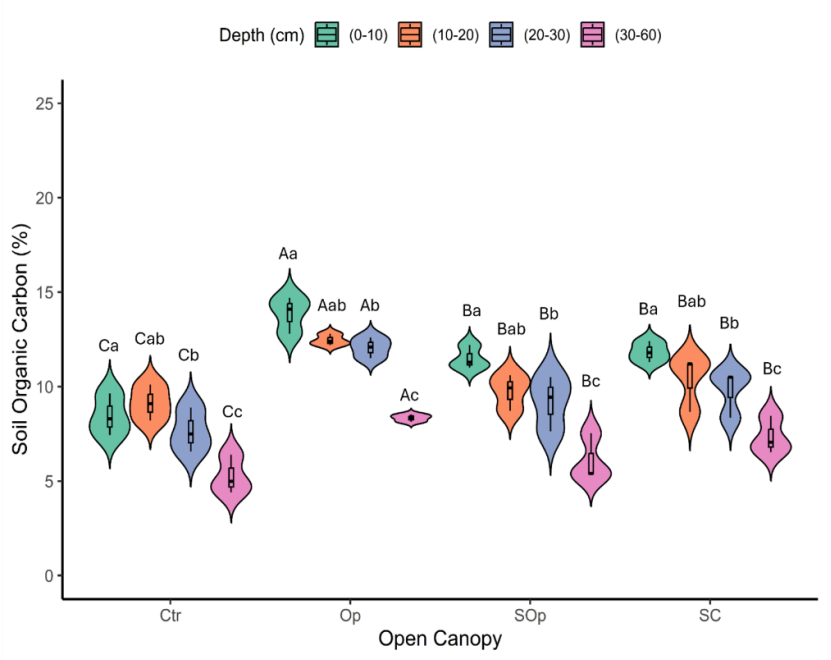

(a)

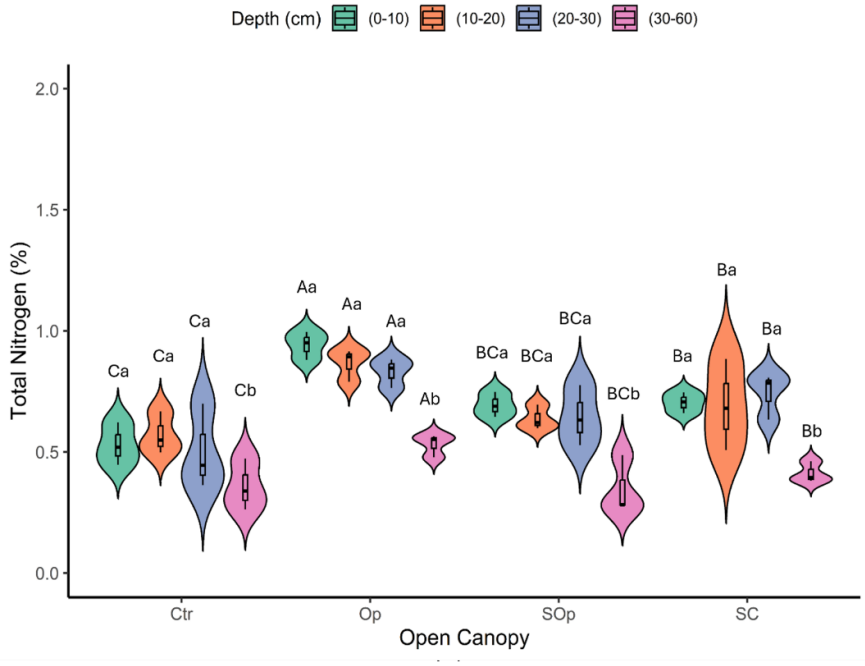

(b)

Figure 5. Violin plot of variables (a) organic carbon (%) and (b) total nitrogen as a function of the factors open canopy (Ctr: control; Op: open; SOp: semi-open; SC: semi-closed) and soil depth (0–10; 10–20; 20–30; and 30–60 cm). Uppercase letters indicate

significant differences between open canopy levels, while lowercase letters indicate significant differences between soil depths. Differences were considered significant according to Tukey's test ($p < 0.05$).

The OC content in the soil showed significant differences between the evaluated depths ($p \leq 0.05$) (Figure 5a). The highest concentrations were found in the surface horizons (0–10 cm). This pattern is consistent with the dynamics of C in soils, since the surface horizons receive greater contributions of leaf litter and other organic residues that, when decomposed, favor the accumulation of C and as the depth of the profile increases, the percentage of C decreases due to the lower amount of fresh OM and the more limited microbial activity [41].

On the other hand, significant differences were observed between the different open canopy levels ($p \leq 0.05$). The Op canopy showed the highest concentrations of C, despite having the least tree cover and being the most degraded area. This finding coincides with previous studies [31] and could be associated with the history of agricultural burning in this area, mainly of potato cultivation, which generates pyrogenic carbon (PyC) [24]. This form of C is evidenced by the presence of charcoal fragments and an intense black color in the soil samples. PyC is highly resistant to oxidation due to its polyaromatic structure, being a persistent fraction of the TC, making it an important long-term C reservoir [42].

Although the study sites are close to the Op zone, the distribution of treatments does not suggest a uniform pattern of PyC influence across the other treatments. Although SOp is close to Op, it does not show similar values, indicating that the transport of pyrogenic carbon is not a dominant factor. Therefore, we maintain that only the Op condition presents PyC, which supports our results. Another important point is the presence of black charcoal in the Op samples, a material previously identified in earlier studies by Ortiz et al. However, this material has not been visually observed in the samples from the other treatments, reinforcing the idea that the influence of pyrogenic carbon is concentrated exclusively in Op.

Furthermore, silvopastoral management conditions showed a higher percentage C compared to the non-silvopastoral treatment (Op > SC > SOp > Ctr). This suggests that

SPSs promote soil recovery, increasing C accumulation, possibly through the increase in the amount of available OM contributed by animals to the system. In general, the estimated C concentrations were higher than those observed in other soil conservation systems; an example of this is the study by Poblete-Grant et al. [43], which reports OC levels in Andisol soils under grasslands in southern Chile with prolonged application of poultry manure, which were lower than those found in this study. Our results are, however, similar to those reported by Gomez et al. [30], who evaluated these parameters under similar agroforestry conditions in a temperate native forest in Argentina, working with the tree species *Nothofagus antartica*. This species, like *N. obliqua*, is a deciduous tree that contributes a continuous level of leaf litter to the soil throughout the year, which is related to high C level inputs.

The total N% showed significant differences between the open canopy conditions evaluated and soil depths ($p \leq 0.05$) (Figure 5b). The total N% of (0–10 cm) varied between 0.45 and 1.0 (±0.15) where Op > SC > Sop > Ctr. The values obtained in this study are higher than those reported by Crovo et al. [44] for native forest Andisols. However, the inorganic forms of nitrogen available to plants, NO_3^- and NH_4^+, were lower than the minimum requirements necessary for plant growth (Table A1. Average NO_3^- values ranged from 7.77 to 14.7 mg/kg (Ctr > SC > Op > SOp), while NH_4^+ values ranged from 3.01 to 12.83 mg/kg (SOp > SC > Op > Ctr), respectively. Previous studies have shown a similar trend or behavior at the same site in previous years [31,45], although an increase in NH_4^+ levels as a form of bioavailable nitrogen would have been expected due to the incorporation of animal feces, or also an increase in the potential N mineralization pool due to the leguminous species incorporated in 2016.

In terms of C sequestration, the results indicate that the Op treatment is the most effective, as it presents the highest SOC stocks at all depths (Figure 6). The highest Op levels with respect to the rest of the treatments were observed in the surface horizons 0–10 cm and deep horizons 30–60 cm, where values of 84.2 Mg C ha^{-1} and 189.6 Mg C ha^{-1} were reached, respectively. On the other hand, the SOp and SC treatments also showed high values at all depths analyzed, although not as high as Op; this could be due to differences in management practices associated with agricultural

burning, which influence the dynamics of C in the soil. The Ctr presented the lowest C stock values with respect to the rest of the treatments, especially at the depth of 30–60 cm, where it barely reached values close to 90 Mg C ha^{-1}. This suggests that soil in unmanaged degraded native forests has a lower capacity to retain C, and that the implementation of practices such as SPSs are effective in promoting long-term C storage.

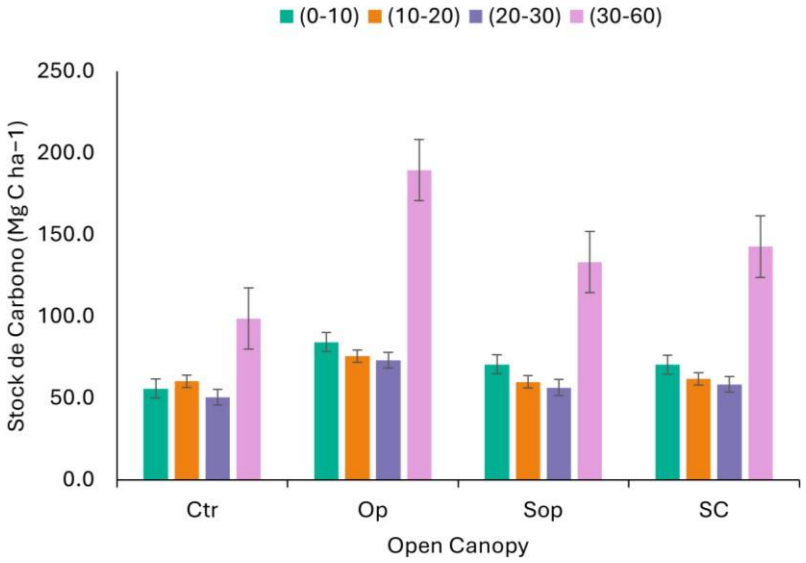

Figure 6. Figure 6. SOC stocks as a function of open canopy (Ctr: control; Op: open; SOp: semi-open; SC: semi-closed) and soil depth (0–10; 10–20; 20–30; and 30–60 cm). The error bars represent the standard deviation SD.

The results revealed that the C:N ratio (C/N) of the unfractionated samples did not show significant differences in terms of open canopy ($p > 0.05$) but did differ in terms of soil depth ($p \leq 0.05$) (Figure 7a). The C/N ratio of the unfractionated samples varied between 12.66 and 19.25 with an average of 15.6 ±1, which is within the distribution of C/N averages (9.9 to 25.8) found for soils around the world [46], although it is below the C/N ratio reported by Katsumi [47], who worked with Andisols (n = 14) under different land uses and found an average C/N ratio of 26.3. These results for the site could be highly related to the quality of the substrate, since the tree species present at the site is deciduous and its litter has a relatively lower lignin content (lignin: N of 21.79) and, consequently, lower C:N ratios [48].

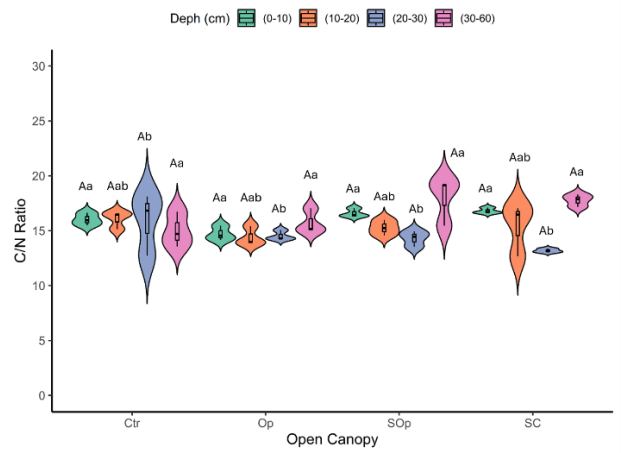
Depth (cm) (0-10) (10-20) (20-30) (30-60)
C/N Ratio
Open Canopy
Ctr
Op
SOp
SC

(a)

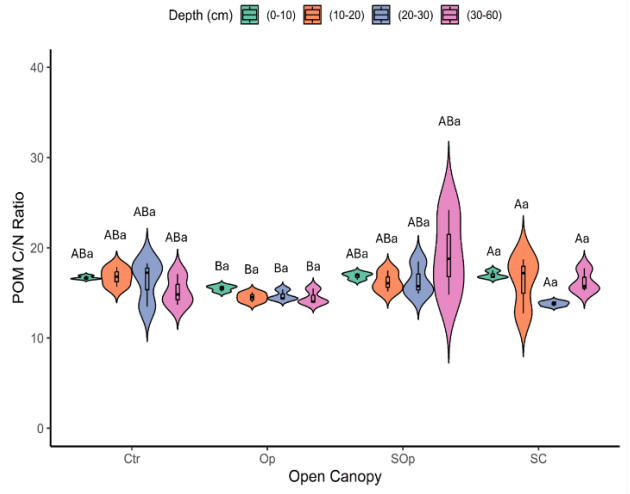
Depth (cm) (0-10) (10-20) (20-30) (30-60)
POM C/N Ratio
Open Canopy
Ctr
Op
SOp
SC

(b)

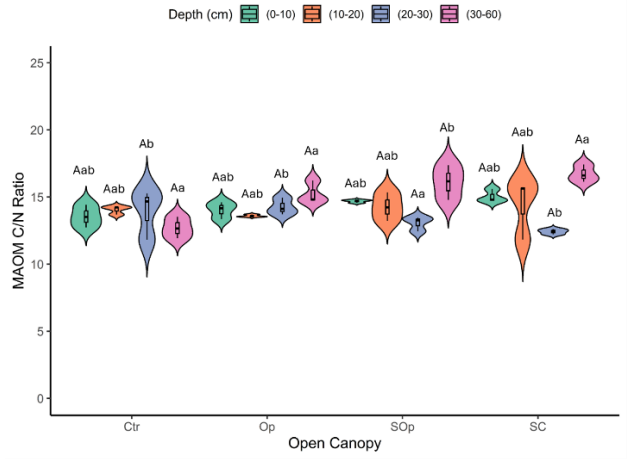
Depth (cm) (0-10) (10-20) (20-30) (30-60)
MAOM C/N Ratio
Open Canopy
Ctr
Op
SOp
SC

(c)

Figure 7. Violin plot of the variables: (a) C/N ratio, (b) POM C/N ratio, and (c) MAOM C/N ratio as a function of open canopy (Ctr: control; Op: open; SOp: semi-open; SC: semi-closed) and soil depth (0–10; 10–20; 20–30 and 30–60 cm).Uppercase letters indicate significant differences between open canopy levels, while lowercase letters indicate significant differences between soil depths. Differences were considered significant according to Tukey's test ($p < 0.05$).

The C/N ratio of the POM fraction showed significant differences depending on the open canopy conditions ($p \leq 0.05$) (Figure 7b). On the other hand, the C/N ratio of the MAOM fraction showed significant differences both in depth and in open canopy ($p \leq 0.05$) (Figure 7c). In the particulate fraction, the highest C/N ratios were observed at depths of 30–60 cm, particularly in SC, while in the surface horizons (0–10 cm), the values were more uniform between treatments. On the other hand, in the mineral fraction, C/N values were more homogeneous throughout the depths, although the surface horizons showed lower C/N ratios, with Ctr being the treatment with the lowest values.

Overall, the C/N ratio of MAOM (11–17, mean = 14.24 ± 1) was very similar to that of POM (12–24, mean = 16.02 ± 2), although more contrasting values between both fractions would have been expected (Figure 7c). As reported by Lavallee et al. [21], POM generally presents C/N ratios between 10 and 40, while MAOM has narrower C/N ratios, between 8 and 13. This would be expected, given that the C/N ratios of POM and MAOM largely reflect the characteristics of the source material. POM is associated with the C/N of plant litter, while MAOM corresponds to the C/N of microbial necromass and metabolites. Plant litter shows high variability in its C/N ratio (e.g., from 40 to 120 in a subset of NEON sites; [49]), while soil microorganisms have a significantly lower and restricted C/N ratio (between 3 and 15; [50]). This analysis would be based on the hypothesis that MAOM is dominated by microbially derived OM; however, POM and MAOM fractions are also known to contain mixtures of faster and slower cycling C pools with likely contributions from both plant and microbial detritus [51,52,53]. A study by Yu et al. [54] suggests that plant-derived OM may also contribute substantially to MAOM, especially in humid forests (with MAOM C/N > 15), which could explain the similarity observed between fractions in this study.

Cnox concentrations in unfractionated samples varied significantly with respect to opening condition and depth ($p \leq 0.05$) (Figure 8a). Cnox decreases with depth in all treatments. The highest values are found in the Op and SC treatments in the surface horizons despite being the most different treatments in terms of degradation condition, but this is not the case at the depth of 30–60 cm where the differences between all treatments tend to be less marked.

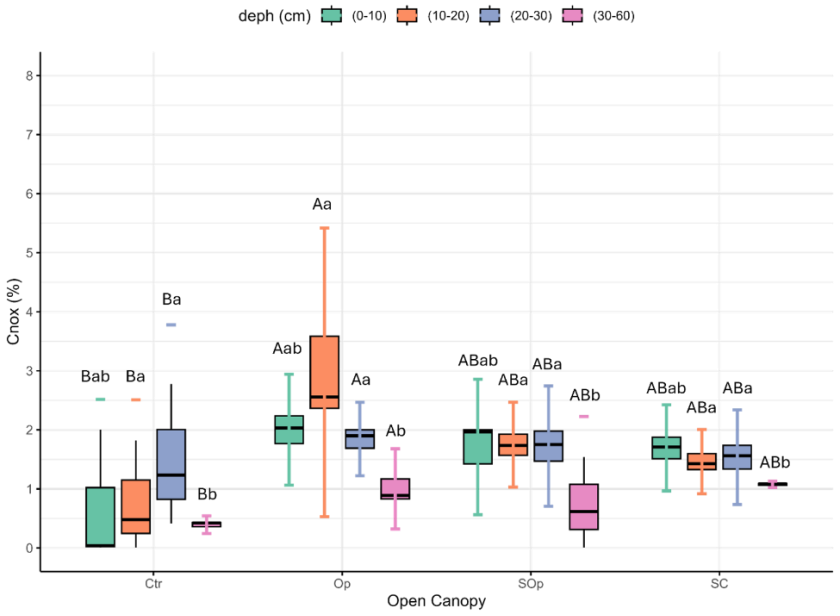

(a)

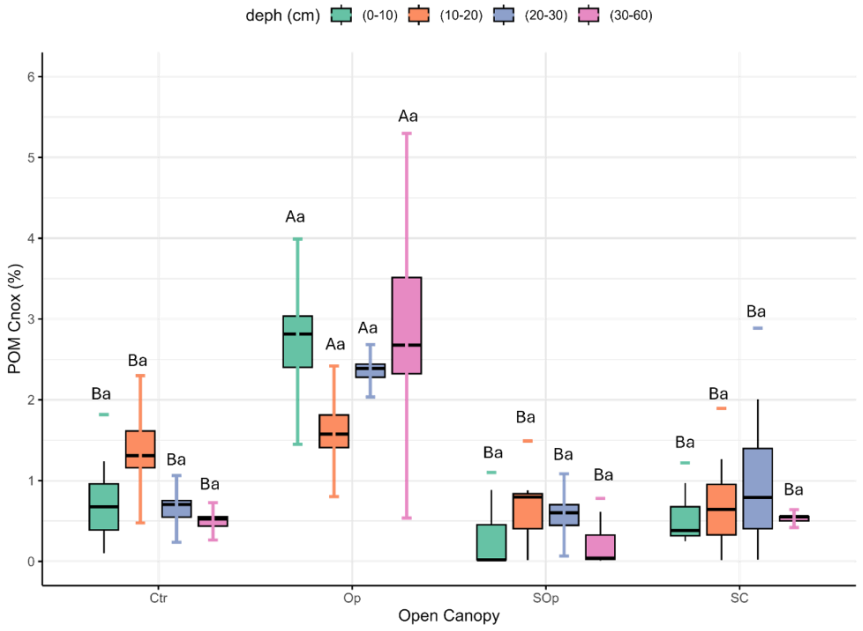

(b)

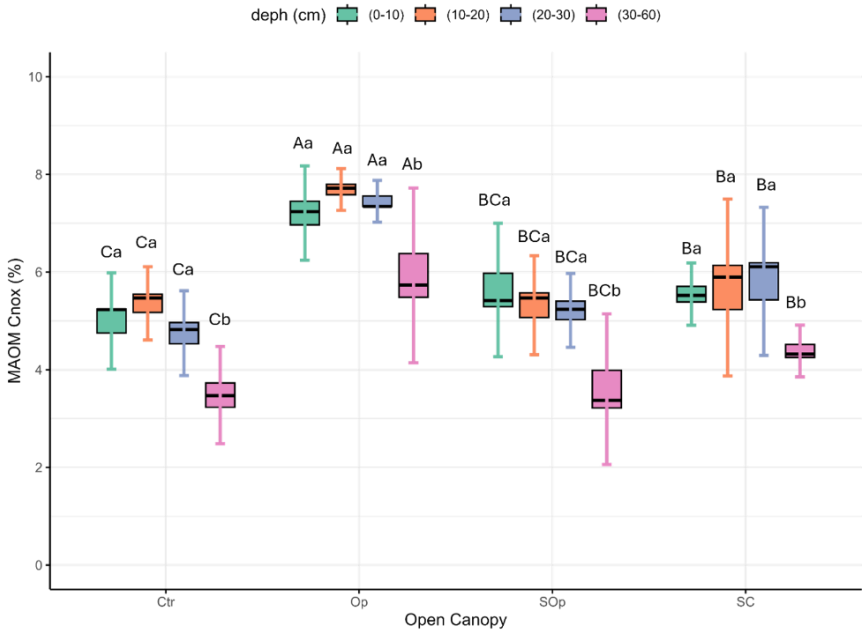

(c)

Figure 8. (**a**) Non-oxidizable carbon (Cnox %), (**b**) non-oxidizable carbon in particulate fraction (POM Cnox %), (**c**) non-oxidizable carbon in mineral fraction (MAOM Cnox %) as a function of open canopy (Ctr: control; Op: open; SOp: semi-open; SC: semi-closed) and soil depth (0–10; 10–20; 20–30 and 30–60 cm). Uppercase letters indicate significant differences between open canopy levels, while lowercase letters indicate significant differences between soil depths. Differences were considered significant

according to Tukey's test ($p < 0.05$). The box-and-whisker plot shows the distribution of the data in the box and the whiskers show the deviation. The line shows the mean of the data. The concentration of POM Cnox and MAOM Cnox showed significant differences depending on the open canopy conditions ($p \leq 0.05$). In addition, the MAOM Cnox fraction also showed significant differences depending on the depth ($p \leq 0.05$) (Figure 8b,c). In general, the values of POM Cnox and MAOM Cnox tend to be higher in the surface horizons (0–10 cm) and progressively decrease with depth, following a pattern similar to that observed in the unfractionated samples.

As reported by Sierra et al. [55], it is expected that as the soil profile goes deeper, the fraction of Cnox will increase proportionally, reflecting the accumulation of more recalcitrant and stable forms of OM in the deeper layers. This phenomenon is due to the presence of recalcitrant compounds such as lignin, tannins [56], cutins, and suberins [57], which are more abundant in the roots [58]. On the other hand, it is expected that the concentrations of Cox will be higher in both fractions (POM and MAOM) in the surface horizons, due to the contribution of OC from leaf litter.

In this study, both Cox and Cnox showed the highest concentrations in the surface horizon (0–10 cm) (Figure A1a). Yu et al. [54], in a study that included a large transect of soil types, found that forest soils tend to vary the chemical and isotopic properties of the OM fractions of the soil and that this occurs mainly in the surface horizons. These authors found that in the surface horizons of forest soils there is a high abundance of aliphatic compounds (aliphatic C–H/C=O) compared to carbonyl groups (C=O), which are associated with more oxidized compounds. These observations reinforce the relationship between C dynamics in the different OM fractions and the fact that the C stabilization processes in our study are not only occurring at depth.

In terms of open canopy, the Op treatment showed the highest concentrations of both fractions. However, MAOM Cnox concentrations are more homogeneous throughout the depths compared to the POM fraction, which presents greater variability. This behavior could be related to the different dynamics of C stabilization in each fraction, where MAOM is more associated with stabilized microbial SOM, while POM reflects a more direct influence of litter and other materials in initial decomposition processes. In addition, Cnox is determined as a more stable fraction of C and is expected to include highly recalcitrant forms of C, including PyC or black carbon, and/or organic

compounds strongly associated with the clay fraction. This is why the Op condition, despite being the most degraded, presents the highest values and this is associated with the historical anthropogenic practices of burning stubble.

PCA explained 80.4% of the total variation in the data with the first two components (Figure 9). The results revealed clear clusters for biological and C and N analyses in the samples and their fractions indicating that agroforestry practices have a significant impact on SOC properties and dynamics.

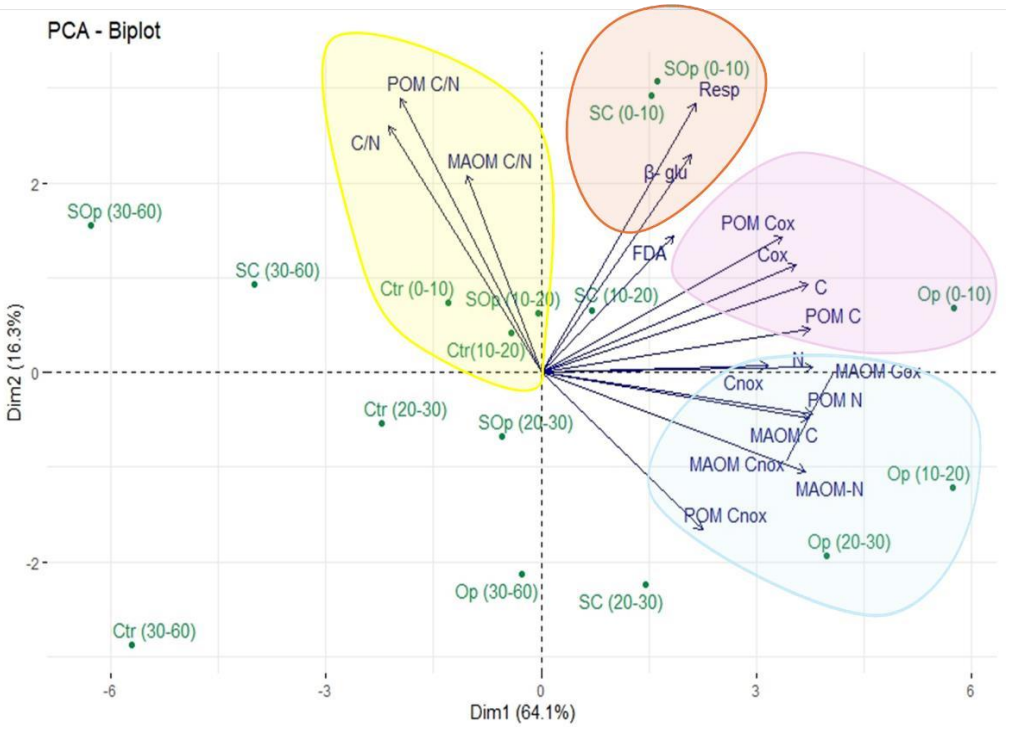

Figure 9. Principal component analysis (PCA) of soil chemical and biological indicators under different open canopy levels (Ctr, Op, SOp, and SC) and soil depths (0–10, 10–20, 20–30, and 30–60 cm). Arrows represent the original variables projected into the space of the first two principal components (Dim1 and Dim2), which explain 80.4% of the total variance, respectively. Colored ellipses group observations according to their similarities, providing information on the relationship between variables under different open canopy levels and depths. Arrows indicate the contribution of each response variable to the variability explained by the principal components, highlighting the differences in parameters under each treatment.

At shallow depths of 0–10 cm and 10–20 cm for the SOp and SC systems, they are grouped together, showing an association with the variables of enzymatic activity and soil respiration. This indicates that SPSs at shallow depths present a high biological

activity, which is consistent with their greater exposure to the input of OM and conditions that favor microbial activity. The Op system and the depths of 20–30 cm and 30–60 cm tend to group together, showing an association with the content of Cox and Cnox in different fractions. This suggests that in this system, although it is more degraded, the accumulation of stable C could be promoted by historical management practices (such as burning), which generate PyC resistant to degradation. The Ctr is not grouped with the variables of labile C content and enzymatic activity. This suggests a lower level of C and lower biological activity, which could be determined since this system does not present silvopastoralism.

This study provides relevant information on the impact of silvopastoral systems on carbon and nitrogen dynamics in degraded soils. Although previous studies exist at this site, long-term research (more than 20 years) is required to evaluate the persistence of these effects, which could be addressed in future studies. In addition, environmental factors such as climatic variability, soil type, and tree component can significantly influence the response of these systems, which underscores the need for studies under diverse ecological conditions, especially those that include the native forest component, which are still limited. Also, the inclusion of additional indicators, such as microbial biodiversity, would allow a more complete evaluation of the impact of silvopastoral systems. Analysis of the soil microbial community, which includes the diversity of bacteria, fungi, and other microorganisms, would provide a detailed profile that would help identify the composition and relative abundance of different microbial groups and the contribution and pathways of carbon formation in soils. In addition, molecular compositional techniques would be useful to understand the pathways of formation and the contribution of plant material in the generation of soil organic matter. Furthermore, the analysis of Al and Fe pedogenic oxides, stable aggregates (≥63 μm) [59], and/or Al-organomineral complexes [60] will also contribute to a better understanding of C stabilization in C-rich soils in temperate climates.

4. Conclusions

This study highlights the critical role agroforestry systems based on native forests can play in restoring degraded soils. The increased levels of stable C and nitrogen observed in SPS treatments, compared to the Ctr, emphasize the potential of these practices to enhance long-term C sequestration and improve soil quality in degraded landscapes. The distinct dynamics of C across various OM fractions, coupled with the observation that C stabilization in this study is not confined to deeper soil layers, may be characteristic of humid forest ecosystems. PyC contributed to the higher concentration found in the Op treatments. However, our findings do not support the fact that its transport to the other treatments is a dominant factor. Future research should incorporate more advanced methodologies, such as fractionation techniques that separate SOM by particle size and density, and target more specific analyses to identify PyC. These approaches would enable a more nuanced understanding of the mechanisms and pathways driving SOM formation and stabilization, thereby advancing our knowledge of its dynamics across diverse ecological and management contexts.

Author Contributions

Conceptualization, E.Z., F.D. and C.R.; methodology, C.R., E.Z., F.D., L.P., S.T. and J.P.F.; validation, C.R., E.Z., F.D., L.P., S.T. and J.P.F.; formal analysis, C.R. and E.Z.; investigation, C.R., E.Z., J.I.-Á. and J.O.; resources, E.Z. and F.D.; data curation, C.R., E.Z., S.T., F.D. and J.O.; writing—original draft preparation, C.R. and E.Z.; writing—review and editing, C.R., E.Z., F.D., J.I.-Á., L.P., S.T. and J.P.F.; visualization, C.R., E.Z., J.I.-Á. and J.O.; supervision, C.R. and E.Z.; project administration, E.Z., F.D. and C.R.; funding acquisition, E.Z. and C.R. All authors have read and agreed to the published version of the manuscript.

Funding

This research was funded by ANID (Agencia Nacional de Investigación y Desarrollo)/Programa/Beca Doctorado Nacional 2022-21221453 to the Doctoral

Program in Agronomy Sciences, Faculty of Agronomy 2021300163 and to the Department of Soil Sciences and Natural Resources, Universidad de Concepción.

Data Availability Statement

Data is contained within the article.

Acknowledgments

We would like to express our gratitude to the staff of the Ranchillo Alto Research Center at the University of Concepción, as well as to the Department of Soils and Natural Resources, particularly to the Spectroscopy Laboratory (Vis-IR) and Sustainable Soil Management department. We extend special thanks to Katherine Rebolledo for her valuable collaboration. We also thank the Department of Forestry, Faculty of Forestry Sciences, and the Doctoral Program in Agronomy Sciences at the University of Concepción. Additionally, we are grateful to the National Agency for Research and Development (ANID) for the funding provided through the National Doctoral Scholarship 2022-21221453 awarded to R.C. This research is part of R.C.'s doctoral thesis, and we thank the Universidad de Concepción for approving its publication.

Conflicts of Interest

The authors declare no conflicts of interest.

Abbreviations

Abbreviation	Description
Mha	million hectares
SPSs	silvopastoral systems
C	carbon
SOC	soil organic carbon
IPCC	Intergovernmental Panel on Climate Change
FAO	Food and Agriculture Organization of the United Nations

SOM	soil organic matter
POM	particulate organic matter
MAOM	matrix-associated organic matter minerals
N	nitrogen
Op	open
SOp	semi-open
SC	semi-closed
Ctr	control
WFPS	water-filled pore space
BD	bulk density
PD	particle density
OM	organic matter
P	phosphorous
K^+	potassium
ECEC	effective cation exchange capacity
Al_{EXCH}	exchangeable aluminum
Ca^{2+}_{EXCH}	exchangeable calcium
Mg^{2+}_{EXCH}	exchangeable magnesium
NH_4^+	ammonium
NO_3^-	nitrate
K^+_{EXCH}	exchangeable potassium
Na^+_{EXCH}	exchangeable sodium

Al_{SAT}	aluminum saturation
K^{+}_{SAT}	potassium saturation
Ca^{2+}_{SAT}	calcium saturation
Mg^{2+}_{SAT}	magnesium saturation
FDA	fluorescein diacetate
CO_2	carbon dioxide
TC	total carbon
Cox	oxidizable carbon
TOC	total organic carbon
Cnox	non-oxidizable carbon
C stock	carbon stock
PyC	pyrogenic carbon
	C:N ratio

C/N

Appendix A

Table A 2. Chemical properties of soil under different open canopy levels and depths.

Supplementary results of **Table 3**.

Condition/ Depths	NH_4^+	NO_3^-	K^+_{EXCH}	Na^+_{EXCH}	Al_{SAT}	K^+_{SAT}	Ca^{2+}_{SAT}	Mg^{2+}_{SAT}
Ctr (0–30)	[illegible] ± 0.07	14.7 ± 4.88	0.28 ± 1.34	0.07 ± 0.00	3.85 ± 2.19	8.64 ± 2.77	70.79 ± 8.49	13.75 ± 2.04
Ctr (30–60)	[illegible] ± 0.00	5.90 ± 3.18	0.10 ± 0.59	0.07 ± 0.00	2.20 ± 0.43	8.72 ± 3.78	64.84 ± 1.32	17.24 ± 2.29
OP (0–30)	[illegible] ± 0.05	11.60 ± 0.05	0.23 ± 0.05	0.04 ± 0.05	9.40 ± 0.05	12.54 ± 0.05	63.41 ± 0.05	12.85 ± 0.05
OP (30–60)	[illegible] ± 0.04	5.80 ± 0.04	0.12 ± 0.04	0.04 ± 0.04	8.69 ± 0.04	13.60 ± 0.04	54.12 ± 0.04	17.81 ± 0.04
SOp (0–30)	[illegible] ± 1.87	7.77 ± 1.87	0.16 ± 0.05	0.03 ± 0.00	5.14 ± 3.49	8.51 ± 2.64	71.12 ± 10.20	12.89 ± 2.77
SOp (30–60)	6.47 ± 1.83	4.37 ± 1.83	0.12 ± 0.06	0.07 ± 0.00	1.46 ± 0.53	9.88 ± 1.77	65.83 ± 6.86	15.82 ± 4.46
SC (0–30)	[illegible] ± 3.03	14.7 ± 3.03	0.23 ± 0.05	0.04 ± 0.00	6.98 ± 7.49	7.87 ± 2.51	71.37 ± 11.92	12.30 ± 1.63
SC (30–60)	[illegible] ± 0.37	10.07 ± 0.37	0.21 ± 0.10	0.07 ± 0.03	8.08 ± 8.28	11.28 ± 1.88	61.77 ± 14.10	14.54 ± 2.89

Appendix B

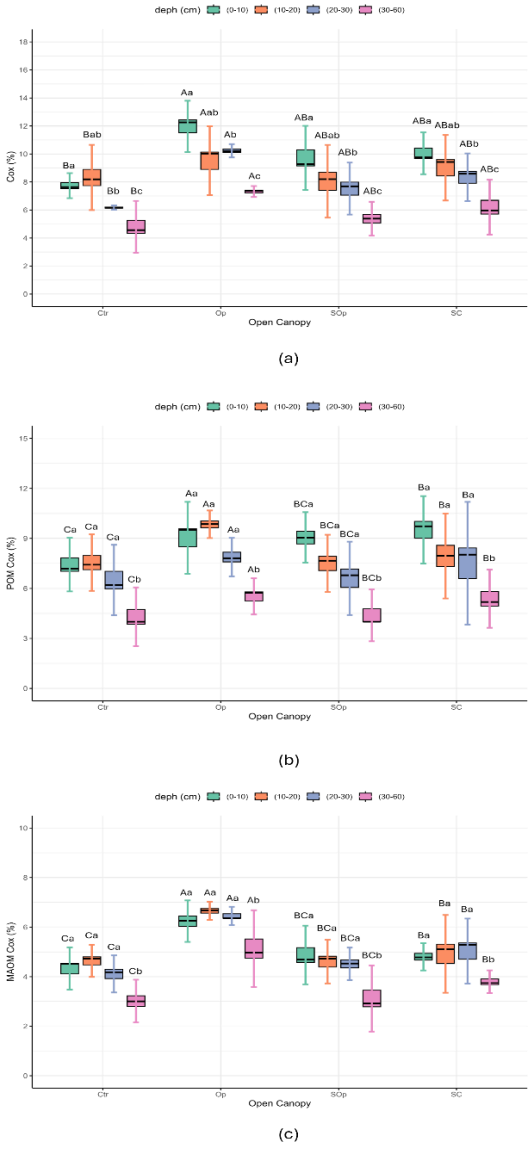

Figure A 0-1. (**a**) oxidizable carbon (%); (**b**) oxidizable carbon in the particulate fraction (POM Cox %); and (**c**) oxidizable carbon in the mineral fraction (MAOM Cox %) as a function of the factors of canopy openness (Ctr: control; Op: open; SOp: semi-open; SC: semi-closed) and soil depth (0–10; 10–20; 20–30; and 30–60 cm). Uppercase letters indicate significant differences between canopy conditions, while lowercase letters indicate significant differences between soil depths. Differences were considered significant according to Tukey's test ($p < 0.05$).

References

1. Casanova, M.; Salazar, O.; Seguel, O.; Luzio, W. Human-Induced Soil Degradation in Chile. In The Soils of Chile; World Soils Book Series; Springer: Dordrecht, The Netherlands, 2013; pp. 121–158. ISBN 978-94-007-5948-0. [Google Scholar]
2. Flores, J.P.; Martínez, E.; Espinosa, M.; Avendaño, P.; Ahumada, I.; Henríquez, G.; Torres, P. Determinación de La Erosión Actual y Potencial de Los Suelos de Chile: Región Del Bío Bío. Síntesis de Resultados. (Pub. Ciren N° 148). 2010. Available online: https://bibliotecadigital.ciren.cl/items/114f1067-d6bb-4e0f-aa24-b259ad15e901 (accessed on 27 March 2025).
3. Lara, A.; Solari, M.E.; Prieto, M.D.R.; Peña, M.P. Reconstrucción de La Cobertura de La Vegetación y Uso Del Suelo Hacia 1550 y Sus Cambios a 2007 En La Ecorregión de Los Bosques Valdivianos Lluviosos de Chile (35°–43° 30′ S). Bosque Valdivia **2012**, 33, 3–4. [Google Scholar] [CrossRef]
4. Nair, P.K.R.; Kumar, B.M.; Nair, V.D. Carbon Sequestration and Climate Change Mitigation. In An Introduction to Agroforestry; Springer International Publishing: Cham, Switzerland, 2021; pp. 487–537. ISBN 978-3-030-75357-3. [Google Scholar]
5. Udawatta, R.P.; Gantzer, C.J.; Jose, S. Agroforestry Practices and Soil Ecosystem Services. In Soil Health and Intensification of Agroecosytems; Elsevier: Amsterdam, The Netherlands, 2017; pp. 305–333. ISBN 978-0-12-805317-1. [Google Scholar]
6. Yasin, G.; Nawaz, M.F.; Sinha, D.; Qadir, I.; Altaf, M.; Ashraf, M.N.; Soufan, W.; Mammadov, A.; Zulfiqar, U.; Rahman, S.U. Agroforestry Status, Services, and Its Role in Climate Change Mitigation through Carbon Sequestration under Semi-Arid Conditions. Trees For. People **2024**, 17, 100640. [Google Scholar] [CrossRef]
7. Ramachandran Nair, P.K.; Nair, V.D.; Mohan Kumar, B.; Showalter, J.M. Carbon Sequestration in Agroforestry Systems. In Advances in Agronomy; Elsevier:

Amsterdam, The Netherlands, 2010; Volume 108, pp. 237–307. ISBN 978-0-12-381031-1. [Google Scholar]

8. Ortiz, J.; Dube, F.; Neira, P.; Hernández Valera, R.R.; De Souza Campos, P.M.; Panichini, M.; Pérez-San Martín, A.; Stolpe, N.B.; Zagal, E.; Curaqueo, G. Comparative Study between Silvopastoral and Agroforest Systems on Soil Quality in a Disturbed Native Forest of South-Central Chile. Agronomy **2023**, 13, 2683. [Google Scholar] [CrossRef]
9. IPCC. Summary for Policymakers; IPCC: Geneva, Switzerland, 2019. [Google Scholar]
10. Cai, Z.; Aguilar, F.X. Economic Valuation of Agroforestry Ecosystem Services. In Agroforestry and Ecosystem Services; Udawatta, R.P., Jose, S., Eds.; Springer International Publishing: Cham, Switzerland, 2021; pp. 477–494. ISBN 978-3-030-80059-8. [Google Scholar]
11. Kay, S.; Graves, A.; Palma, J.H.N.; Moreno, G.; Roces-Díaz, J.V.; Aviron, S.; Chouvardas, D.; Crous-Duran, J.; Ferreiro-Domínguez, N.; García De Jalón, S.; et al. Agroforestry Is Paying off—Economic Evaluation of Ecosystem Services in European Landscapes with and without Agroforestry Systems. Ecosyst. Serv. **2019**, 36, 100896. [Google Scholar] [CrossRef]
12. FAO. Scaling up Agroecology to Achieve the Sustainable Development Goals. In Proceedings of the 2nd FAO International Symposium on Agroecology, Rome, Italy, 3–5 April 2018; FAO: Rome, Italy, 2019. [Google Scholar]
13. Smith, P.; Cotrufo, M.F.; Rumpel, C.; Paustian, K.; Kuikman, P.J.; Elliott, J.A.; McDowell, R.; Griffiths, R.I.; Asakawa, S.; Bustamante, M.; et al. Biogeochemical Cycles and Biodiversity as Key Drivers of Ecosystem Services Provided by Soils. Soil **2015**, 1, 665–685. [Google Scholar] [CrossRef]
14. Voltr, V.; Menšík, L.; Hlisnikovský, L.; Hruška, M.; Pokorný, E.; Pospíšilová, L. The Soil Organic Matter in Connection with Soil Properties and Soil Inputs. Agronomy **2021**, 11, 779. [Google Scholar] [CrossRef]
15. Hayes, M.H.B.; Swift, R.S. An Appreciation of the Contribution of Frank Stevenson to the Advancement of Studies of Soil Organic Matter and Humic

Substances. J. Soils Sediments **2018**, 18, 1212–1231. [Google Scholar] [CrossRef]

16. Cambardella, C.A.; Elliott, E.T. Particulate Soil Organic-Matter Changes across a Grassland Cultivation Sequence. Soil Sci. Soc. Am. J. **1992**, 56, 777–783. [Google Scholar] [CrossRef]
17. Cotrufo, M.F.; Ranalli, M.G.; Haddix, M.L.; Six, J.; Lugato, E. Soil Carbon Storage Informed by Particulate and Mineral-Associated Organic Matter. Nat. Geosci. **2019**, 12, 989–994. [Google Scholar] [CrossRef]
18. Follett, R.F.; Stewart, C.E.; Pruessner, E.G.; Kimble Retired, J.M. Great Plains Climate and Land-Use Effects on Soil Organic Carbon. Soil Sci. Soc. Am. J. **2015**, 79, 261–271. [Google Scholar] [CrossRef]
19. Heckman, K.; Hicks Pries, C.E.; Lawrence, C.R.; Rasmussen, C.; Crow, S.E.; Hoyt, A.M.; Von Fromm, S.F.; Shi, Z.; Stoner, S.; McGrath, C.; et al. Beyond Bulk: Density Fractions Explain Heterogeneity in Global Soil Carbon Abundance and Persistence. Glob. Change Biol. **2022**, 28, 1178–1196. [Google Scholar] [CrossRef]
20. Witzgall, K.; Vidal, A.; Schubert, D.I.; Höschen, C.; Schweizer, S.A.; Buegger, F.; Pouteau, V.; Chenu, C.; Mueller, C.W. Particulate Organic Matter as a Functional Soil Component for Persistent Soil Organic Carbon. Nat. Commun. **2021**, 12, 4115. [Google Scholar] [CrossRef] [PubMed]
21. Lavallee, J.M.; Soong, J.L.; Cotrufo, M.F. Conceptualizing Soil Organic Matter into Particulate and Mineral-associated Forms to Address Global Change in the 21st Century. Glob. Change Biol. **2020**, 26, 261–273. [Google Scholar] [CrossRef]
22. Cotrufo, M.F.; Lavallee, J.M. Soil Organic Matter Formation, Persistence, and Functioning: A Synthesis of Current Understanding to Inform Its Conservation and Regeneration. In Advances in Agronomy; Elsevier: Amsterdam, The Netherlands, 2022; Volume 172, pp. 1–66. ISBN 978-0-323-98953-4. [Google Scholar]

23. Rumpel, C.; Kögel-Knabner, I. Deep Soil Organic Matter—A Key but Poorly Understood Component of Terrestrial C Cycle. Plant Soil **2011**, 338, 143–158. [Google Scholar] [CrossRef]
24. Sandoval, E.; Dorner, F.; Seguel, S.; Cuevas, B.; Rivera, S. Métodos de Análisis Físicos del Suelo. 2012. Available online: https://hdl.handle.net/20.500.14001/59208 (accessed on 27 March 2025).
25. Sadzawka, R.; Carrasco, R.; Adriana, M.; Grez, Z.; Mora, G.; de la Luz, M.; Flores, P.; Neaman, A. Métodos de Análisis Recomendados para los Suelos de Chile. Revisión 2006; SIDALC: Turrialba, Costa Rica, 2006. [Google Scholar]
26. Alef, K. Nitrogen Mineralization in Soils. In Methods Appl. Soil Microbiol. Biochem.; Academic Press: London, UK, 1995; pp. 234–245. [Google Scholar]
27. Tabatabai, M.A. Soil Enzymes. In SSSA Book Series; Weaver, R.W., Angle, S., Bottomley, P., Bezdicek, D., Smith, S., Tabatabai, A., Wollum, A., Eds.; Soil Science Society of America: Madison, WI, USA, 2018; pp. 775–833. ISBN 978-0-89118-865-0. [Google Scholar]
28. Craine, J.M.; Fierer, N.; McLauchlan, K.K. Widespread Coupling between the Rate and Temperature Sensitivity of Organic Matter Decay. Nat. Geosci. **2010**, 3, 854–857. [Google Scholar] [CrossRef]
29. Wright, A.F.; Bailey, J.S. Organic Carbon, Total Carbon, and Total Nitrogen Determinations in Soils of Variable Calcium Carbonate Contents Using a Leco CN-2000 Dry Combustion Analyzer. Commun. Soil Sci. Plant Anal. **2001**, 32, 3243–3258. [Google Scholar] [CrossRef]
30. Gomez, F.; Von Müller, A.; Tarabini, M.; La Manna, L. Resilient Andisols under Silvopastoral Systems. Geoderma **2022**, 418, 115843. [Google Scholar] [CrossRef]
31. Ortiz, J.; Dube, F.; Neira, P.; Panichini, M.; Stolpe, N.B.; Zagal, E.; Martínez-Hernández, P.A. Soil Quality Changes within a (*Nothofagus Obliqua*) Forest Under Silvopastoral Management in the Andes Mountain Range, South Central Chile. Sustainability **2020**, 12, 6815. [Google Scholar] [CrossRef]

32. Nissen, J.; Quiroz, C.; Seguel, O.; Mac Donald, R.; Sch, A.E. Variacion del potencial matrico durante el movimiento de agua en andisoles. Agro Sur **2005**, 33, 36–47. [Google Scholar] [CrossRef]
33. Vásquez, H.V.; Valqui, L.; Bobadilla, L.G.; Arbizu, C.I.; Alegre, J.C.; Maicelo, J.L. Influence of Arboreal Components on the Physical-Chemical Characteristics of the Soil under Four Silvopastoral Systems in Northeastern Peru. Heliyon **2021**, 7, e07725. [Google Scholar] [CrossRef]
34. Doetterl, S.; Stevens, A.; Six, J.; Merckx, R.; Van Oost, K.; Casanova Pinto, M.; Casanova-Katny, A.; Muñoz, C.; Boudin, M.; Zagal Venegas, E.; et al. Soil Carbon Storage Controlled by Interactions between Geochemistry and Climate. Nat. Geosci. **2015**, 8, 780–783. [Google Scholar] [CrossRef]
35. Renwick, L.L.R.; Celedón, A.; Nájera, F.; Fuentes Espoz, J.-P.; Celedón, D.; Arellano, C.; Salazar, O. Integrated Crop-Livestock Farms Have Higher Topsoil Nitrogen and Carbon than Crop-Only Farms in Chilean Mediterranean Climate Volcanic Soils. Agric. Syst. **2025**, 222, 104172. [Google Scholar] [CrossRef]
36. Banerjee, A.; Jhariya, M.K.; Yadav, D.K.; Raj, A. (Eds.) Environmental and Sustainable Development Through Forestry and Other Resources; Apple Academic Press: New York, NY, USA, 2020; ISBN 978-0-429-27602-6. [Google Scholar]
37. Borie, F.; Aguilera, P.; Castillo, C.; Valentine, A.; Seguel, A.; Barea, J.M.; Cornejo, P. Revisiting the Nature of Phosphorus Pools in Chilean Volcanic Soils as a Basis for Arbuscular Mycorrhizal Management in Plant P Acquisition. J. Soil Sci. Plant Nutr. **2019**, 19, 390–401. [Google Scholar] [CrossRef]
38. Lambers, H.; Finnegan, P.M.; Jost, R.; Plaxton, W.C.; Shane, M.W.; Stitt, M. Phosphorus Nutrition in Proteaceae and Beyond. Nat. Plants **2015**, 1, 15109. [Google Scholar] [CrossRef]
39. Poirier, V.; Basile-Doelsch, I.; Balesdent, J.; Borschneck, D.; Whalen, J.K.; Angers, D.A. Organo-Mineral Interactions Are More Important for Organic Matter Retention in Subsoil Than Topsoil. Soil Syst. **2020**, 4, 4. [Google Scholar] [CrossRef]

40. Reyes, F.; Lillo, A.; Ojeda, N.; Reyes, M.; Alvear, M. Efecto de La Exposición y La Toposecuencia Sobre Actividades Biológicas Del Suelo En Bosque Relicto Del Centro-Sur de Chile. Bosque Valdivia **2011**, 32, 255–265. [Google Scholar] [CrossRef]
41. Masebo, N.; Birhane, E.; Takele, S.; Lucena, J.J.; Araceli, P.-S.; Yunta, F.; Belay, Z.; Anjulo, A. Microbial Biomass Carbon Distribution under Agroforestry Practices and Soil Depth Variations in Southern Ethiopia. Agrofor. Syst. **2025**, 99, 56. [Google Scholar] [CrossRef]
42. Lavallee, J.M.; Conant, R.T.; Haddix, M.L.; Follett, R.F.; Bird, M.I.; Paul, E.A. Selective Preservation of Pyrogenic Carbon across Soil Organic Matter Fractions and Its Influence on Calculations of Carbon Mean Residence Times. Geoderma **2019**, 354, 113866. [Google Scholar] [CrossRef]
43. Poblete-Grant, P.; Suazo-Hernández, J.; Condron, L.; Rumpel, C.; Demanet, R.; Malone, S.L.; Mora, M.D.L.L. Soil Available P, Soil Organic Carbon and Aggregation as Affected by Long-Term Poultry Manure Application to Andisols under Pastures in Southern Chile. Geoderma Reg. **2020**, 21, e00271. [Google Scholar] [CrossRef]
44. Crovo, O.; Costa-Reidel, C.D.; Rodríguez, R.; Aburto, F. Livestock grazing reduces soil quality and threatens recovery of a degraded andean araucaria forest. 2021. Authorea **2021**, preprints. [Google Scholar] [CrossRef]
45. Alfaro, M.; Dube, F.; Zagal, E. Soil Quality Indicators in an Andisol under Different Tree Covers in Disturbed *Nothofagus Forests*. Chil. J. Agric. Res. **2018**, 78, 106–116. [Google Scholar] [CrossRef]
46. Batjes, N.H. Total Carbon and Nitrogen in the Soils of the World. Eur. J. Soil Sci. **2014**, 65, 10–21. [Google Scholar] [CrossRef]
47. Katsumi, T. Soil Excavation and Reclamation in Civil Engineering: Environmental Aspects. Soil Sci. Plant Nutr. **2015**, 61, 22–29. [Google Scholar] [CrossRef]

48. Decker, K.L.M.; Boerner, R.E.J. Mass Loss and Nutrient Release from Decomposing Evergreen and Deciduous *Nothofagus* Litters from the Chilean Andes. Austral Ecol. **2006**, 31, 1005–1015. [Google Scholar] [CrossRef]
49. Hall, S.J.; Ye, C.; Weintraub, S.R.; Hockaday, W.C. Molecular Trade-Offs in Soil Organic Carbon Composition at Continental Scale. Nat. Geosci. **2020**, 13, 687–692. [Google Scholar] [CrossRef]
50. Manral, V.; Bargali, K.; Bargali, S.S.; Karki, H.; Chaturvedi, R.K. Seasonal Dynamics of Soil Microbial Biomass C, N and P along an Altitudinal Gradient in Central Himalaya, India. Sustainability **2023**, 15, 1651. [Google Scholar] [CrossRef]
51. Angst, G.; Mueller, K.E.; Nierop, K.G.J.; Simpson, M.J. Plant- or Microbial-Derived? A Review on the Molecular Composition of Stabilized Soil Organic Matter. Soil Biol. Biochem. **2021**, 156, 108189. [Google Scholar] [CrossRef]
52. Hall, S.J.; Silver, W.L. Reducing Conditions, Reactive Metals, and Their Interactions Can Explain Spatial Patterns of Surface Soil Carbon in a Humid Tropical Forest. Biogeochemistry **2015**, 125, 149–165. [Google Scholar] [CrossRef]
53. Poeplau, C.; Don, A.; Six, J.; Kaiser, M.; Benbi, D.; Chenu, C.; Cotrufo, M.F.; Derrien, D.; Gioacchini, P.; Grand, S.; et al. Isolating Organic Carbon Fractions with Varying Turnover Rates in Temperate Agricultural Soils—A Comprehensive Method Comparison. Soil Biol. Biochem. **2018**, 125, 10–26. [Google Scholar] [CrossRef]
54. Yu, W.; Huang, W.; Weintraub-Leff, S.R.; Hall, S.J. Where and Why Do Particulate Organic Matter (POM) and Mineral-Associated Organic Matter (MAOM) Differ among Diverse Soils? Soil Biol. Biochem. **2022**, 172, 108756. [Google Scholar] [CrossRef]
55. Sierra, M.; Martínez, F.J.; Verde, R.; Martín, F.J.; Macías, F. Soil-Carbon Sequestration and Soil-Carbon Fractions, Comparison between Poplar Plantations and Corn Crops in South-Eastern Spain. Soil Tillage Res. **2013**, 130, 1–6. [Google Scholar] [CrossRef]

56. Kraus, T.E.C.; Dahlgren, R.A.; Zasoski, R.J. Tannins in Nutrient Dynamics of Forest Ecosystems—A Review. Plant Soil **2003**, 256, 41–66. [Google Scholar] [CrossRef]
57. Tegelaar, E.W.; De Leeuw, J.W.; Holloway, P.J. Some Mechanisms of Flash Pyrolysis of Naturally Occurring Higher Plant Polyesters. J. Anal. Appl. Pyrolysis **1989**, 15, 289–295. [Google Scholar] [CrossRef]
58. Goering, H.K.; Soest, P.J.V. Forage Fiber Analyses (Apparatus, Reagents, Procedures, and Some Applications); U.S. Agricultural Research Service: Washington, DC, USA, 1970.
59. Wasner, D.; Abramoff, R.; Griepentrog, M.; Venegas, E.Z.; Boeckx, P.; Doetterl, S. The role of climate, mineralogy and stable aggregates for soil organic carbon dynamics along a geoclimatic gradient. Glob. Biogeochem. Cycles **2024**, 38, e2023GB007934. [Google Scholar] [CrossRef]
60. Matus, F.; Salazar, O.; Aburto, F.; Zamorano, D.; Nájera, F.; Jovanović, R.; Guerra, C.; Reyes-Rojas, L.; Seguel, O.; Pfeiffer, M.; et al. Perspective of soil carbon sequestration in Chilean volcanic soils. npj Mater. Sustain. **2024**, 2, 32. [Google Scholar] [CrossRef]

III. CHAPTER II: LITTER QUALITY, MINERAL MATRIX CAPACITY, AND CANOPY STRUCTURE INTERACT TO CONTROL CARBON STABILIZATION IN NATIVE FOREST ANDISOLS

Camila Ramos[1], Erick Zagal[2]*, Salme Timmusk[3], Francis Dube[4], David Contreras[5] Leandro Paulino[6], Juan Ortiz[6], Jean Intriago-Ávila[1] y Juan Pablo Fuentes[7]

[1]Doctoral Program in Agronomy Sciences, Faculty of Agronomy, Universidad de Concepción, Chillán 3812120, Chile

[2]Spectroscopy Laboratory (Vis-IR) and Sustainable Soil Management, Soils and Natural Resources Department, Faculty of Agronomy, University of Concepción, Chillán 3812120, Chile

[3]Department of Forest Mycology and Pathology, Uppsala BioCenter, P.O. Box 7026, SE-75007 Uppsala, Sweden

[4]Department of Silviculture, Faculty of Forest Sciences, University of Concepción, Victoria 631, Concepción 4030000, Chile

[5]Department of Analytical and Inorganic Chemistry, Faculty of Chemical Sciences, University of Concepción, Edmundo Larenas 129, Concepción 4030000, Chile

[6]Soils and Natural Resources Department, Faculty of Agronomy, University of Concepción, Chillán 3812120, Chile

[7]Department of Silviculture and Nature Conservation, Faculty of Forest Sciences and Nature Conservation, University of Chile, Santiago 8820808, Chile

*ezagal@udec.cl

Submitted to Plant and Soil on October 10, 2025.

Abstract.

The quality of leaf litter is a key factor in soil organic matter (SOM) dynamics, but questions remain about how its initial chemistry influences carbon © stabilization in fractions of varying stability. We evaluated the effect of good-quality (GQ) (low C/N ≈ 27) and low-quality (LQ) (high C/N≈ 105) on C stabilization in particulate organic matter (POM) and mineral-associated organic matter (MAOM) in native forest Andisols, under three canopy openings and two depths, through 120-day incubations. Total C and Nitrogen (N), labile and stable fractions, and C use efficiency estimation based on C_MAOM (CUE_MAOM) were determined. Fourier-transform infrared spectroscopy (FTIR) detected chemical shifts during organic matter transformation, while structural equation modeling (SEM) identified key factors controlling CUE_MAOM. Low-quality

(LQ) litter enhanced direct POM→MAOM transfer and stabilization, whereas high-quality (GQ) litter prolonged labile-phase residence, favoring respiratory carbon losses before mineral association. FTIR showed POM enriched in aliphatic signals and MAOM in oxidized carbonyl groups. Canopy opening modulated the effects of substrate quality, and FTIR applied to bulk soil samples exhibited limited sensitivity to substrate changes in the short-term. The results highlight that substrate chemistry, canopy structure, and mineral capacity jointly control C stabilization in native forest Andisols.

Keywords: Substrate quality, carbon efficiency use, soil organic matter stabilization, POM–MAOM fractionation, Carbon and nitrogen dynamics.

1. Introduction.

Soil organic matter (SOM) constitutes the largest terrestrial reservoir of organic carbon (OC), storing approximately 1,500–2,400 Pg Carbon © in the top meter of soils globally and represents a key component of ecosystem resilience to climate change (Georgiou et al. 2022b). Longtime and efficient carbon sequestration in soils compensates CO_2-concentrations in the atmosphere and is the bases for soil organic matter and soil fertility (Timmusk and de-Bashan 2022). This in turn does safeguard soil biodiversity, water retention, nutrient provision and recycling. All of which are crucial to stabilize productivity, enhance resilience and ensure sustainable food production under climate change (Timmusk et al. 2017; Timmusk and de-Bashan 2022).

Traditionally, its stability was explained by the “recalcitrance hypothesis,” which attributed carbon longevity to the chemical composition of plant debris: lignin, cutin, and other molecules with high C/N ratios were considered intrinsically recalcitrant (Thevenot et al. 2010). However, there is growing evidence that C persistence actually depends on microbial activity and its interaction with mineral matrix (Cotrufo et al. 2013; Buckeridge et al. 2022; Tao et al. 2023ª; Manzoni and Cotrufo 2024; Elias et al. 2024). This paradigm shift is reflected in the Microbial Efficiency–Matrix Stabilization (MEMS) framework, which proposes that long-term C stabilization results from two coupled mechanisms: (i) the efficiency microorganisms transform fresh litter into microbial biomass, leaving in the process more stable necromass and (ii) the physicochemical

protection of this stable necromass mediated by mineral matrix (Cotrufo et al. 2013). From this perspective, high-quality litters (low C/N ratio and nutrient-rich) can, paradoxically, generate more stable C, as they more efficiently fuel the microbial pathway leading to mineral-associated organic matter (MAOM), even though they mineralize faster than nutrient-poor litters (Cotrufo et al. 2013; Sokol et al. 2022).

Alongside this conceptual reinterpretation, methods for characterizing SOM have also evolved. Classical chemical fractionations (acid-base extractions, oxidations) that distinguished "humins," "humic acids," and "fulvic acids" have been questioned for altering SOM, also producing analytical artifacts. Currently, physical fractionations (by size and/or density), which isolate fractions with specific characteristics and dynamics such as particulate organic matter (POM) and MAOM, have become more common. However, protocols still lack standardization, making comparisons across studies difficult (Lavallee et al. 2020; Leuthold et al. 2024).

To address this limitation, Lavallee et al. (2020) proposed a physical operational fractionation that separates SOM only into POM and MAOM. This minimal classification facilitates: (i) distinguishing formation pathways (plant debris → POM vs. microbial necromass → MAOM); (ii) assigning residence times (years–decades for POM; decades–centuries for MAOM); and (iii) linking functional indicators (respiration, N mineralization, enzymatic activity) to actual C stabilization (Lavallee et al. 2020).

Fourier transformed infrared spectroscopy (FTIR) has been widely used in soils to characterize organic matter and its transformations (Calderón et al. 2013; Gholizadeh et al. 2013). The DRIFT-FTIR modality has been described as a suitable and non-destructive complement to physical fractionation(Thabit et al. 2024; Walden et al. 2025), as it allows the identification, based on diagnostic absorbance bands (e.g., 2920/2850 cm^{-1} for aliphatic C-H and 1620 cm^{-1} for aromatic C=C), the transformation of plant substrates into microbially processed compounds associated with minerals (Margenot et al. 2023; Thabit et al. 2024). These advances position FTIR spectroscopy as a high-throughput tool for monitoring C-stabilization pathways alongside wet-chemistry based protocols.

Despite conceptual and methodological advances, recent studies qualify and sometimes question this unidirectional view proposed by the MEMS framework (Yu et al. 2022; Elias et al. 2024). The original MEMS formulation assumes a mostly linear progression from plant residues → POM → microbial transformation → MAOM, with limited feedback or cycling of material among pools (Cotrufo et al. 2013; Robertson et al. 2019). However, more recent work, including MEMS 2.0 and the "two-pathway" model of (Zhang et al. 2021) acknowledges that litter-derived material, DOM, microbial by-products and necromass may recycle between particulate, dissolved, and mineral-associated pools before being stabilized (Zhang et al. 2021; Cotrufo and Lavallee 2022).

Most studies evaluating the MEMS framework have focused on large spatial and temporal scales, mainly along climatic gradients and ecosystem transects, where multiple environmental factors can mask or attenuate the signal of substrate quality (Yu et al. 2022; Li et al. 2023). This limits the ability to predict how different leaf litter qualities contribute to the long-term stabilization of C in soils.

In this context, microbial carbon use efficiency (CUE), defined as the fraction of assimilated organic carbon allocated to microbial growth relative to that lost as respiration (CO_2), has emerged a key concept for understanding how litter quality translates into long-term C stabilization. Traditionally, CUE is estimated from microbial growth and respiration rates, but alternative formulas can provide complementary information. In this case, we adopted an approach based on cumulative C fluxes, contrasting the C retained in MAOM with that respired as CO_2 (CUE→MAOM), which directly links microbial processing with stabilization pathways in soils (Manzoni et al. 2012; Geyer et al. 2019). To further unravel the complexity of these processes, we applied structural equation models (SEM) to assess the direct and indirect pathways connecting litter quality, microbial activity, and SOM fractions. SEMs are increasingly used in soil science to capture multivariate relationships between C pools and identify the mechanisms underlying stabilization (Fan et al. 2016; Geyer et al. 2019). This integrative framework allows us to test whether efficient microbial processing of high-

quality litter promotes MAOM formation, while low-quality litter is preferentially retained in POM.

Therefore, the objective of this study is to evaluate how litter quality influences the formation of stable soil organic matter under different canopy openings (OP, SOp, SC) and soil depths (0–30 and 30–60 cm), by incubating two litter-derived substrates with contrasting stoichiometries *Nothofagus obliqua* (C/N ≈ 27) and *Festuca arundinacea* (C/N ≈ 105) in a controlled laboratory experiment. By combining the operational fractionation proposed by (Lavallee et al. 2020) with carbon and nitrogen balances, respiration measurements, FTIR spectroscopy, and a structural equation modeling (SEM) approach, we tested whether high-quality litter promotes more efficient carbon fluxes into MAOM, while low-quality litter leads to greater retention in POM, and how these patterns are modulated by canopy structure and soil depth.

2. Materials and Methods.

2.1 Soil Sampling

The soils used in this study corresponded to “Santa Bárbara” series (typic medial, amorphic, mesic Haploxerands), associated to secondary *Nothofagus sp* native forests at Ñuble Region, Chile. Particularly, studied area is located at Ranchillo Alto state-owned property (37°04′52″ S, 71°39′14″ W; 1,200–2,000 m a.s.l.), with an approximate area of 635 ha, which has been under prolonged degradation processes (Ortiz et al. 2020; Ramos et al. 2025). In 2016, silvopastoral treatments (SPS) were implemented in the northern and southern sectors of the property to restore the ecosystem value of the forest. This study was conducted in the period 2023-2024 and focused on three SPS located in the southern sector, covering 12 ha in total (4 ha each). These SPS represent different levels of canopy openings, defined according to the degree of previous disturbance of the forest. The sites were classified as open (Op) +++, semi-open (SOp) ++ and semi-closed (SC) + previously described by (Ramos et al. 2025). A completely randomized design with three replicates (plots) randomly distributed in each treatment was used for soil sampling. Soil samples were collected from each plot, consisting of five random subsamples taken at two depths: 0–30 cm and 30–60 cm.

Samples were placed in a cool box with ice for transport from the forest to the laboratory, where they were stored at 4 °C. All samples were sieved with a 2 mm stainless steel sieve and then divided into two parts: one was air-dried for subsequent physicochemical analysis, and the other was conditioned at 60 % WFSP for biological analysis. The chemical and physical analyses were carried out at the Laboratory for Soil and Plant Chemical Analysis, and the biological analyses at the Spectroscopy Laboratory (Vis-IR) and Sustainable Soil Management of the Faculty of Agronomy, and FTIR analyses were conducted at the Advanced Oxidation Processes Laboratory, Department of Analytical and Inorganic Chemistry, Faculty of Chemical Sciences, Universidad de Concepcion (UdeC).

2.2 Characterization of Soil Properties

Prior to incubation with plant materials, the soil was characterized in terms of physical, chemical and biological properties.

For physical analyses, bulk density (BD) was determined using the cylinder method. Particle density (PD) was assessed by the pycnometer method and texture was analyzed by the Bouyoucos hydrometer method, all following the methodology described by (Sandoval E. et al. 2012).

Soil chemical analyses, including pH (H_2O; 1:2.5 soil-to-distilled water suspension), organic matter (OM), $N_{(AVAILABLE)}$, P Olsen, effective cation exchange capacity (ECEC), exchangeable Al, Ca, Mg, K, Na (Al_{EXCH}, Ca^{2+}_{EXCH}, Mg^{2+}_{EXCH}, K^{+}_{EXCH}, Na^{+}_{EXCH}), NH_4^+, NO_3^-; Al, K, Ca, and Mg saturation (Al_{SAT}, K^{+}_{SAT}, Ca^{2+}_{SAT} and Mg^{2+}_{SAT}) were performed according to the protocols of (Sadzawka R. et al. 2006).

Total potential enzymatic activity was assessed by fluorescein diacetate (FDA) hydrolysis: 1 g moist soil was incubated with phosphate buffer and FDA at 25 °C for 1 h; acetone was added, samples filtered, and absorbance read at 490 nm (ALEF 1995). β-Glucosidase activity was measured by incubating soil with 25 mM p-nitrophenyl-β-D-glucopyranoside in buffer solution MUB-HCl (pH 6) at 37 °C for 1 h, followed by centrifugation, pH adjustment with $CaCl_2$/THAM-NaOH (pH 12), and reading at 400 nm (Tabatabai 2018). Urease activity was determined following Tabatabai et al. (Tabatabai

and Bremner 1972): 1 g moist soil was incubated with 0.1 M urea in phosphate buffer (pH 7) at 37 °C for 2 h; released NH_4^+ was extracted with 2 M KCl, and quantified by indophenol colorimetry at 630 nm.

For soil respiration, 20 g soil at 60 % WFSP were incubated in sealed 50 mL Falcon tubes (using rubber plugs with septum), at 22 °C for 14 days; on days 3, 5, 7, 10, and 14, headspace was homogenized (1 mL cycling, extraction and reinjection) and gas samples were injected into an NDIR analyzer (LI-820, Li-COR Bioscience) to measure CO_2 emission (Craine et al. 2010) (see also section *2.4* for details).

Detailed results of chemical (Table S1), physical (Table S2) and biological (Table S3) characterization are presented in the supplementary material.

2.3 Sampling and preparation of plant material

Leaves of the five most representative species from studied area were collected and transported to the laboratory in paper bags. There they were washed with distilled water, dried in an oven at 60 °C until constant weight and ground to a fine powder. The pulverized material was analyzed for total C and N, in an elemental analyzer by dry combustion (Truspec CN, LECO, USA) to determine the carbon and nitrogen content (Table S4).

Among the five analyzed litter species (Table S4), *Nothofagus obliqua* (roble) and *Festuca arundinacea* occupy opposite ends of the stoichiometric spectrum. Consequently, we designated *N. obliqua* litterfall as high quality (GQ) and *Festuca* litterfall as low quality (LQ) for subsequent soil incubation treatments.

According to the most recent conceptual frameworks, the chemical quality of leaf litter drives the stabilization pathway of SOM, favoring its incorporation either as particulate organic matter (POM) or as mineral-associated organic matter (MAOM). Based on this approach, we anticipate clearly contrasting responses linking the stoichiometry of roble (GQ) and fescue (LQ) litterfall and with the distribution of C between the POM and MAOM fractions. Table 2 shows expected functional impacts of contrasting litter (festuca vs. roble) on CO_2 dynamics, N cycling, and soil organic matter fractions.

2.3.1 Chemical Analysis of Leaf Litter

The concentrations of P, K, Ca, Mg y S in GQ and LQ leaf litters were determined according to protocols described in Sadzawka etal. [21]: P by molybdate blue colorimetry, K by atomic emission spectrophotometry (EAA), Ca and Mg using atomic absorption spectrophotometry, and S by sulfate turbidimetry. Fe, Mn, Zn, Cu and B micronutrients were quantified by atomic absorption spectrophotometry after HNO_3–$HClO_4$ digestion.

2.4 Soil Incubation Experiment

For soil incubation, 20 g of 60 % WFSP conditioned wet soil was weighed in Falcon tubes (triplicates). Each replicate was duplicated under equal conditions containing 20 g of 60 % WFSP conditioned moist soil: to one was added 0.20 g of high quality plant material (roble litter) and to the other, 0.20 g of low quality plant material (*Festuca spp*. litter) maintaining a soil:litter ratio of 100:1. After carefully mixing the soil with the litter, the tubes were sealed with caps incorporating a septum for gas extraction by precision syringe. Samples were incubated at 22 °C for 120 days under controlled temperature, periodically adjusting humidity to ensure homogeneous conditions. Basal CO_2 emission was determined at days 3, 5, 7, 10, 14, 14, 30, 60, 60, 90, and 120; prior to each measurement, the headspace was homogenized by extracting and reinjecting 1 mL of gas three times, and then 1 mL was taken for injection into a dual-wavelength non-dispersive infrared (NDIR) analyzer Li-820 CO_2 (Li-COR Bioscience, Lincoln, NE, 284 USA) according to the modification described by (Craine et al. 2010).

For each incubated tube (20 g soil + 0.20 g litter), before and after the incubation period the available ammonium (NH_4^+) and nitrate (NO_3-) were quantified. For this purpose, 5 g of wet soil were extracted with 25 mL of K_2SO_4 2 M, shaking for 1 h. The supernatant was obtained by decantation and centrifugation, and the anions were subsequently determined using a modified colorimetric method based on the protocol described by (Robarge et al. 1983).

To quantify the net mineralization or immobilization of inorganic N, two indicators of net N change (ΔN) were calculated according to:

$$\Delta N\_GQ = NpostGQ - Npre \quad (1)$$

$$\Delta N\_LQ = NpostLQ - Npre \quad (2)$$

Where N_{post} = post incubation soil mineral N, and N_{pre} = preincubation soil mineral N. Thus, a negative ΔN indicates net N immobilization by microbial activity during incubation.

2.5 Physical Soil Fractionation

To characterize the organic matter fractions of the soil before and after incubation with both plant materials, a physical soil fractionation was performed following the method described by Lavalle etal. (Leuthold et al. 2024). For this purpose, 5 g of soil previously dried at 60 °C were taken and dispersed in 15 mL of 0.5 % sodium hexametaphosphate solution together with five 1 mm glass beads, stirring on a reciprocating shaker for 18 h. After dispersion, the suspension was washed over a 53 µm mesh sieve; the fraction that passed through the sieve (< 53 µm) was collected as mineral-associated organic matter (MAOM) and the retained material was defined as particulate organic matter (POM).

Total C (TC) and total N were determined in each of the soil samples and their fractions using the dry combustion method based on the Dumas principle (Wright and Bailey 2001). The different samples and their fractions were subjected to chemical oxidation with sodium dichromate dihydrate to determine the oxidizable C (Cox) ratio, following the Walkley-Black method (Sadzawka R. et al. 2006). Since there is no inorganic C in this volcanic soil, TC = total organic carbon (TOC). Non-oxidizable carbon (Cnox) was determined by the difference between TC and Cox (Cnox = TOC - Cox).

2.6 Stabilization-Oriented CUE Estimate (CUE_MAOM)

In the literature, microbial carbon use efficiency (CUE) is commonly estimated using isotopic tracers that quantify growth relative to respiration(Manzoni et al. 2012; Hu et al. 2025). Since our goal was to explicitly link microbial processing with mineral stabilization, we used a stabilization-oriented proxy, called CUE_MAOM, defined as the fraction of processed C that is stabilized as MAOM relative to the sum of stabilized carbon and respired carbon:

$$CUE\_MAOM = \frac{C\_MAOM}{C_{MAOM} + Cresp} \quad (3)$$

C-MAOM was calculated based on the relative contribution of MAOM to total soil mass and its C concentration:

$$\text{MAOM\_C} = \text{MAOM\_C}\ (\%) \times \text{MAOM mass proportion}\ (\text{g}) \quad (4)$$

Respiratory C was estimated from the CO_2 accumulated during incubation, converted to C equivalents:

$$Cresp = mg\ \text{CO}^2 acum^* 0.2727 \quad (5)$$

This stabilization-oriented approach complements the classical estimation of CUE using isotopes, as it focuses on the fate of microbially processed C within the MEMS framework, highlighting the balance between mineral association and respiratory losses.

2.7 Soil Organic Matter Characterization by FTIR

After incubation, the samples with the different plant materials and their POM and MAOM fractions were analyzed by FTIR to detect changes in functional groups, for example, the intensity of bands associated with C-O, C=O bonds or aromatic features reflecting chemical transformations induced by microbial decomposition. Fourier transform infrared (FTIR) spectra were acquired on a PerkinElmer Spectrum Two spectrometer equipped with ZnSe ATR accessory. Each dry sample (approx. 2 mg) was deposited directly on the ATR crystal, and 32 scans were recorded in the range of 4 000 to 400 cm-¹ with 4 cm-¹ resolution. Baseline correction and normalization of the band intensity centered at 1 650 cm^{-1} was applied for data processing using Spectrum™ v.10 software (PerkinElmer) (Lei et al. 2023) .

2.8 Statistical Analysis

The assumptions of normality of residuals and homogeneity of variances were verified using the Shapiro-Wilk and Levene tests, respectively.

To evaluate the main effects and interactions between the factors canopy opening (OP, SOp, SC), sampling depth (0-30 and 30-60 cm) and incubation phase (Pre-incubation, Post GQ and Post LQ), a three-way ANOVA factorial model (opening × depth ×

incubation) was used, applying type III sums of squares using the Anova function of the R's car package.

Subsequently, to identify significant differences between the levels of each factor, multiple comparisons were performed using Tukey's test. The estimated/adjusted marginal means (emmeans) and their confidence intervals were calculated with the emmeans package, generating homogeneous groups using the cld function.

In addition, in order to explore significant relationships between key variables such as chemical quality of plant material (C:N ratio), cumulative CO_2 emissions, degree of nitrogen immobilization or mineralization, as well as carbon and nitrogen distribution between organic matter fractions (POM and MAOM), correlation analyses were performed using Pearson's correlation coefficient, considering significant those values with $p < 0.05$.

Structural equation models (SEM) were adjusted separately for each litter quality (high/low) to evaluate the pathways proposed by the MEMS framework. The models were estimated using the lavaan package, considering carbon use efficiency (CUE) as an endogenous variable and POM_C, MAOM_C, Cox, C/N_POM, and C/N_MAOM as predictors. Based on the standardized path coefficients (β), adjacency matrices were constructed and visualized as networks using the qgraph package. In these representations, the thickness and color of the edges encode the magnitude (|β|) and sign of the relationships, respectively, while insignificant paths ($p \geq 0.05$) were attenuated.

To evaluate differences in functional composition detected by FTIR, for each individual spectrum we calculated the average relative absorbance in three predefined functional bands: aliphatic (2800–3000 cm^{-1}), carbonyl (1600–1700 cm^{-1}), and "aromatic" (1000–1200 cm^{-1}), averaging the signal within each wavelength range (individual spectra were included in the Supplementary Material). From these averages, we obtained the functional ratios Aromatic/Aliphatic and Carbonyl/Aliphatic per sample. For each combination of fraction (total soil, POM, MAOM) and band or ratio, we compared high vs. low litter quality treatments using one-way ANOVA. Normality was tested (Shapiro–Wilk) and p-values were adjusted by Bonferroni for multiple comparisons.

All statistical analyses were performed in R (version 4.5.1; R Core Team, 2024) using several specialized packages. Specifically, the car package (Fox, John; Weisberg, Sanford 2019) was used for factorial ANOVA, the emmeans package (Lenth, Russell V.) for estimated marginal means and post-hoc Tukey comparisons, and the lavaan package (Rosseel 2012) for structural equation modeling. Network visualization based on standardized path coefficients was performed using the qgraph package (Epskamp et al. 2012).

3. Results.

3.1 Chemical and Nutritional Profiles of Experimental Litters

Table 1 shows the macro- and micronutritional composition of the two contrasting leaf litter samples selected for incubation. Letters indicate significant differences between litters ($p < 0.05$). The high-quality leaf litter (*Nothofagus obliqua*, GQ) showed significantly higher concentrations of most of the macronutrients and micronutrients analyzed. Among the macronutrients, the N content (1.90 ± 0.06%) was much higher than that of the LQ litter, and like Ca and K, it showed significant differences ($p < 0.05$), while Mg showed no differences ($p > 0.05$). Among the micronutrients, Fe, Mn, and Zn were significantly higher in GQ leaf litter ($p < 0.05$), while S and P did not vary significantly ($p > 0.05$), suggesting greater homogeneity in these elements between the two species.

Table 1. Macro- and micronutrient composition (dry-weight basis) of the contrasting litter types used in the incubation experiment: high-quality *Nothofagus obliqua* litter ("GQ", low C/N) versus low-quality litter ("LQ", high C/N).

Nutrient	High-quality litter (GQ)	Low-quality litter (LQ)
Carbon (C)*	52.6± 0.12a	48.3± 0.17b
Nitrogen (N)*	1.90 ± 0.06a	0.42 ± 0.01b
Phosphorus (P)*	0.11 ± 0.26a	0.04 ± 0.01a
Potassium (K)*	0.64 ± 0.02a	0.32 ± 0.01b
Calcium (Ca)*	0.71 ± 0.01a	0.25 ± 0.03b
Magnesium (Mg)*	0.12 ± 0.01a	0.08 ± 0.01a
Iron (Fe)**	139.00 ± 0.58a	116.00 ± 1.15b
Manganese (Mn)**	340.00 ± 1.15a	69.50 ± 0.87b
Zinc (Zn)**	32.00 ± 0.29a	5.50 ± 0.29b
Copper (Cu)**	5.00 ± 0.06a	1.50 ± 0.06b
Sulfur (S)*	0.18 ± 0.01a	0.15 ± 0.01a
Boron (B)**	27.50 ± 0.29a	6.30 ± 0.17b

*Macronutrients are expressed in %, **micronutrients in mg kg^{-1}. GQ = good-quality litter (low C/N); LQ = low-quality litter (high C/N) (dry-weight basis). Values are means ± standard error (n = 3). Different letters within a row denote significant differences between GQ and LQ litters according to an independent t-test ($p < 0.05$).

3.2 Time-Integrated CO_2 Efflux During Incubation

Cumulative CO_2 fluxes during the 120 days of incubation showed highly significant effects of depth, litter quality, and canopy openness (Table S5). Cumulative CO_2 fluxes (Figure 1) showed a rapid decomposition phase in the first 15 d, followed by a plateau until day 120 of incubation. Throughout the period, GQ released more CO_2 than LQ, but the greatest difference was observed under SOp canopies, followed by SC. For the surface layer (0–30 cm), the differences between GQ and LQ were most pronounced under all three openness conditions. This trend suggests a combined effect of plant material quality and canopy degradation/openness conditions at each site on soil microbial activity and respiration (Table S5). At depth (30–60 cm), although CO_2 fluxes were lower compared to the surface layer, the general trend was maintained that treatments with GQ showed higher accumulated emissions.

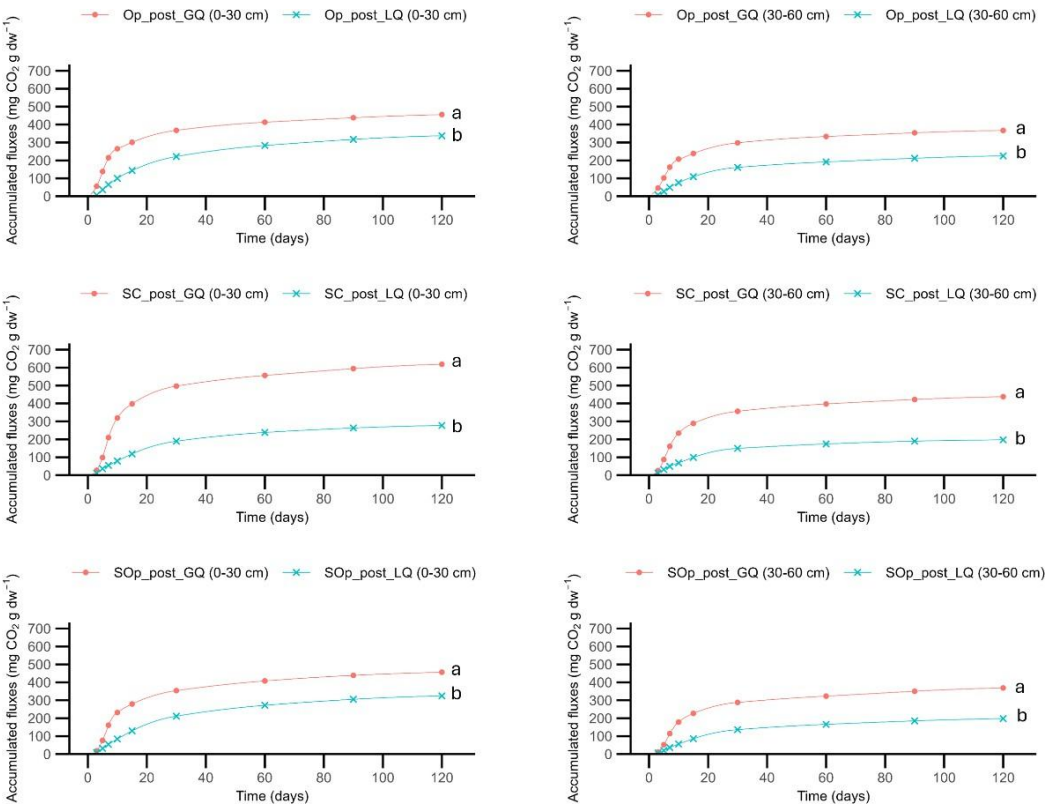

Fig.1. Cumulative CO_2 fluxes (mg CO_2 g dw^{-1}) during 120 days of incubation for soils at two depths (0–30 and 30–60 cm) and three canopy opening conditions (Op: open, SC: semi-closed and SOp: semi-open), incubated with good quality (GQ) and poor quality (LQ) plant material. The circle symbols "●" for GQ and the "×" symbols for LQ mark the reading days (3, 5, 7, 10, 15, 30, 60, 90, and 120).

3.3 Decomposition Kinetics of GQ and LQ Leaf Litters.

The accumulated CO_2 respiration data were adjusted using a two-compartment decomposition model (see supplementary material , Eq. S1), which separates a labile fraction (C_1) and a more stable or slow fraction (C_2), with their respective decomposition constants (k_1 and k_2)(Paul et al. 1999). The values obtained for each treatment are presented in Table 2.

In general, treatments with GQ showed higher values of C_1 and C_2, indicating a greater amount of potentially decomposable C, both in the fast and slow fractions. In the SC condition (0–30 cm) with GQ, one of the highest values of C_1 (318.9 ± 47.8 mg C g dw^{-1}) and C_2 (299.7 ± 18.2 mg C g dw^{-1}) was observed, along with a constant k_1 of

0.116 ± 0.003 day⁻¹, suggesting a rapid initial release of CO_2. This trend was maintained at depth (30–60 cm), although with lower values of available C. In contrast, LQ treatments showed reduced C_1 values, especially in the deep layer. For example, in SOp (30–60 cm), C_1 was 56.1 ± 8.1 mg C kg⁻¹, with a much lower initial release than GQ (178.1 ± 25.2 mg C kg⁻¹). This indicates a lower initial availability of labile C in low-quality residues.

Table 2. Cumulative CO_2 values (mg CO_2 g dw⁻¹) of labile (C_1) and stable (C_2) carbon fractions and their respective rate constants (k_1 and k_2; day^{-1}), on day 120 of incubation (post) in soils at two depths (0–30 and 30–60 cm), under three canopy opening conditions (Op: open, SOp: semi-open, SC: semi-closed), incubated with good quality (GQ) and low quality (LQ) plant material. Values are the means of replicates (n=3).

Tratamiento	C_1	C_2	k_1	k_2	R^2
Op_GQ (0-30)	265.2±84.5	190.5±29.8	0.14±0.01	0.027±0.003	0.986±0.006
Op_GQ (30-60)	207.3±20.4	159.8±10.1	0.13±0.01	0.028±0.003	0.987±0.008
Op_LQ (0-30)	100.0±5.5	237.4±11.1	0.06±0.01	0.028±0.002	0.993±0.001
Op_LQ (30-60)	75.9±5.9	149.3±18.6	0.09±0.01	0.028±0.002	0.986±0.005
SC_GQ (0-30)	318.8±47.7	299.7±18.2	0.12±0.01	0.03±0.002	0.974±0.006
SC_GQ (30-60)	234.4±14.5	203.3±35.3	0.12±0.01	0.031±0.005	0.976±0.002
SC_LQ (0-30)	79.1±12.6	198.0±89.9	0.06±0.02	0.033±0.006	0.993±0.002
SC_LQ (30-60)	68.7±6.7	128.4±3.8	0.08±0.01	0.033±0.004	0.989±0.007
SOp_GQ (0-30)	231.7 ±23.2	224.8±30.5	0.11±0.0	0.028±0.001	0.98 ±0.003
SOp_GQ (30-60)	178.1±25.2	190.7±35.4	0.11±0.01	0.028±0.003	0.972±0.002
SOp_LQ (0-30)	84.2 ± 16.7	240.3 ± 44.8	0.05±0.01	0.029±0.005	0.992±0.002
SOp_LQ (30-60)	56.1 ± 8.1	141.7 ± 26.7	0.07± 0.01	0.028±0.003	0.988±0.0

Values for rapid decomposition constants (k_1) were generally higher in the GQ treatments, ranging from 0.111–0.14 day⁻¹ on the surface, compared to lower values in LQ (0.049–0.086 day⁻¹). In contrast, results from slow fraction constant (k_2), were more stable between treatments, with values between 0.027 and 0.033 day⁻¹, without a clear trend attributable to the type of residue and/or canopy condition. The model fits (R^2) were high in all treatments (≥ 0.972), indicating an excellent ability of the two-

compartment model to represent the decomposition dynamics observed in the incubation.

3.4 Nitrogen Mineralization and Net N Dynamics

The concentration of inorganic N in the soil showed a general decrease after 120 days of incubation in all treatments, with variations depending on depth, canopy openness, and the quality of the incorporated plant material (Table 3).

When analyzing the difference between mineral N concentrations (NH_4^+ + NO_3^-) before (N_pre) and after (N_post) incubation, we observed that in all treatments the average value of ΔN (ΔN = N_post – N_pre) was less than zero. None of the treatments showed net N mineralization; instead, the soils presented a negative mineral N balance, indicating that inorganic N was not released during incubation but, on the contrary, was immobilized.

Table 3. Mineral nitrogen concentrations before (N_pre) and after incubation (120 d, Npost), with good (GQ) and poor-quality (LQ) plant materials and their net difference (ΔN = N_post – N_pre), for each treatment (n = 3)

Treatment	N_pre	N_post_GQ	N_post_LQ	ΔN GQ	ΔN LQ
Op (0-30)	122.84±10.8	64.76±3.4a	15.23±6.6b	-58.08±5.6a	-107.61±1.3b
Op (30-60)	78.14±3.3	57.07±0.3 a	5.81±5.7b	-21.08±6.8a	-72.33±7.0b
SOp (0-30)	117.47±2.1	71.15±6.9a	16.33±3.4b	-46.32±8.8a	-101.15±6.2b
SOp (30-60)	66.12±3.0	60.56±2.8a	11.73±2.3b	-5.56±1.1a	-54.39±3.8b
SC (0-30)	123.63±9.8	10.17±4.8b	19.80±3.0b	-113.46±4.0b	-103.83±3.5a
SC (30-60)	42.65±11.3	3.63±2.1a	13.67±2.9b	-39.03±2.9a	-28.98±2.0b

Values are mean ± standard error (n = 3) in mg N kg^{-1}. Different letters within a row denote significant differences between plant materials (GQ = good-quality litter; LQ = low-quality litter) for each treatment (paired t-test, $p < 0.05$). N_pre: inorganic N before incubation. N post_GQ and N_post_LQ: inorganic N after incubation with GQ and LQ, respectively. ΔN GQ and ΔN LQ were calculated as (N_post − N_pre); negative values indicate net N immobilization.

In the surface layer (0–30 cm), the greatest reduction in N was observed in soils under SC, with a decrease of 113.46 mg N kg^{-1} in the GQ treatment and 103.83 mg N kg^{-1} in

LQ. This was followed by Op and SOp conditions, which also showed substantial N losses, especially when LQ material was applied, indicating possible more intense microbial immobilization or lower N availability for mineralization. In the deep layer (30–60 cm), N losses were lower in magnitude. Under Op conditions, the decrease was -21.08 mg N kg^{-1} in GQ and -72.33 mg N kg^{-1} in LQ, while in SC, a more marked reduction was observed in GQ (-39.03 mg N kg^{-1}) than in LQ (-28.98 mg N kg^{-1}). The SOp treatment showed the smallest variations at this depth.

3.5 Litter-Driven Alterations in Soil Carbon and Nitrogen Fractions

The three-factor ANOVA (depth × canopy opening × incubation phase) showed that the incorporation of plant material significantly altered all C fractions (C_total, POM-C, MAOM-C, C_ox, and C_nox) and N_total. Of the main effects, depth explained most of the variance: contents were systematically higher at a depth of 0–30 cm than at a depth of 30–60 cm. Canopy openness was also significant, with higher values in Op followed by SOp. The incubation phase mainly affected the labile compartments (POM-C and C_ox) and, to a lesser extent, the organo-mineral fraction (MAOM-C), and had no significant effect on the stable reserve (C_nox).

In the interactions, the only consistently significant term was canopy openness × incubation phase. This interaction showed that the increases induced by both high- and low-quality litter were intensified in the Op and SOp plots, while in SC the effect was smaller or nonexistent. The depth × phase and depth × opening interactions, as well as the triple interaction, did not reach significance in any of the variables, indicating that the response of soil C and N to the addition of fresh biomass depends fundamentally on the combination of canopy opening and temporal substrate quality, rather than on position in the profile when these factors were considered simultaneously.

Adjusted mean comparisons (emmeans) confirm this pattern: both GQ and LQ increased significantly after incubation but did not differ from each other within each combination of opening and depth (Figure 2). Canopy opening established a consistent gradient Op > SOp ≈ SC in all soil C fractions and total N, while changes in C_ox were limited to the surface layer and C_nox remained unchanged, underscoring its

recalcitrant nature, which makes it virtually immune to short-term disturbances, unlike the labile fractions that respond quickly.

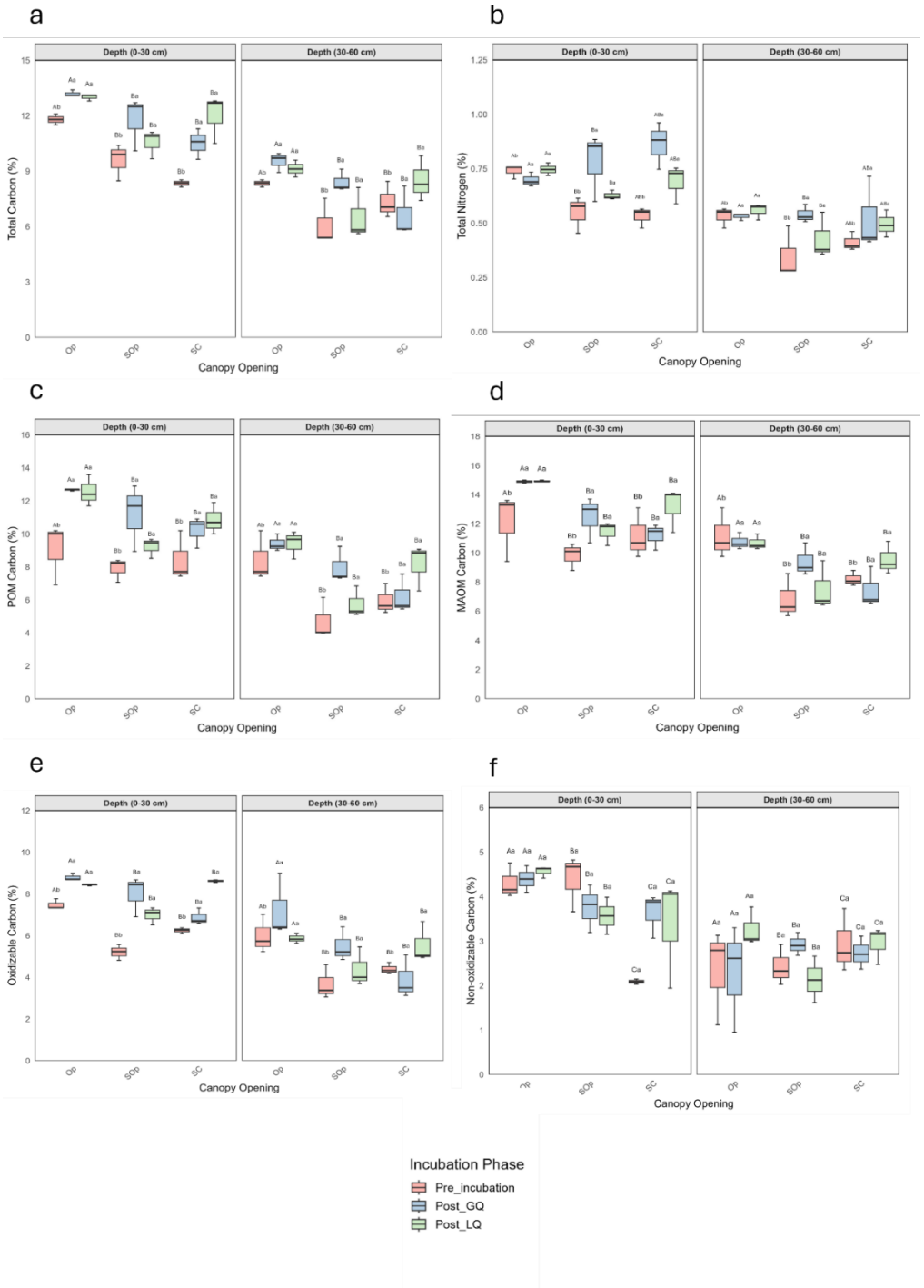

Fig. 2 (a) Total carbon; (b) total nitrogen; (c) particulate-organic-matter carbon (POM Carbon); (d) mineral-associated-organic-matter carbon (MAOM_C); (e)

oxidizable carbon; and (f) non-oxidizable carbon. Box-and-whisker plots depict each fraction across three canopy-opening classes—open (Op), semi-open (SOp) and semi-closed (SC)—at two sampling depths (0–30 cm and 30–60 cm) and three incubation phases: Pre-incubation, Post GQ (high-quality litter) and Post LQ (low-quality litter). Boxes represent the inter-quartile range, the central line the median, and whiskers 1.5 × IQR. Different uppercase letters within the same depth denote significant differences among canopy-opening classes, whereas different lower-case letters indicate significant differences among incubation phases (Tukey test, $p < 0.05$)

3.6 Carbon-Use Efficiency and Piecewise Structural Equation Models (SEM) for GQ and LQ Litter

Microbial carbon use efficiency (CUE_MAOM) ranged from 0.16 ± 0.01 to 0.39 ± 0.02 (Fig. 3a), indicating that microorganisms retained 16% to 39% of the C assimilated as biomass and respired the rest as CO_2. The highest values were recorded in the surface layer (0–30 cm), while the lowest were observed at a depth of 30–60 cm. The overall average CUE depends on the approach used: it reaches an average of 0.59 when using the ^{13}C-labeled substrate approach, while it decreases to 0.34 in the stoichiometric modeling and ^{18}O water tracing approaches (Hu et al. 2025). Our CUE_MAOM results show a decrease, with soil depth.

In all combinations of depth and openness, incubation with LQ produced significantly higher CUE_MAOM than GQ litter. This gap was most pronounced under SC, where CUE_MAOM with LQ was statistically higher than that obtained with GQ; under Op and SOp, the difference was reduced, although it remained significant. In absolute terms, the highest CUE_MAOM values (0.30–0.39) were achieved with LQ, while GQ yielded the lowest figures (0.16–0.30). Interestingly, this pattern suggests that high C/N substrates may induce a more efficient allocation of processed carbon into MAOM despite their lower nutrient content, a trend consistent across canopy conditions.

The correlation matrices (Fig. 3b) show that the addition of the two leaf litter types produced contrasting patterns of C allocation between the labile compartments (POM-C, C_ox) and the more stable compartment (MAOM-C). With GQ litter, POM-C and C_ox were strongly correlated with each other (r = 0.92) and MAOM-C (r =

0.96), while MAOM-C showed an equally high correlation with C_ox (r = 0.94). CUE_MAOM was weakly associated with total C (r = 0.37) and with POM C (r = 0.33). In contrast, with LQ, the link between POM-C and C_ox remained high (r = 0.95), but MAOM-C showed stronger correlations with total C (r = 0.99) and, in turn, with CUE_MAOM (r = 0.80).

The structural equation models (SEM) of the C pools (Fig. 3c) revealed very different flow architectures depending on the quality of the litter. With GQ litter, CUE_MAOM received a direct positive effect from MAOM-C (standardized coefficient = +1.56) and a negative effect from POM-C (–1.11); the C/N ratio of POM acted as a secondary positive driver of CUE_MAOM (+0.70). In turn, MAOM-C was driven by C_ox (+0.28) and POM_C (+0.66). In the LQ litter (C/N ≈ 105), CUE_MAOM was mainly controlled by the C/N of MAOM (+1.92) and MAOM-C (+1.05), while the C/N of POM had a negative influence (–1.28). There was a robust positive path between POM-C and MAOM-C (+0.93); the paths from C_ox were weak and not significant. Overall, the estimated trajectories reflect the correlation patterns shown in Fig. 3b: with nutrient-rich litter, the labile pools (POM-C, C_ox) remain closely linked to MAOM-C, while with nutrient-poor litter, MAOM-C is more closely linked to CUE_MAOM and partially detached from the labile fractions.

a

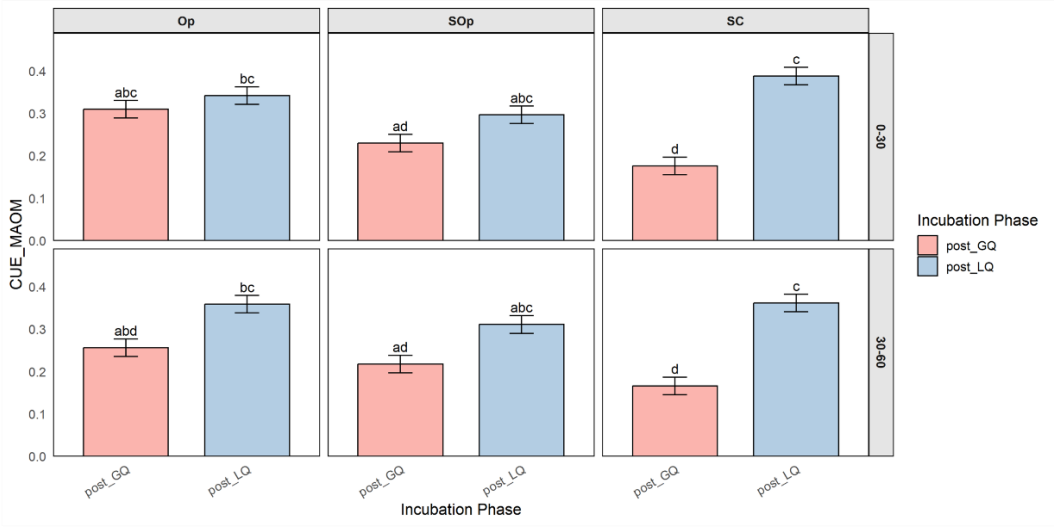
Op
SOp
SC
0-30
30-60
CUE_MAOM
Incubation Phase
post_GQ
post_LQ
abc
bc
ad
abc
d
c
abd
bc
ad
abc
d
c
Incubation Phase
post_GQ
post_LQ

b

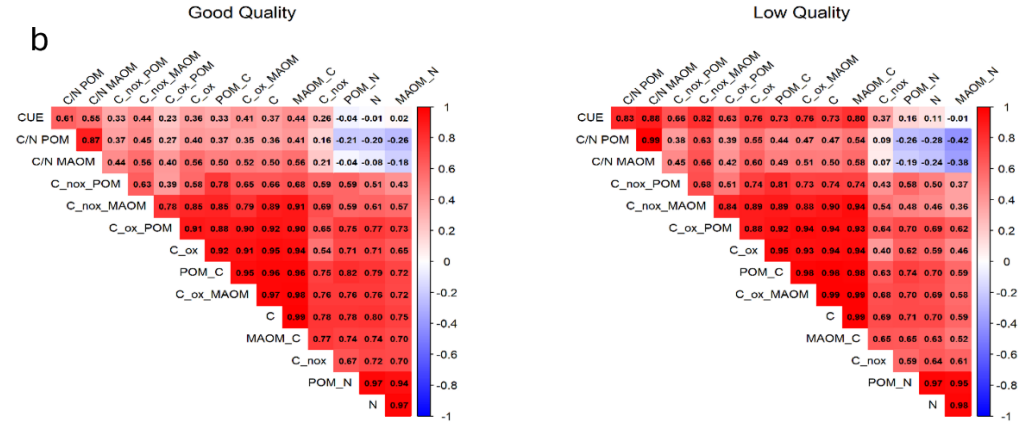
Good Quality
Low Quality
C/N POM
C/N MAOM
C_nox_POM
C_nox_MAOM
C_ox_POM
C_ox
POM_C
C_ox_MAOM
C
MAOM_C
C_nox
POM_N
N
MAOM_N
CUE

c

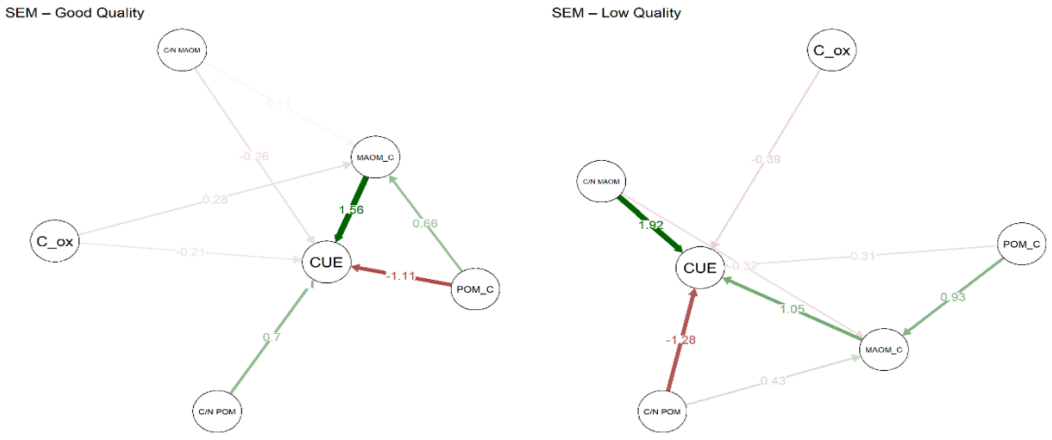
SEM – Good Quality
SEM – Low Quality
C/N MAOM
MAOM_C
C_ox
CUE
POM_C
C/N POM
0.11
-0.26
0.28
1.56
0.66
-0.21
-1.11
0.7
C_ox
C/N MAOM
CUE
POM_C
MAOM_C
C/N POM
-0.39
1.92
-0.32
-0.31
0.93
1.05
-1.28
0.43

Fig. 3 (a) Microbial carbon-use efficiency (CUE) at 0–30 cm and 30–60 cm after incubation with GQ litter (C_post_GQ) and LQ litter (C_post_LQ) under three canopy-opening levels: open (OP), semi-open (SOp) and semi-closed (SC). Bars represent SE. Distinct lower-case letters above the bars denote significant differences among incubation-phase × canopy combinations within the same depth (Tukey, $p < 0.05$). **(b)** Pearson correlation matrices (|r|) between CUE and soil organic-matter pools after 120 days of incubation with good-quality (GQ) litter (left) or low-quality (LQ) litter (right). Red color indicates positive correlations and blue negative correlations; colour intensity scales with |r|. Abbreviations: POM_C, particulate-organic-matter carbon; MAOM_C, mineral-associated-organic-matter carbon; C_ox, oxidizable carbon; C_nox, non-oxidizable carbon; C/N POM and C/N MAOM, C:N ratios of the respective pools; N, total nitrogen. **(c)** Piecewise structural-equation models (SEM) for the GQ (left) and LQ (right) litter treatments. Numbers on arrows indicate standardized path coefficients (β). Higher |β| values represent stronger effects, while smaller values represent weaker effects. Green = positive relationships, red = negative relationships; arrow width is proportional to the effect size. Non-significant paths ($p \geq 0.05$) were excluded. Note: In panels (b)–(c), the label "CUE" is used as shorthand for the CUE_MAOM proxy shown in (a)

3.7 Spectroscopic Fingerprints of Litter Chemistry (FTIR)

The normalized mid-infrared FTIR spectra (Fig. 4) allows us to track the evolution of the main functional groups in the total soil and in the physical fractions. Three diagnostic regions were considered: (a) aliphatic C–H stretching (2,950–2,850 cm^{-1}), (b) carbonyl C=O stretching (~1,720 cm^{-1}), and (c) aromatic C=C stretching (1,600–1,510 cm^{-1}, reference band).

In the total soil, the spectra obtained after incubation with GQ and LQ leaf litter overlap almost completely, indicating that at the whole-soil scale, substrate-specific signatures are largely diluted after 120 days. In the POM fraction, LQ shows slightly higher absorbance in the aliphatic region compared with GQ, suggesting a greater relative contribution of lipid- and wax-type compounds associated with nutrient-poor litter inputs. In contrast, carbonyl and aromatic bands exhibit nearly identical intensities between treatments, indicating no clear substrate-specific signal in these regions.

In the MAOM fraction, absorbance patterns are also very similar between treatments in all functional regions, although a subtle tendency towards higher aliphatic absorbance under LQ is observed, while carbonyl and aromatic signals remain almost unchanged. These results indicate that substrate quality exerts only a minor effect on

the distribution of functional groups, mainly reflected in a modest enrichment of aliphatic structures under LQ conditions.

The processed FTIR spectra allowed us to obtain mean relative absorbance values in the selected functional bands: aliphatic (2800–3000 cm^{-1}), carbonyl (1600–1700 cm^{-1}), and aromatic (1450–1600 cm^{-1}). The box plots show the mean relative absorbance values in these bands for the bulk soil, POM, and MAOM fractions with GQ and LQ incubations (Figure 5).

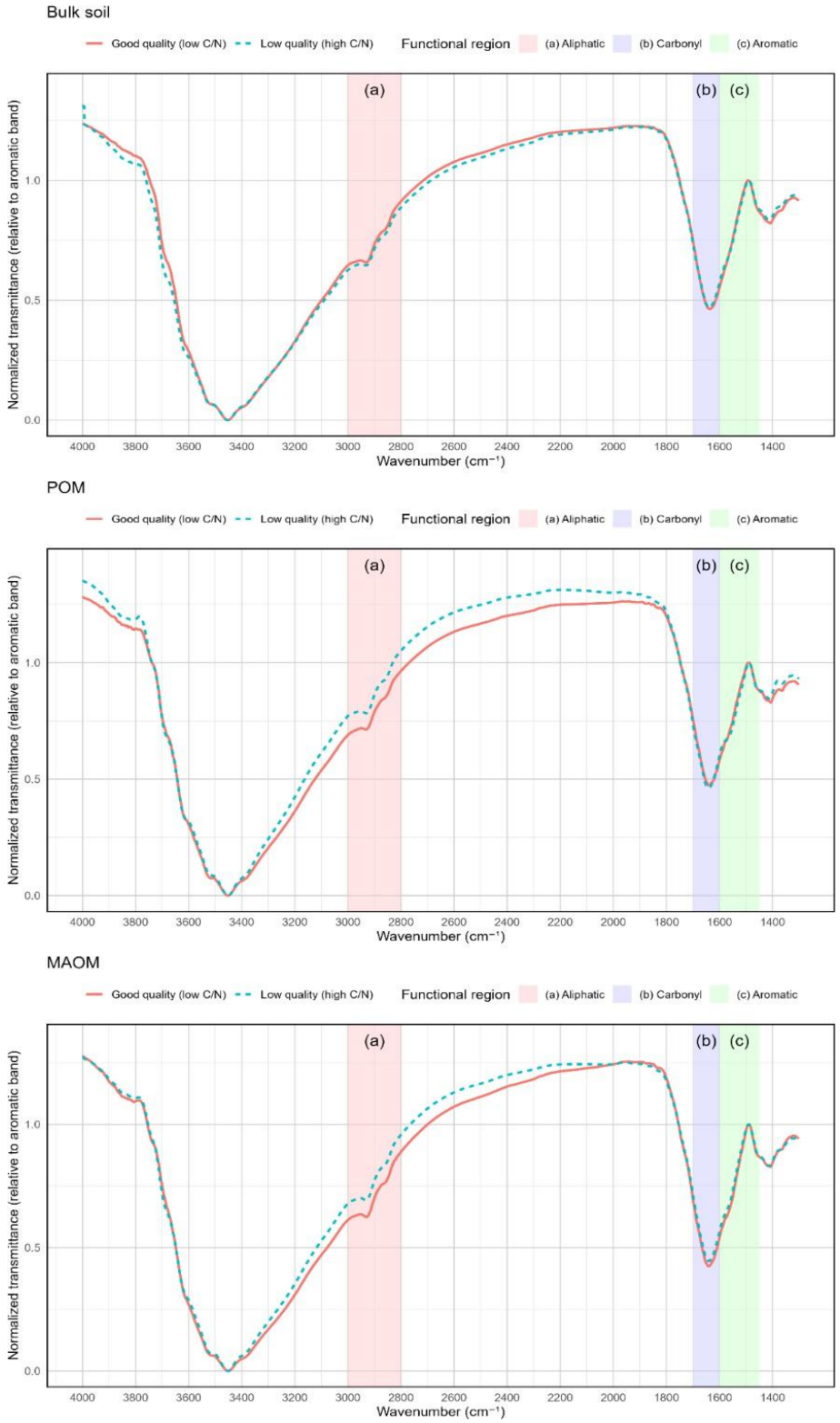

Fig. 4 Normalized FTIR transmittance spectra (relative to the aromatic band, 1450–1600 cm^{-1}) for bulk soil, POM, and MAOM fractions under good-quality (GQ;

low C/N) and low-quality (LQ; high C/N) leaf litter treatments. The shaded regions correspond to functional groups: (a) aliphatic (2800–3000 cm^{-1}, red), (b) carbonyl (1600–1700 cm^{-1}, blue), and (c) aromatic (1450–1600 cm^{-1}, green). The spectra are presented as the average of the normalized spectra for each treatment and fraction

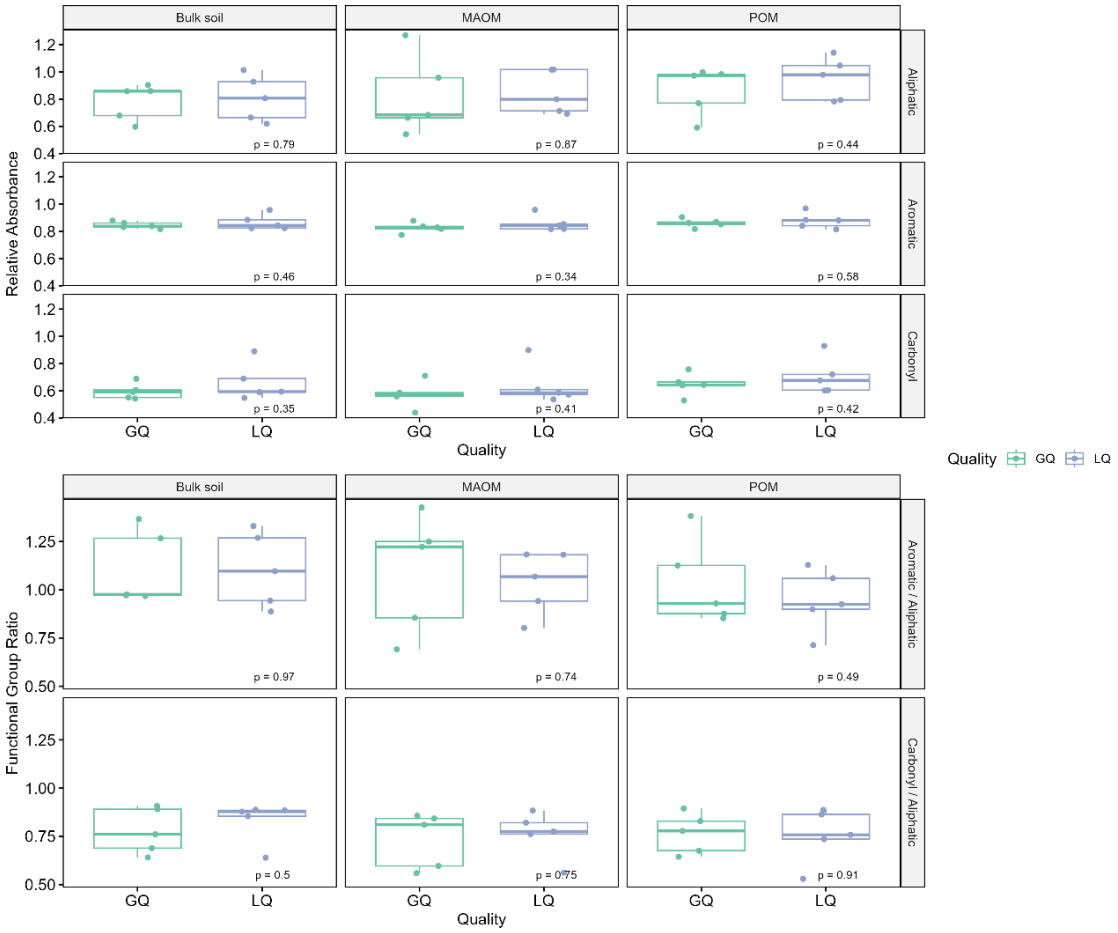

Fig. 5 Relative absorbance (upper panels) and ratios between functional groups (lower panels) in bulk soil, POM, and MAOM fractions under good quality GQ) and low quality (LQ) leaf litter treatments. The relative absorbance values correspond to the normalized transmittance (corrected for baseline and normalized with respect to the aromatic band, 1450–1600 cm^{-1}), averaged within each functional region: aliphatic (2800–3000 cm^{-1}), carbonyl (1600–1700 cm^{-1}), and aromatic (1450–1600 cm^{-1}).

Functional group ratios were calculated as aromatic/aliphatic and carbonyl/aliphatic based on these normalized values. Box plots show individual spectra, means, and p-values obtained from one-way ANOVAs comparing GQ and LQ treatments within each fraction and metric. No statistically significant differences (all $p > 0.05$) in relative

absorbances or functional group ratios were detected between GQ and LQ in any fraction or functional band. Nevertheless, a slight but non-significant tendency toward higher aliphatic absorbance under LQ in the POM fraction was observed, consistent with the normalized spectra shown in Fig. 4. Similarly, marginal increases in the aromatic/aliphatic and carbonyl/aliphatic ratios under LQ were noted, although they were not statistically significant. Overall, these results indicate that litter quality did not produce significant changes in the functional composition of soil organic matter, and any potential effects are subtle and largely confined to the aliphatic domain.

4. Discussion.

The marked stoichiometric differences between GQ and LQ litter can significantly impact decomposition processes and soil nutrient dynamics (Table 1). Previous studies have linked the C/N ratio and nutrient content to microbial activity and mineralization rates (Manzoni et al. 2010; Berg and McClaugherty 2020). GQ had higher concentrations of macronutrients (N, K, Ca, Mg) and micronutrients (Fe, Mn, Zn, Cu, B), along with a lower C/N ratio, suggesting greater availability of labile substrates, which, according to (Cornwell et al. 2008; Berg and McClaugherty 2020), favors faster rates of decomposition and mineralization. In contrast, the lower nutrient concentration in LQ slows down microbial activity and promotes the accumulation of more recalcitrant compounds, such as lignin and polyphenols(Cornwell et al. 2008).

In addition, the chemical profile of GQ, characterized by high levels of Mn (and, to a lesser extent, Zn) (Table 1), has been associated in previous studies with higher rates of decomposition and the generation of microbial compounds capable of stabilizing as MAOM (Neupane et al. 2023; Wang et al. 2025). Mn, as a cofactor of manganese peroxidases, participates in the oxidation of lignin (Alfaro et al. 2018; Ortiz et al. 2020), thus promoting greater initial release of C and a possible increase in the formation of stable fractions, a pattern that was reflected in the accumulated CO_2 respiration fluxes (Figure 1).

The cumulative CO_2 fluxes observed in the GQ leaf litter treatments confirm the essential role of initial nutrient availability in soil microbial activity, especially in the surface layer

(0–30 cm) (Figure 1). Recent studies show that greater nutrient availability drives rapid organic matter turnover and accelerates CO_2 production by soil microorganisms, strengthening the relationship between nutrient availability and microbial respiration (Sun et al. 2025). Our results show a rapid decomposition flash during the first 15 days, followed by a plateau, a classic pattern of decomposition in temperate forests where the initial stage is mainly due to the decomposition of labile components, while later stages degrade more recalcitrant compounds (Kriiska et al. 2021).

Furthermore, the marked increase observed under SC suggests that the quality of the canopy-bound substrate interacts with microclimatic conditions such as greater moisture retention, lower temperature fluctuations, and reduced evaporation to regulate soil respiration rates. These conditions likely create a more stable and favorable microenvironment for decomposer communities, explaining the stronger respiration response compared with more open canopy treatments, consistent with previous studies (Feng et al. 2024). In addition, part of the added carbon may have been mineralized as CO_2 not only from the litter itself but also from native soil organic matter, through a positive priming effect induced by the fresh inputs. This microbial stimulation can accelerate the decomposition of pre-existing SOM, potentially offsetting the net C gains in bulk soil pools (Kuzyakov et al. 2000; Yin et al. 2025).

The parameters of the two-compartment model support this interpretation (Table 2). GQ presented higher values of C_1 and C_2, indicating greater available C in both the fast and slow fractions. The higher rapid decomposition rates (k_1) in GQ, with k_2 constant between treatments, suggest that litter quality predominantly affects the initial phases, while the slow phase is governed by factors such as physicochemical stabilization. This pattern is consistent with previous studies in temperate forests, which show that high-quality litter drives microbial processes that potentially stabilize C, although they do not always reflect an increase in C in the mineral fraction.

Together, these results show that the chemical quality of leaf litter and canopy conditions not only determines decomposition rates and C release but also modulates mineral N fluxes. As shown in Table 3, both leaf litters recorded negative mineral ΔN, indicating net N immobilization during the 120 days of incubation. This differs from expectations, as

greater availability of nutrients such as N, K, and Ca increases microbial efficiency and favors early N mineralization(Dang et al. 2024). However, the observed net immobilization (ΔN < 0) may reflect a negative priming effect, in which microorganisms preferentially assimilate available inorganic N to process the new C inputs, thereby reducing N mineralization from native SOM and retaining N in microbial biomass or organic forms (Kuzyakov et al. 2000; Yin et al. 2025). In our study, immobilization was more pronounced with LQ in open and semi-open sites, probably due to its low N and the consequent microbial need to capture mineral N to balance its C/N ratio; however, even GQ showed negative ΔN, suggesting that the initial demand for N was high enough to retain the available inorganic N in microbial biomass or organic forms, masking any early release.

This pattern (ΔN<0) is probably related to the origin of the soil used for incubation (degraded native forest with agroforestry systems since 2016), where despite the high total N present in the soil (0.9%), no sustained increase in NH_4^+ or NO_3^- has been recorded in the medium to long term. In silvopastoral systems with livestock, higher levels of inorganic N are commonly expected due to the contribution of organic matter and excreta(Sarabia et al. 2020); however, previous studies at the site report net N immobilization over time (Alfaro et al. 2018; Ortiz et al. 2020).

Based on the marked difference in leaf litter chemistry (Table 1) and respiration dynamics (Figure 1), under the MEMS framework, we expected GQ leaf litter to increase total C and N levels more at the end of incubation and show more noticeable increases in MAOM-C and C_ox, while LQ would be expressed mainly in POM-C and C_ox (Cotrufo et al. 2013). The significant increase in C_total, POM-C, and MAOM-C after the incorporation of litter confirms that the input of fresh biomass is a key driver for C accumulation in forest soils, especially in the labile compartments (Dörner et al. 2010; Matus et al. 2014). The greater sensitivity of POM-C and C_ox to the incubation phase suggests that these fractions respond rapidly to pulses of recently added organic matter, in line with studies that indicate that POM acts as a temporary C reservoir before its stabilization or mineralization (Elakiya 2024; Rong et al. 2025). However, although there were changes between Pre and Post incubation, the Post-GQ and Post-LQ treatments

were very similar (Gentile et al. 2011; Lyu et al. 2023); the clearest differences were associated with canopy opening rather than litter quality, as the only significant interaction was canopy opening × incubation phase, suggesting that the response to the addition of fresh biomass is more conditioned by the microclimate associated with canopy structure and the timing of decomposition than by soil depth (Prescott 2010). Such microclimatic variations, together with changes in soil chemical properties under different canopy conditions, can also influence the structure and activity of microbial communities including shifts in the fungi-to-bacteria biomass ratio thereby modifying decomposition pathways and the efficiency of organic matter processing (Six et al. 2006).

Beyond these biological and microclimatic controls, the physical and mineralogical properties of Andisols may have influenced the patterns observed. These soils are highly porous, have low bulk density, and are rich in low-crystallinity minerals, characteristics that favor the formation of carbon associated with the MAOM (Dörner et al. 2010; Matus et al. 2014). Although organo-mineral associations and reactive Al and Fe fractions were not directly evaluated, their presence could explain the convergence between treatments, since carbon stabilization depends not only on substrate quality but also on the matrix's ability to retain microbial products, as proposed by the MEMS framework (Cotrufo et al. 2013). In this regard, future studies should incorporate mineralogical and structural analyses to better understand how these properties interact with substrate quality and microclimate in carbon stabilization in Andisols (Dörner et al. 2022; Matus et al. 2024).

The similarity between Post-GQ and Post-LQ treatments could also reflect compensatory dynamics driven by priming, were rapid decomposition of native SOM offsets fresh C additions, reducing treatment contrasts. Such interactions between new inputs and existing C pools are increasingly recognized as central to understanding soil C stabilization (Kuzyakov et al. 2000; Yin et al. 2025). These results may have been influenced by the following factors: (i) a relatively short incubation period (120 days), which allows rapid responses to be observed in POM-C and C_ox, but is generally insufficient to show sustained changes in MAOM and, especially, in C_nox (Börger et al.

2022; Elias et al. 2024). (ii) proximity to mineral saturation in C-rich Andisols, which limits additional sequestration in MAOM despite new inputs. Most incubation studies designed to evaluate stabilization processes report that detectable changes in MAOM often require longer timescales from several months to multiple years because mineral-associated carbon accumulates slowly through repeated microbial turnover and organo-mineral interactions (Cotrufo et al. 2013; Lavallee et al. 2020). Our 120-day period was therefore intended to capture the early dynamics of decomposition and stabilization, but not the full trajectory of MAOM formation.

In line with fractionation procedure, we estimated an 'alternative' CUE_MAOM focused on C stabilization in the mineral fraction. CUE is usually estimated using isotopic tracers (e.g., incorporation of ^{18}O from water into DNA or partitioning of ^{13}C from labeled substrates between biomass and CO_2) (Hu et al. 2025). The global average microbial CUE in soil depends on the approach: 0.59 for the 13 C-substrate approach, and 0.34 for stoichiometric modeling and for the 18 O-water approaches (Hu et al. 2025). Our results are consistent with previous estimates and decrease with depth, consequently with the limitation of microbial activity in deeper layer (Pei et al. 2025).

The differences observed in CUE_MAOM between the GQ and LQ litters indicate that nutrient availability and substrate stoichiometry modulate the partitioning of processed C between its stabilization in MAOM and its release as CO_2, consistent with the MEMS framework and with the stoichiometric control of CUE described in the literature (Manzoni et al. 2012; Cotrufo et al. 2013). The higher CUE_MAOM observed in LQ, particularly at the surface, is consistent with a *negative priming response* under nutrient-limited conditions, where microbes channel a larger proportion of processed C into stable MAOM rather than respiring it as CO_2 (Soares and Rousk 2019; Yin et al. 2025). Our higher CUE_MAOM values in LQ especially in the surface layer (SC) reflect that a greater fraction of processed C ended up as MAOM relative to accumulated CO_2. This pattern is consistent with recent findings in subtropical forests, where the addition of low-quality litter significantly increased microbial CUE, while high-quality litter had no effect, resulting in greater incorporation of litter C into soil organic matter (Lyu et al. 2023). However, caution is warranted when interpreting this comparison, as our experiment was

conducted under temperate conditions characterized by lower temperatures and higher seasonal moisture variability compared with subtropical sites. Such climatic differences can strongly influence microbial physiology, turnover rates, and C stabilization dynamics, potentially amplifying or dampening CUE responses to litter quality. It is worth noting that our CUE_MAOM was calculated from absolute C_MAOM (as a measure of stabilization efficiency), not from microbial growth (Manzoni et al. 2012; Geyer et al. 2016). Therefore, it does not directly contradict the MEMS framework, which states that stabilization depends jointly on microbial efficiency and mineral matrix capacity (Cotrufo et al. 2013). Figures 3b–c show that substrate stoichiometry and flows between organic fractions (POM ↔ MAOM) modulate CUE_MAOM differently depending on litter quality. In LQ, CUE_MAOM was strongly related to the C/N ratio and MAOM_C, and SEM showed dominant pathways from both variables to CUE_MAOM, indicating a close coupling between N limitation and direct transfer to MAOM. In GQ, although MAOM_C maintained a positive effect on CUE, the feeding of MAOM C by the labile fractions POM_C and Cox suggests that part of the C remains longer in labile fractions before stabilizing, which increases respiratory losses. Thus, CUE_MAOM in GQ depends more on C stabilized in MAOM than on C retained in POM, but with greater prior recirculation, in line with the observations of Elias et al. (2024), where high substrate quality does not always translate into more efficient MAOM formation. This pattern is not consistent with the original MEMS framework (Cotrufo et al. 2013), which proposed mainly unidirectional flows from POM or litter to MAOM, but it is consistent with later concepts that incorporate dynamic transfer between fractions and C recirculation between labile and stable forms before final stabilization (Cotrufo et al. 2015; Sokol et al. 2019; Lavallee et al. 2020).and it is also a more holistic interpretation of C dynamics, since environmental conditions and other components of the ecosystems were incorporated in the analysis.

FTIR spectra normalized to the aromatic band shows that convergence in bulk soil (Fig. 4ª) is consistent with our C results (Fig. 2ª). This is to be expected because FTIR in bulk soil captures relative proportions and tends to attenuate subtle changes in complex matrices (Parikh et al. 2014; Margenot et al. 2023). In POM (Fig. 4b), a greater relative contribution of aliphatic signals (≈3000–2800 cm^{-1}) was observed compared to aromatic

signals, consistent with fresher and more labile plant residues(Parikh et al. 2014; Margenot et al. 2023). In MAOM (Fig. 4c), on the other hand, the carbonyl region (≈1700–1600 cm^{-1}) was enhanced, indicative of more oxidized carboxyl and amide groups, which have a high affinity for mineral surfaces and favor the formation of stable organo-mineral associations (Volkov et al. 2021). This set of fingerprints (↑carbonyl/aromatic in MAOM and ↑aliphatic/aromatic in POM) supports a shift of C from operationally labile fractions to more oxidized forms susceptible to mineral sorption (Parikh et al. 2014), in line with the POM→MAOM flow suggested by our correlations and SEM. Furthermore, a slight, non-significant tendency toward a higher relative proportion of aromatic and carbonyl signals in POM under LQ was observed, which is consistent with high C:N substrates (more lignin/polyphenols) showing lower degradability and greater relative persistence (Figure 5) (Kögel-Knabner 2002).

This study provides evidence that leaf litter quality is a key factor in the formation of stabilized organic matter in MAOM and, therefore, a useful focus for guiding management practices aligned with soil health and C sequestration; this is consistent with current frameworks linking microbial efficiency with stabilization in the mineral matrix (Cotrufo et al. 2013). At the same time, our results reinforce that SOM is complex and dynamic, whose response integrates substrate traits, microbial pathways, and mineralogical constraints (Kögel-Knabner 2002). Importantly, we also show that canopy structure exerts a strong modulatory effect on these processes. Differences among canopy openings (Op, SOp, SC) significantly influenced decomposition dynamics, microbial C allocation, and stabilization pathways, highlighting that microclimatic conditions (e.g., temperature, moisture, and litter–soil contact) interact with substrate quality to determine the fate of C in soils. These findings emphasize that future management or modeling efforts should consider not only litter chemistry but also canopy configuration as a key driver of long-term C sequestration potential. Consequently, longer-term studies are needed to assess the persistence of these effects. Future lines of research should integrate isotopic tracers (^{13}C in plant material; ^{18}O-DNA to estimate growth CUE), quantify stabilization capacity (e.g., Fe/Al oxides typical of Andisols) (Jia et al. 2024), and complement FTIR with ^{13}C-NMR (Mathers et al.

2007) and Py-GC/MS (Haddix et al. 2016) to discriminate between new and native C and strengthen the interpretation of CUE/CUE_MAOM and its implications for C sequestration in native forests.

5. Conclusions

Our results show that litter quality partially determines the magnitude and the pathway of C stabilization in native forest Andisols. Low-quality litter (high C/N) promoted a more direct POM→MAOM transfer and greater stabilization efficiency, while high-quality litter prolonged the permanence in labile fractions, favoring respiratory losses prior to mineral association. Canopy openness modulated these patterns, highlighting the interaction between microclimatic conditions and stabilization processes. FTIR confirmed chemical differences consistent with the observed pathways, although total soil analysis showed low sensitivity to short-term changes.

Taken together, these findings indicate that C stabilization is not solely determined by substrate quality but emerges from the interaction of substrate stoichiometry, microclimatic conditions, and mineral matrix capacity. Moreover, microbial processes such as the priming effect which can either accelerate native SOM decomposition (positive priming) or enhance its stabilization (negative priming) may further modulate these outcomes by shaping decomposition pathways, nutrient cycling, and ultimately C persistence. These results suggest that management strategies aiming to enhance soil C sequestration in native forests should consider not only the chemical quality of litter inputs but also canopy structure, soil mineral saturation, and microbial dynamics as key drivers of SOM stabilization.

Future research should include a baseline characterization of the soil microbiome, explore the role of microbial efficiency and community composition in controlling C fate, and evaluate potential temporal shifts associated with different energy use efficiencies. Additionally, incorporating other locally relevant plant residues and litters could provide broader insights into the variability of stabilization processes under field conditions.

References:

1. ALEF K (1995) Nitrogen mineralization in soils. Methods Appl Soil Microbiol Biochem 234–245
2. Alfaro M, Dube F, Zagal E (2018) Soil quality indicators in an Andisol under different tree covers in disturbed *Nothofagus forests.* Chil J Agric Res 78:106–116. https://doi.org/10.4067/S0718-58392018000100106
3. Amoakwah E, Lucas ST, Didenko NA, et al (2022) Impact of deforestation and temporal land-use change on soil organic carbon storage, quality, and lability. PLOS ONE 17:e0263205. https://doi.org/10.1371/journal.pone.0263205
4. Aryal DR, Morales-Ruiz DE, López-Cruz S, et al (2022) Silvopastoral systems and remnant forests enhance carbon storage in livestock-dominated landscapes in Mexico. Sci Rep 12:16769. https://doi.org/10.1038/s41598-022-21089-4
5. Aynekulu E, Suber M, Van Noordwijk M, et al (2020) Carbon Storage Potential of Silvopastoral Systems of Colombia. Land 9:309. https://doi.org/10.3390/land9090309
6. Berg B, McClaugherty C (2020) Plant Litter: Decomposition, Humus Formation, Carbon Sequestration. Springer International Publishing, Cham
7. Börger M, Bublitz T, Dyckmans J, et al (2022) Microbial carbon use efficiency of litter with distinct C/N ratios in soil at different temperatures, including microbial necromass as growth component. Biol Fertil Soils 58:761–770. https://doi.org/10.1007/s00374-022-01656-7
8. Buckeridge KM, Mason KE, Ostle N, et al (2022) Microbial necromass carbon and nitrogen persistence are decoupled in agricultural grassland soils. Commun Earth Environ 3:1–10. https://doi.org/10.1038/s43247-022-00439-0
9. Calderón F, Haddix M, Conant R, et al (2013) Diffuse-Reflectance Fourier-Transform Mid-Infrared Spectroscopy as a Method of Characterizing Changes in Soil Organic Matter. Soil Sci Soc Am J 77:1591–1600. https://doi.org/10.2136/sssaj2013.04.0131

10. Cardinael R, Chevallier T, Cambou A, et al (2017) Increased soil organic carbon stocks under agroforestry: A survey of six different sites in France. Agric Ecosyst Environ 236:243–255. https://doi.org/10.1016/j.agee.2016.12.011
11. Centro de Información de Recursos Naturales (CIREN) (2010) Determinación de la erosión actual y potencial de los suelos de Chile. Ministerio de Agricultura, Gobierno de Chile, Santiago, Chile
12. Cornwell WK, Cornelissen JHC, Amatangelo K, et al (2008) Plant species traits are the predominant control on litter decomposition rates within biomes worldwide. Ecol Lett 11:1065–1071. https://doi.org/10.1111/j.1461-0248.2008.01219.x
13. Cotrufo MF, Lavallee JM (2022) Chapter One - Soil organic matter formation, persistence, and functioning: A synthesis of current understanding to inform its conservation and regeneration. In: Sparks DL (ed) Advances in Agronomy. Academic Press, pp 1–66
14. Cotrufo MF, Soong JL, Horton AJ, et al (2015) Formation of soil organic matter via biochemical and physical pathways of litter mass loss. Nat Geosci 8:776–779. https://doi.org/10.1038/ngeo2520
15. Cotrufo MF, Wallenstein MD, Boot CM, et al (2013) The M icrobial E fficiency- M atrix S tabilization (MEMS) framework integrates plant litter decomposition with soil organic matter stabilization: do labile plant inputs form stable soil organic matter? Glob Change Biol 19:988–995. https://doi.org/10.1111/gcb.12113
16. Craine JM, Fierer N, McLauchlan KK (2010) Widespread coupling between the rate and temperature sensitivity of organic matter decay. Nat Geosci 3:854–857. https://doi.org/10.1038/ngeo1009
17. Dang R, Liu J, Lichtfouse E, et al (2024) Soil microbial carbon use efficiency and the constraints. Ann Microbiol 74:37. https://doi.org/10.1186/s13213-024-01780-9
18. De Macêdo Carvalho CB, De Mello ACL, Da Cunha MV, et al (2024) Ecosystem services provided by silvopastoral systems: a review. J Agric Sci 162:417–432. https://doi.org/10.1017/S0021859624000595

19. Del Pozo A, Catenacci-Aguilera G, Acosta-Gallo B (2024) Consequences of Land Use Changes on Native Forest and Agricultural Areas in Central-Southern Chile during the Last Fifty Years. Land 13:610. https://doi.org/10.3390/land13050610
20. Don A, Schumacher J, Freibauer A (2011) Impact of tropical land-use change on soil organic carbon stocks - a meta-analysis: SOIL ORGANIC CARBON AND LAND-USE CHANGE. Glob Change Biol 17:1658–1670. https://doi.org/10.1111/j.1365-2486.2010.02336.x
21. Dörner J, Dec D, Peng X, Horn R (2010) Effect of land use change on the dynamic behaviour of structural properties of an Andisol in southern Chile under saturated and unsaturated hydraulic conditions. Geoderma 159:189–197. https://doi.org/10.1016/j.geoderma.2010.07.011
22. Dörner J, Zúñiga Ugalde F, Ordónez Vásquez I, et al (2022) Physical properties of volcanic ash soils related to soil biodiversity: effects of pasture improvement managements. pp 300–313
23. Elakiya DN (2024) Soil Particulate Organic Matter Does Matter. 4:
24. Elias DMO, Mason KE, Goodall T, et al (2024) Microbial and mineral interactions decouple litter quality from soil organic matter formation. Nat Commun 15:10063. https://doi.org/10.1038/s41467-024-54446-0
25. Epskamp S, Cramer AOJ, Waldorp LJ, et al (2012) **qgraph** : Network Visualizations of Relationships in Psychometric Data. J Stat Softw 48:. https://doi.org/10.18637/jss.v048.i04
26. Fan Y, Chen J, Shirkey G, et al (2016) Applications of structural equation modeling (SEM) in ecological studies: an updated review. Ecol Process 5:19. https://doi.org/10.1186/s13717-016-0063-3
27. FAO (2022) The State of the World's Land and Water Resources for Food and Agriculture 2021 – Systems at breaking point. FAO ;
28. Feng J, Wang C, Gao J, et al (2024) Changes in plant litter and root carbon inputs alter soil respiration in three different forests of a climate transitional

region. Agric For Meteorol 358:110212. https://doi.org/10.1016/j.agrformet.2024.110212

29. Fox, John; Weisberg, Sanford (2019) car: Companion to Applied Regression
30. Gentile R, Vanlauwe B, Six J (2011) Litter quality impacts short- but not long-term soil carbon dynamics in soil aggregate fractions. Ecol Appl Publ Ecol Soc Am 21:695–703. https://doi.org/10.1890/09-2325.1
31. Georgiou K, Jackson RB, Vindušková O, et al (2022a) Global stocks and capacity of mineral-associated soil organic carbon. Nat Commun 13:3797. https://doi.org/10.1038/s41467-022-31540-9
32. Georgiou K, Jackson RB, Vindušková O, et al (2022b) Global stocks and capacity of mineral-associated soil organic carbon. Nat Commun 13:3797. https://doi.org/10.1038/s41467-022-31540-9
33. Geyer KM, Dijkstra P, Sinsabaugh R, Frey SD (2019) Clarifying the interpretation of carbon use efficiency in soil through methods comparison. Soil Biol Biochem 128:79–88. https://doi.org/10.1016/j.soilbio.2018.09.036
34. Geyer KM, Kyker-Snowman E, Grandy AS, Frey SD (2016) Microbial carbon use efficiency: accounting for population, community, and ecosystem-scale controls over the fate of metabolized organic matter. Biogeochemistry 127:173–188. https://doi.org/10.1007/s10533-016-0191-y
35. Gholizadeh A, Borůvka L, Saberioon M, Vašát R (2013) Visible, Near-Infrared, and Mid-Infrared Spectroscopy Applications for Soil Assessment with Emphasis on Soil Organic Matter Content and Quality: State-of-the-Art and Key Issues. Appl Spectrosc 67:1349–1362. https://doi.org/10.1366/13-07288
36. Gomes VM, Miranda Júnior MS, Silva LJ, et al (2025) A Global Meta-Analysis of Soil Carbon Stock in Agroforestry Coffee Cultivation. Agronomy 15:480. https://doi.org/10.3390/agronomy15020480
37. Guerra CA, Rosa IMD, Valentini E, et al (2020) Global vulnerability of soil ecosystems to erosion. Landsc Ecol 35:823–842. https://doi.org/10.1007/s10980-020-00984-z

38. Haddix ML, Magrini-Bair K, Evans RJ, et al (2016) Progressing towards more quantitative analytical pyrolysis of soil organic matter using molecular beam mass spectroscopy of whole soils and added standards. Geoderma 283:88–100. https://doi.org/10.1016/j.geoderma.2016.07.027
39. Hu J, Cui Y, Manzoni S, et al (2025) Microbial Carbon Use Efficiency and Growth Rates in Soil: Global Patterns and Drivers. Glob Change Biol 31:e70036. https://doi.org/10.1111/gcb.70036
40. Huaico Malhue A (2018) Análisis de la evolución de las áreas ambientalmente degradadas en Chile. Rev Fac Cienc For Conserv Nat 50:
41. Jia N, Li L, Guo H, Xie M (2024) Important role of Fe oxides in global soil carbon stabilization and stocks. Nat Commun 15:10318. https://doi.org/10.1038/s41467-024-54832-8
42. Kögel-Knabner I (2002) The macromolecular organic composition of plant and microbial residues as inputs to soil organic matter. Soil Biol Biochem 34:139–162. https://doi.org/10.1016/S0038-0717(01)00158-4
43. Kriiska K, Lõhmus K, Frey J, et al (2021) The Dynamics of Mass Loss and Nutrient Release of Decomposing Fine Roots, Needle Litter and Standard Substrates in Hemiboreal Coniferous Forests. Front For Glob Change 4:. https://doi.org/10.3389/ffgc.2021.686468
44. Kuzyakov Y, Friedel JK, Stahr K (2000) Review of mechanisms and quantification of priming effects. Soil Biol Biochem 32:1485–1498. https://doi.org/10.1016/S0038-0717(00)00084-5
45. Lavallee JM, Soong JL, Cotrufo MF (2020) Conceptualizing soil organic matter into particulate and mineral-associated forms to address global change in the 21st century. Glob Change Biol 26:261–273. https://doi.org/10.1111/gcb.14859
46. Lebuy R, Mancilla-Ruiz D, Manríquez H, De La Barrera F (2022) Degraded Landscapes in Hillside Systems with Agricultural Use: An Integrated Analysis to Establish Restoration Opportunities in Central Chile. Land 12:5. https://doi.org/10.3390/land12010005

47. Lehmann J, Kleber M (2015) The contentious nature of soil organic matter. Nature 528:60–68. https://doi.org/10.1038/nature16069
48. Lei W, Pan Q, Teng P, et al (2023) How does soil organic matter stabilize with soil and environmental variables along a black soil belt in Northeast China? An explanation using FTIR spectroscopy data. CATENA 228:107152. https://doi.org/10.1016/j.catena.2023.107152
49. Lenth, Russell V. emmeans: Estimated Marginal Means, aka Least-Squares Means
50. Leuthold S, Lavallee JM, Haddix ML, Cotrufo MF (2024) Contrasting properties of soil organic matter fractions isolated by different physical separation methodologies. Geoderma 445:116870. https://doi.org/10.1016/j.geoderma.2024.116870
51. Li X, Yang T, Hicks LC, et al (2023) Latitudinal patterns of particulate and mineral-associated organic matter down the soil profile in drylands. Soil Tillage Res 226:105580. https://doi.org/10.1016/j.still.2022.105580
52. López-Sampson A, Andrade HJ (2024) Agroforestry systems in Latin America. Agrofor Syst 98:1075–1078. https://doi.org/10.1007/s10457-024-01002-w
53. Lyu M, Homyak PM, Xie J, et al (2023) Litter quality controls tradeoffs in soil carbon decomposition and replenishment in a subtropical forest. J Ecol 111:2181–2193. https://doi.org/10.1111/1365-2745.14167
54. Manzoni S, Cotrufo MF (2024) Mechanisms of soil organic carbon and nitrogen stabilization in mineral-associated organic matter – insights from modeling in phase space. Biogeosciences 21:4077–4098. https://doi.org/10.5194/bg-21-4077-2024
55. Manzoni S, Taylor P, Richter A, et al (2012) Environmental and stoichiometric controls on microbial carbon-use efficiency in soils. New Phytol 196:79–91. https://doi.org/10.1111/j.1469-8137.2012.04225.x
56. Manzoni S, Trofymow JA, Jackson RB, Porporato A (2010) Stoichiometric controls on carbon, nitrogen, and phosphorus dynamics in decomposing litter. Ecol Monogr 80:89–106. https://doi.org/10.1890/09-0179.1

57. Margenot AJ, Parikh SJ, Calderón FJ (2023) Fourier-transform infrared spectroscopy for soil organic matter analysis. Soil Sci Soc Am J 87:1503–1528. https://doi.org/10.1002/saj2.20583
58. Mathers NJ, Jalota RK, Dalal RC, Boyd SE (2007) 13C-NMR analysis of decomposing litter and fine roots in the semi-arid Mulga Lands of southern Queensland. Soil Biol Biochem 39:993–1006. https://doi.org/10.1016/j.soilbio.2006.11.009
59. Matus F, Rumpel C, Neculman R, et al (2014) Soil carbon storage and stabilisation in andic soils: A review. CATENA 120:102–110. https://doi.org/10.1016/j.catena.2014.04.008
60. Matus F, Salazar O, Aburto F, et al (2024) Perspective of soil carbon sequestration in Chilean volcanic soils. Npj Mater Sustain 2:32. https://doi.org/10.1038/s44296-024-00038-4
61. Miranda A, Altamirano A, Cayuela L, et al (2017) Native forest loss in the Chilean biodiversity hotspot: revealing the evidence. Reg Environ Change 17:285–297. https://doi.org/10.1007/s10113-016-1010-7
62. Neupane A, Herndon EM, Whitman T, et al (2023) Manganese effects on plant residue decomposition and carbon distribution in soil fractions depend on soil nitrogen availability. Soil Biol Biochem 178:108964. https://doi.org/10.1016/j.soilbio.2023.108964
63. Ortiz J, Dube F, Neira P, et al (2023) Comparative Study between Silvopastoral and Agroforest Systems on Soil Quality in a Disturbed Native Forest of South-Central Chile. Agronomy 13:2683. https://doi.org/10.3390/agronomy13112683
64. Ortiz J, Dube F, Neira P, et al (2020) Soil Quality Changes within a (*Nothofagus obliqua)* Forest Under Silvopastoral Management in the Andes Mountain Range, South Central Chile. Sustainability 12:6815. https://doi.org/10.3390/su12176815
65. Parikh SJ, Goyne KW, Margenot AJ, et al (2014) Chapter One - Soil Chemical Insights Provided through Vibrational Spectroscopy. In: Sparks DL (ed) Advances in Agronomy. Academic Press, pp 1–148

66. Paul EA, Harris D, Collins HP, et al (1999) Evolution of CO2 and soil carbon dynamics in biologically managed, row-crop agroecosystems. Appl Soil Ecol 11:53–65. https://doi.org/10.1016/S0929-1393(98)00130-9
67. Pei J, Li J, Luo Y, et al (2025) Patterns and drivers of soil microbial carbon use efficiency across soil depths in forest ecosystems. Nat Commun 16:5218. https://doi.org/10.1038/s41467-025-60594-8
68. Prescott CE (2010) Litter decomposition: what controls it and how can we alter it to sequester more carbon in forest soils? Biogeochemistry 101:133–149. https://doi.org/10.1007/s10533-010-9439-0
69. Qu X, Li X, Bardgett RD, et al (2024) Deforestation impacts soil biodiversity and ecosystem services worldwide. Proc Natl Acad Sci 121:e2318475121. https://doi.org/10.1073/pnas.2318475121
70. Ramachandran Nair PK, Nair VD, Mohan Kumar B, Showalter JM (2010) Carbon Sequestration in Agroforestry Systems. In: Advances in Agronomy. Elsevier, pp 237–307
71. Ramos C, Zagal E, Timmusk S, et al (2025) Soil Carbon Sequestration in *Nothofagus obliqua* Forests with Different Canopy Cover Levels Under Silvopastoral Management. Agronomy 15:855. https://doi.org/10.3390/agronomy15040855
72. Robarge WP, Edwards A, Johnson B (1983) Water and waste water analysis for nitrate via nitration of salicylic acid. Commun Soil Sci Plant Anal 14:1207–1215. https://doi.org/10.1080/00103628309367444
73. Robertson AD, Paustian K, Ogle S, et al (2019) Unifying soil organic matter formation and persistence frameworks: the MEMS model. Biogeosciences 16:1225–1248. https://doi.org/10.5194/bg-16-1225-2019
74. Rong H, Du Z, Gao W, et al (2025) Long-term pig manure application increases soil organic carbon through aggregate protection and Fe-carbon associations in a subtropical Red soil (Udic Ferralsols). EGUsphere 1–27. https://doi.org/10.5194/egusphere-2025-2405

75. Rosseel Y (2012) **lavaan** : An *R* Package for Structural Equation Modeling. J Stat Softw 48:. https://doi.org/10.18637/jss.v048.i02
76. Sadzawka R. A, Carrasco R. MA, Grez Z. R, et al (2006) Métodos de análisis recomendados para los suelos de Chile. Revisión 2006
77. Sandoval E. M, Dorner F. J, Seguel S. O, et al (2012) Métodos de análisis físicos del suelo
78. Sarabia L, Solorio FJ, Ramírez L, et al (2020) Improving the Nitrogen Cycling in Livestock Systems Through Silvopastoral Systems. In: Meena RS (ed) Nutrient Dynamics for Sustainable Crop Production. Springer Singapore, Singapore, pp 189–213
79. Servicio Agrícola y Ganadero (SAG) (2021) Memoria SIRSD-S 2010–2021. Gobierno de Chile, Ministerio de Agricultura, Santiago, Chile
80. Six J, Frey SD, Thiet RK, Batten KM (2006) Bacterial and Fungal Contributions to Carbon Sequestration in Agroecosystems. Soil Sci Soc Am J 70:555–569. https://doi.org/10.2136/sssaj2004.0347
81. Smith P, Soussana J, Angers D, et al (2020) How to measure, report and verify soil carbon change to realize the potential of soil carbon sequestration for atmospheric greenhouse gas removal. Glob Change Biol 26:219–241. https://doi.org/10.1111/gcb.14815
82. Soares M, Rousk J (2019) Microbial growth and carbon use efficiency in soil: Links to fungal-bacterial dominance, SOC-quality and stoichiometry. Soil Biol Biochem 131:195–205. https://doi.org/10.1016/j.soilbio.2019.01.010
83. Sokol NW, Sanderman J, Bradford MA (2019) Pathways of mineral-associated soil organic matter formation: Integrating the role of plant carbon source, chemistry, and point of entry. Glob Change Biol 25:12–24. https://doi.org/10.1111/gcb.14482
84. Sokol NW, Whalen ED, Jilling A, et al (2022) Global distribution, formation and fate of mineral-associated soil organic matter under a changing climate: A trait-based perspective. Funct Ecol 36:1411–1429. https://doi.org/10.1111/1365-2435.14040

85. Spohn M, Klaus K, Wanek W, Richter A (2016) Microbial carbon use efficiency and biomass turnover times depending on soil depth – Implications for carbon cycling. Soil Biol Biochem 96:74–81. https://doi.org/10.1016/j.soilbio.2016.01.016
86. Sun H, Wang L, Kumar A, et al (2025) Nutrient availability mediates organic carbon turnover in paddy soils through regulating microbial metabolism. Geoderma 458:117313. https://doi.org/10.1016/j.geoderma.2025.117313
87. Tabatabai MA (2018) Soil Enzymes. In: Weaver RW, Angle S, Bottomley P, et al. (eds) SSSA Book Series. Soil Science Society of America, Madison, WI, USA, pp 775–833
88. Tabatabai MA, Bremner JM (1972) Assay of urease activity in soils. Soil Biol Biochem 4:479–487. https://doi.org/10.1016/0038-0717(72)90064-8
89. Tao F, Huang Y, Hungate BA, et al (2023a) Microbial carbon use efficiency promotes global soil carbon storage. Nature 618:981–985. https://doi.org/10.1038/s41586-023-06042-3
90. Tao F, Huang Y, Hungate BA, et al (2023b) Microbial carbon use efficiency promotes global soil carbon storage. Nature 618:981–985. https://doi.org/10.1038/s41586-023-06042-3
91. Thabit FN, Negim OIA, AbdelRahman MAE, et al (2024) Using Various Models for Predicting Soil Organic Carbon Based on DRIFT-FTIR and Chemical Analysis. Soil Syst 8:22. https://doi.org/10.3390/soilsystems8010022
92. Thevenot M, Dignac M-F, Rumpel C (2010) Fate of lignins in soils: A review. Soil Biol Biochem 42:1200–1211. https://doi.org/10.1016/j.soilbio.2010.03.017
93. Timmusk S, Behers L, Muthoni J, et al (2017) Perspectives and Challenges of Microbial Application for Crop Improvement. Front Plant Sci 8:. https://doi.org/10.3389/fpls.2017.00049
94. Timmusk S, de-Bashan LE (2022) Microbiome: A Tool for Plant Stress Management in Future Production Systems. Stresses 2:210–212. https://doi.org/10.3390/stresses2020014

95. Volkov D, Rogova O, Proskurnin M (2021) Organic Matter and Mineral Composition of Silicate Soils: FTIR Comparison Study by Photoacoustic, Diffuse Reflectance, and Attenuated Total Reflection Modalities. Agronomy 11:1879. https://doi.org/10.3390/agronomy11091879
96. Walden L, Sepanta F, Viscarra Rossel RA (2025) FT-MIR Spectroscopic Analysis of the Organic Carbon Fractions in Australian Mineral Soils. Eur J Soil Sci 76:e70084. https://doi.org/10.1111/ejss.70084
97. Wang B, An S, Liang C, et al (2021) Microbial necromass as the source of soil organic carbon in global ecosystems. Soil Biol Biochem 162:108422. https://doi.org/10.1016/j.soilbio.2021.108422
98. Wang S, Zhong Q, Ma W, et al (2025) Effects of exogenous and endogenous Mn on litter decomposition at different stages under continuous N addition in a subtropical forest. For Ecol Manag 585:122614. https://doi.org/10.1016/j.foreco.2025.122614
99. Wright AF, Bailey JS (2001) Organic carbon, total carbon, and total nitrogen determinations in soils of variable calcium carbonate contents using a Leco CN-2000 dry combustion analyzer. Commun Soil Sci Plant Anal 32:3243–3258. https://doi.org/10.1081/CSS-120001118
100. Yin K, Gong L, Ma X, et al (2025) Soil Microbiome Drives Depth-Specific Priming Effects in Picea schrenkiana Forests Following Labile Carbon Input. Microorganisms 13:1729. https://doi.org/10.3390/microorganisms13081729
101. Yu W, Huang W, Weintraub-Leff SR, Hall SJ (2022) Where and why do particulate organic matter (POM) and mineral-associated organic matter (MAOM) differ among diverse soils? Soil Biol Biochem 172:108756. https://doi.org/10.1016/j.soilbio.2022.108756
102. Zhang Y, Lavallee JM, Robertson AD, et al (2021) Simulating measurable ecosystem carbon and nitrogen dynamics with the mechanistically defined MEMS 2.0 model. Biogeosciences 18:3147–3171. https://doi.org/10.5194/bg-18-3147-2021

Author Contributions

Conceptualization, E.Z., F.D. and C.R.; methodology, C.R., E.Z., F.D., D.C., L.P., S.T. and J.P.F.; validation, C.R., E.Z., F.D., D.C., L.P., S.T. and J.P.F.; formal analysis, C.R. and E.Z.; investigation, C.R., D.C., E.Z., J.I.-Á. and J.O.; resources, E.Z. and F.D.; data curation, C.R., E.Z., D.C., S.T., F.D. and J.O.; writing—original draft preparation, C.R. and E.Z.; writing—review and editing, C.R., E.Z., F.D.,D.C., J.I.-Á., L.P., S.T. and J.P.F.; visualization, C.R., E.Z., J.I.-Á. and J.O.; supervision, C.R. and E.Z.; project administration, E.Z., F.D. and C.R.; funding acquisition, E.Z. and C.R. All authors have read and agreed to the published version of the manuscript.

Acknowledgments

We would like to express our gratitude to the staff of the Ranchillo Alto Research Center at the University of Concepción, as well as to the Department of Soils and Natural Resources, particularly to the Spectroscopy Laboratory (Vis-IR) and the Sustainable Soil Management Department. We also extend our thanks to the Advanced Oxidation Processes Laboratory, Department of Analytical and Inorganic Chemistry, Faculty of Chemical Sciences, for their support and technical assistance during this research. Special thanks are given to Katherine Rebolledo for her valuable collaboration. We also thank the Department of Forestry, Faculty of Forestry Sciences, and the Doctoral Program in Agronomy Sciences at the University of Concepción. Additionally, we are grateful to the National Agency for Research and Development (ANID) for the funding provided through the National Doctoral Scholarship 2022-21221453 awarded to R.C. This research is part of R.C.'s doctoral thesis, and we thank the Universidad de Concepción for approving its publication.

Funding

This research was funded by ANID (Agencia Nacional de Investigación y Desarrollo)/Programa/Beca Doctorado Nacional 2022-21221453 to the Doctoral Program in Agronomy Sciences, Faculty of Agronomy 2021300163 and to the Department of Soil Sciences and Natural Resources, Universidad de Concepción.

Competing interests

The authors have no relevant financial or non-financial interests to disclose.

Supplementary Information

1. Two-compartment decomposition model

To describe decomposition kinetics, we fitted a two-pool bi-exponential model (Equation I): Parameters were estimated by nonlinear least squares and used as metrics of the fast (labile) and slow (recalcitrant) phases of decomposition.

$$C(t) = C1 \cdot e\, k1t + C2 \cdot e\, k2t \quad \text{(S1)}$$

Where:

C(t): Remaining carbon or accumulated CO_2 at time t

C_1: Labile fraction of carbon (rapidly decomposed)

C_2: Stable or recalcitrant fraction (slow decomposition)

k1: Decomposition constant of the labile fraction (day^{-1})

k2: Decomposition constant of the stable fraction (day^{-1})

t: Time (usually in days)

Pre-incubation soil characterization. As baseline context, we report the soils' physical (Table S1), chemical (Table S2), and biological (Table S3) properties across canopy openings—open (Op), semi-open (SOp), semi-closed (SC)—and depths (0–30 and 30–60 cm) prior to incubation. Analytical procedures, units, and abbreviations are described in the main text; values are given as mean ± SE.

Table S1. Soil physical properties by canopy opening and depth.

	Op (0–30)	Op (30–60)	SOp (0–30)	SOp (30–60)	SC (0–30)	SC (30–60)
BD	0.61 ± 0.02	0.76 ± 0.08	0.61 ± 0.03	0.72 ± 0.06	0.60 ± 0.01	0.64 ± 0.06
PD	2.14 ± 0.02	2.21 ± 0.00	2.09 ± 0.01	2.12 ± 0.09	2.06 ± 0.01	2.20 ± 0.05
Sand	37.17 ± 0.37	33.80 ± 2.36	40.57 ± 1.23	35.70 ± 1.04	39.77 ± 3.01	37.13 ± 2.53
Silt	45.80 ± 0.37	48.87 ± 0.37	43.90 ± 1.33	50.03 ± 1.59	43.03 ± 0.82	45.07 ± 1.17
Clay	17.03 ± 0.68	17.33 ± 1.41	15.50 ± 0.99	14.27 ± 0.37	17.20 ± 2.12	17.80 ± 2.47

Bulk density (BD) and particle density (PD), together with textural fractions (sand, silt, clay), measured in plots with different canopy opening: open (Op), semi-open (SOp), and semi-closed (SC) at two depths (0–30 and 30–60 cm). Values are mean ± SE. Units: BD and PD in g cm^{-3}; textures in %.

Table S2. Soil chemical properties by canopy opening and depth.

	Op (0–30)	Op (30–60)	SOp (0–30)	SOp (30–60)	SC (0–30)	SC (30–60)
pH (Water)	5.45 ± 0.05	5.41 ± 0.04	5.62 ± 0.21	5.63 ± 0.08	5.50 ± 0.18	5.44 ± 0.12
OM	22.07 ± 0.52	14.38 ± 0.27	17.49 ± 1.44	10.52 ± 1.73	18.37 ± 1.48	12.67 ± 1.39
P	0.67 ± 0.05	0.53 ± 0.04	0.73 ± 19.36	0.67 ± 22.66	0.90 ± 21.32	0.57 ± 38.09
K^+	91.17 ± 0.05	45.27 ± 0.04	62.57 ± 0.05	46.60 ± 0.06	90.50 ± 0.05	81.87 ± 0.06
ECEC	2.14 ± 0.05	0.86 ± 0.04	2.36 ± 1.57	1.20 ± 0.56	3.43 ± 1.52	1.92 ± 0.84
Al_{EXCH} *	0.18 ± 0.05	0.07 ± 0.04	0.07 ± 0.04	0.01 ± 0.00	0.14 ± 0.09	0.09 ± 0.05
Ca^{2+}_{EXCH} *	1.43 ± 0.05	0.49 ± 0.04	1.83 ± 1.43	0.83 ± 0.48	2.62 ± 1.43	1.29 ± 0.69
Mg^{2+}_{EXCH} *	0.26 ± 0.05	0.14 ± 0.04	0.27 ± 0.12	0.16 ± 0.02	0.39 ± 0.13	0.25 ± 0.08
K^+_{EXCH}	0.23 ± 0.05	0.12 ± 0.04	0.16 ± 0.05	0.12 ± 0.06	0.23 ± 0.05	0.21 ± 0.10
$Na+_{EXCH}$	0.04 ± 0.05	0.04 ± 0.04	0.03 ± 0.00	0.07 ± 0.00	0.04 ± 0.00	0.07 ± 0.03
Al_{SAT}	9.40 ± 0.05	8.69 ± 0.04	5.14 ± 3.49	1.46 ± 0.53	6.98 ± 7.49	8.08 ± 8.28
K^+_{SAT}	12.54 ± 0.05	13.60 ± 0.04	8.51 ± 2.64	9.88 ± 1.77	7.87 ± 2.51	11.28 ± 1.88
Ca^{2+}_{SAT}	63.41 ± 0.05	54.12 ± 0.04	71.12 ± 10.20	65.83 ± 6.86	71.37 ± 11.92	61.77 ± 14.10
Mg^{2+}_{SAT}	12.85 ± 0.05	17.81 ± 0.04	12.89 ± 2.77	15.82 ± 4.46	12.30 ± 1.63	14.54 ± 2.89

Soil pH (water), organic matter (OM: is obtained by multiplying %C by 1.724), available phosphorus (P) and potassium (K^+), effective cation exchange capacity (ECEC), exchangeable cations (EXCH: Al^{3+}, Ca^{2+}, Mg^{2+}, K^+, Na^+), and cation saturation indices (SAT for Al, K^+, Ca^{2+}, Mg^{2+}) measured in plots with different canopy opening open (Op), semi-open (SOp), and semi-closed (SC) at two depths (0–30 and 30–60 cm). Values are mean ± SE. Units: pH unitless; OM in %; available P and K^+ in mg kg^{-1}; ECEC and EXCH in cmolc kg^{-1}; SAT in %. ECEC was computed as the sum of exchangeable bases plus exchangeable acidity.

Table S3. Soil biological activities by canopy opening and depth.

	Op (0–30)	Op (30–60)	SOp (0–30)	SOp (30–60)	SC (0–30)	SC (30–60)
β-Glu	0.98±0.1	0.73±0.1	0.98±0.1	0,74±0.1	1,23±0.2	0,82±0.01
MBA	48.06±4.6	57.54±1.6	65.33±0.7	54,90±1.5	56,85±5.1	67,49±5.4
CO_2–C flux	47.56±4.9	36.73±4.6	60.56±3.5	39,62±4.6	50,91±7.5	36,54±0.6
Urs	1180.57±7.6	1183.78±8.8	2302.03±5.1	2049.10±5.1	1497.67±4.6	1382.29±3.1

β-Glucosidase activity (β-Glu), Microbial Biomass Activity (MBA) fluorescein diacetate hydrolysis, respiration as 14-day cumulative (CO_2–C flux), and urease activity (Urs) measured in plots with different canopy openings open (Op), semi-open (SOp), and semi-closed (SC) at two depths (0–30 and 30–60 cm). Values are mean ± SE. Values are mean ± SE. Analytical protocols are described in the main text. Units: β-glucosidase, µg pNP g^{-1} dw h^{-1}; FDA, µg fluorescein g^{-1} dw h^{-1}; respiration, mg CO_2 g^{-1} dw (14 d); urease, µg NH_4^+–N g^{-1} dw h^{-1}. Abbreviations: dw = dry weight.

Table S4. Comparative total nitrogen, total carbon and C/N ratio of the five dominant litter species at Ranchillo Alto (dry-weight basis).

Species	Total N	Total C	C/N ratio	Interpretation
Festuca arundinacea	0.46 ± 0.01	48.3 ± 0.17	105 ± 1.7 a	Very poor-quality litter (high C/N, low N)
Hypericum sp.	0.69 ± 0.32	56.3 ± 0.17	55.2 ± 0.12 b	Intermediate quality; large N variance
Lomatia hirsuta	1.29 ± 0.16	54.4 ± 0.23	49.0 ± 0.58 c	Moderate quality
Berberis sp.	1.09 ± 0.02	50.0 ± 1.15	45.9 ± 0.17 c	Moderate quality
Nothofagus obliqua	1.93 ± 0.01	52.6 ± 0.12	27.3 ± 0.06 d	High-quality litter (low C/N, high N)

*Carbon and nitrogen are expressed in %. Values are expressed as mean ± standard error (n = 3). Different letters within each column indicate significant differences among species according to Tukey's multiple comparison test (α = 0.05).

Table S5. Results of three-way ANOVA (opening canopy × depth × incubation) for CO_2 fluxes and C and N parameters in soil fractions.

	Parámetros estadisticos				
	df	**sumsq**	**meansq**	**F value**	**p.value**
Variables Flujos CO_2 (mg CO_2 g dw^{-1})					
opening_canopy	1	11922	11922	18.305	0.000576 ***
deph	1	49005	49005	75.239	1.91e-07 ***
incub	1	245304	245304	376.622	1.52e-12 ***
opening_canopy x deph	1	3258	3258	5.002	0.039903 *
opening_canopy x incub	1	66718	66718	102.434	2.32e-08 ***
Deph x incub	1	731	731	1.122	0.305122
opening_canopy x deph x incub	1	18892	18892	29.005	6.07e-05 ***
Residuals	16	10421	651		
Effect variables in C (%)					
opening_canopy	2	46.84488	23.42244	28.27494	4.16E-08***
deph	1	152.1074	152.1074	183.6199	1.05E-15***
incub	2	23.35388	11.67694	14.09609	3.01E-05***
opening_canopy x deph	2	2.196478	1.098239	1.325765	0.278256
opening_canopy x incub	4	16.40984	4.102461	4.952381	0.002762**
Deph x incub	2	3.4627	1.73135	2.090039	0.138437
opening_canopy x deph x incub	4	4.418822	1.104706	1.333571	0.2763
Residuals	36	29.82173	0.828381		
Variables effect on N (%)					
opening_canopy	2	0.0704	0.0352	5.219	0.0102 *
deph	1	0.5756	0.5756	85.365	4.92×10^{-11}***
incub	2	0.1685	0.0842	12.494	7.57×10^{-5}***
opening_canopy x deph	2	0.0023	0.0012	0.171	0.844
opening_canopy x incub	4	0.1178	0.0295	4.369	0.0056 **
Deph x incub	2	0.0135	0.0067	1.001	0.378
opening_canopy x deph x incub	4	0.0280	0.0070	1.040	0.400
Residuals	36	0.2427			
Variables effect on POM_C (%)					
opening_canopy	2	60.65	30.32	22.305	4.99×10^{-7} ***
deph	1	112.35	112.35	82.640	7.44×10^{-11}***
incub	2	51.27	25.64	18.857	2.50×10^{-6}***
opening_canopy x deph	2	2.18	1.09	0.802	0.456 0.0188*
opening_canopy x incub	4	18.43	4.61	3.389	
Deph x incub	2	4.67	2.33	1.716	0.194
opening_canopy x deph x incub	4	4.19	1.05	0.770	0.5516
Residuals	36	48.94	1.36		
Variables effect on POM_N (%)					
opening_canopy	2	0.1515	0.0758	10.801	0.000212 ***
deph	1	0.4268	0.4268	60.844	3.01e-09 ***

incub	2	0.1504	0.0752	10.718	0.000223 ***
opening_canopy x deph	2	0.0401	0.0200	2.856	0.070598
opening_canopy x incub	4	0.0997	0.0249	3.554	0.015247 *
Deph x incub	2	0.0122	0.0061	0.867	0.428962
opening_canopy x deph x incub	4	0.0181	0.0045	0.645	0.634101
Residuals	36	0.2525	0.0070		
Variables effect on MAOM_C (%)					
opening_canopy	2	81.80	40.90	25.404	1.32e-07 ***
deph	1	145.01	145.01	90.064	2.47e-11 ***
incub	2	18.45	9.23	5.730	0.00691 **
opening_canopy x deph	2	0.26	0.13	0.082	0.92187
opening_canopy x incub	4	21.34	5.34	3.314	0.02070 *
Deph x incub	2	6.83	3.41	2.120	0.13474
opening_canopy x deph x incub	4	5.12	1.28	0.795	0.53627
Residuals	36	57.96	1.61		
Variables effect on MAOM_N (%)					
opening_canopy	2	0.1060	0.0530	5.819	0.006459 **
deph	1	0.5871	0.5871	64.489	1.54e-09 ***
incub	2	0.1562	0.0781	8.578	0.000898 ***
opening_canopy x deph	2	0.0281	0.0140	1.543	0.227547
opening_canopy x incub	4	0.1685	0.0421	4.628	0.004062 **
Deph x incub	2	0.0163	0.0082	0.896	0.417147
opening_canopy x deph x incub	4	0.0174	0.0043	0.477	0.752138
Residuals	36	0.3277	0.0091		
Variables effect on C/N					
opening_canopy	2	20.76	10.378	11.147	0.000171 ***
deph	1	0.03	0.031	0.034	0.855340
incub	2	19.46	9.728	10.449	0.000264 ***
opening_canopy x deph	2	5.92	2.958	3.178	0.053593.
opening_canopy x incub	4	96.82	24.206	25.999	3.47e-10 ***
Deph x incub	2	6.23	3.114	3.344	0.046537 *
opening_canopy x deph x incub	4	1.78	0.445	0.478	0.751512
Residuals	36	33.52	0.931		
Variables effect on C/N POM					
opening_canopy	2	1.427e-06	7.135e-07	11.940	0.000105 ***
deph	1	6.000e-09	6.500e-09	0.108	0.744242
incub	2	1.586e-06	7.929e-07	13.269	4.82e-05 ***
opening_canopy x deph	2	3.140e-07	1.568e-07	2.624	0.086343 .

opening_canopy x incub	4	5.885e-06	1.471e-06	24.622	7.06e-10 ***
Deph x incub	2	2.000e-07	1.000e-07	1.674	0.201835
opening_canopy x deph x incub	4	7.100e-08	1.770e-08	0.296	0.878376
Residuals	36	14.165	0.393		
Variables effect on C/N MAOM					
opening_canopy	2	47.37	23.686	37.403	1.63e-09 ***
deph	1	0.39	0.385	0.609	0.44039
incub	2	9.52	4.762	7.519	0.00187 **
opening_canopy x deph	2	2.95	1.475	2.330	0.11183
opening_canopy x incub	4	118.06	29.515	46.607	9.34e-14 ***
Deph x incub	2	4.56	2.281	3.602	0.03750 *
opening_canopy x deph x incub	4	0.93	0.232	0.366	0.83149
Residuals	36	22.80	0.633		
Variables effect on en Cox (%)					
opening_canopy	2	56.87	28.43	28.522	3.78e-08 ***
deph	1	134.34	134.34	134.758	9.99e-14 ***
incub	2	33.92	16.96	17.011	6.30e-06 ***
opening_canopy x deph	2	2.12	1.06	1.062	0.3563
opening_canopy x incub	4	32.43	8.11	8.133	8.85e-05 ***
Deph x incub	2	6.62	3.31	3.319	0.0475 *
opening_canopy x deph x incub	4	1.24	0.31	0.312	0.8683
Residuals	36	35.89	1.00		
Variables effect on Cnox (%)					
opening_canopy	2	2.988	1.494	3.797	0.03188 *
deph	1	16.889	16.889	42.924	1.28e-07 ***
incub	2	0.569	0.285	0.723	0.49217
opening_canopy x deph	2	6.541	3.270	8.311	0.00108 **
opening_canopy x incub	4	3.632	0.908	2.307	0.07681.
Deph x incub	2	0.184	0.092	0.233	0.79304
opening_canopy x deph x incub	4	3.818	0.955	2.426	0.06568.
Residuals	36	14.165	0.393		

*Signif. codes: 0 '***' 0.001 '**' 0.01 '*' 0.05 '.' 0.1 ' ' 1*

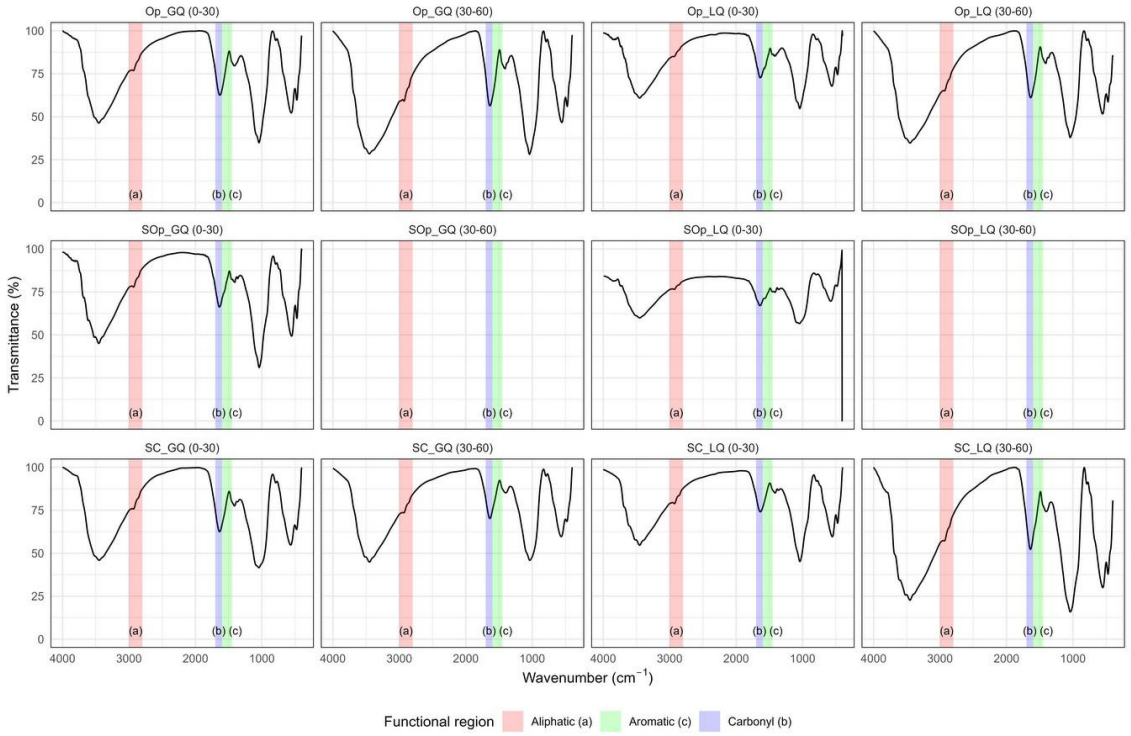

Fig. S1 FTIR transmittance spectra (%) for whole samples under good quality (GQ) and low quality (LQ) leaf litter treatments, different canopy opening levels, and soil depths (0–30 and 30–60 cm). The shaded regions correspond to functional groups: (a) aliphatic (2800–3000 cm^{-1}, red), (b) carbonyl (1600–1700 cm^{-1}, blue), and (c) aromatic (1450–1600 cm^{-1}, green).
The letters (a), (b), and (c) indicate the positions of the respective functional regions in the spectrum

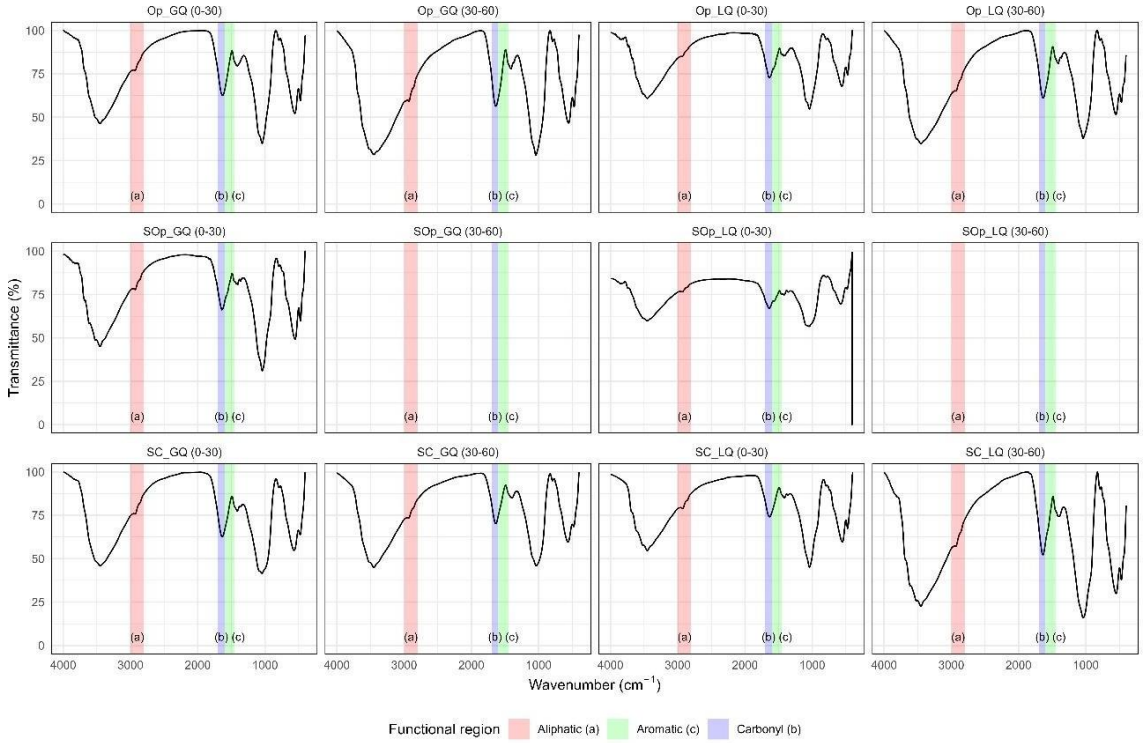

Fig. S2 FTIR transmittance (%) spectra for POM fractions under good quality (GQ) and low quality (LQ) leaf litter treatments, different canopy opening levels, and soil depths (0–30 and 30–60 cm).The shaded regions correspond to functional groups: (a) aliphatic (2800–3000 cm^{-1}, red), (b) carbonyl (1600–1700 cm^{-1}, blue), and (c) aromatic (1450–1600 cm^{-1}, green).
The letters (a), (b), and (c) indicate the positions of the respective functional regions in the spectrum

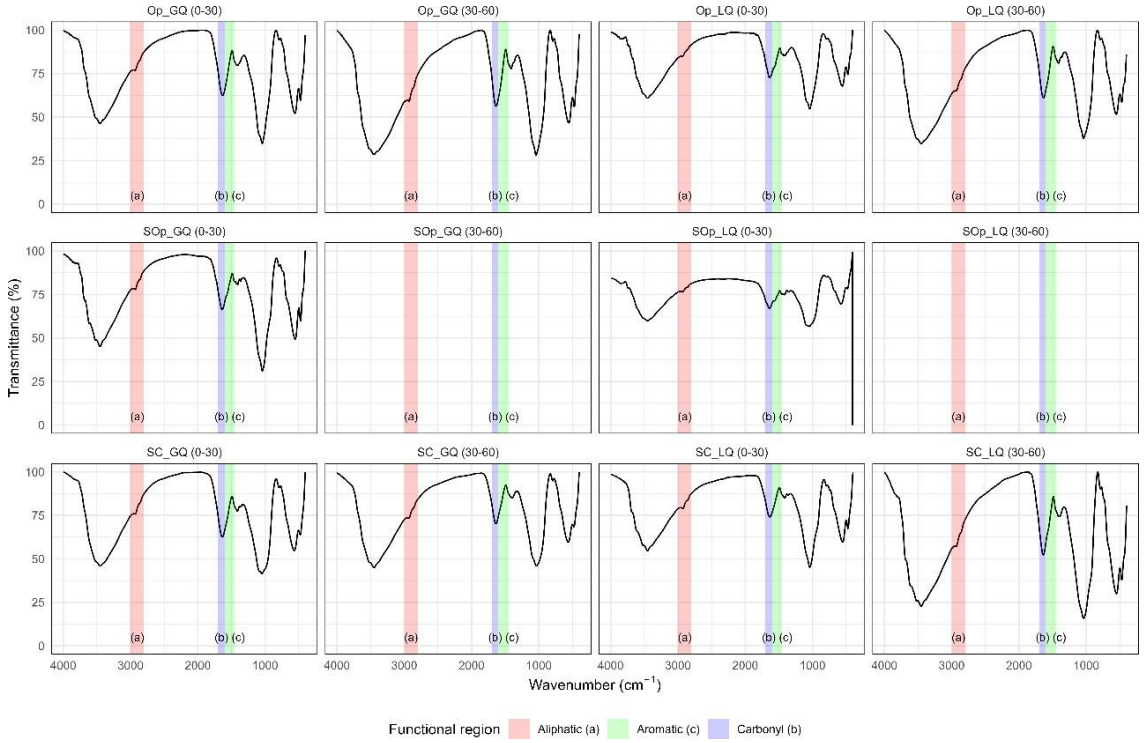

Fig. S3 FTIR transmittance (%) spectra for MAOM fractions under good quality (GQ) and low quality (LQ) leaf litter treatments, different canopy opening levels, and soil depths (0–30 and 30–60 cm). The shaded regions correspond to functional groups: (a) aliphatic (2800–3000 cm^{-1}, red), (b) carbonyl (1600–1700 cm^{-1}, blue), and (c) aromatic (1450–1600 cm^{-1}, green).
The letters (a), (b), and (c) indicate the positions of the respective functional regions in the spectrum

IV. Conclusiones Generales

Este trabajo demuestra que los sistemas agroforestales basados en bosques de *Nothofagus obliqua* constituyen una estrategia eficaz para recuperar suelos degradados, al mejorar el almacenamiento y la estabilización del carbono (C) y el nitrógeno (N) a través de la interacción entre el manejo silvopastoril, la estructura del dosel, la profundidad del suelo y la calidad del material vegetal incorporado.

Los tratamientos silvopastoriles incrementaron de manera consistente las fracciones estables de la MOS incluida la MAOM y el C no oxidable (Cnox) respecto del control, evidenciando su capacidad para fortalecer la estabilidad del C en suelos degradados. La estabilización del C no se restringió a los horizontes superficiales, sino que ocurrió a lo largo de todas las profundidades evaluadas, un patrón característico de ecosistemas templados húmedos. Las altas concentraciones de C y N observadas en el sistema abierto (Op) sugieren la posible influencia de prácticas antropogénicas históricas, como la quema, lo que indicaría un rol importante del carbono pirogénico en el almacenamiento de C a largo plazo.

La calidad de la hojarasca emergió como un regulador clave de las rutas de estabilización del C. La hojarasca de buena calidad (baja relación C/N) mostró mayores pérdidas respiratorias y una tendencia a promover la incorporación de C a la fracción mineral, mientras que la hojarasca de baja calidad favoreció una transferencia más directa POM→MAOM y una mayor permanencia del C en fracciones lábiles. Las variaciones en C y N tras la incubación evidencian la influencia de procesos microbianos como el efecto de “priming” (priming effect), que modularon tanto la descomposición como la estabilización de la materia orgánica nativa. Además, las características propias del sitio influyeron en la disponibilidad de N, afectando directamente las rutas de estabilización del C.

Los análisis FTIR fueron coherentes con estas dinámicas, aunque los análisis de suelo total mostraron baja sensibilidad para detectar cambios en el C estable de largo plazo.

En conjunto, los resultados indican que la estabilización del C en Andisoles, como el de este estudio, bajo bosque nativos e un proceso emergente que depende de la interacción entre la estequiometría del sustrato, el microclima regulado por el dosel, la eficiencia de la actividad microbiana, y la capacidad de la matriz mineral. Por ello, las estrategias de manejo orientadas a mejorar el secuestro de C deben considerar simultáneamente la calidad de las entradas orgánicas, el microclima del suelo generado por el dosel, la matriz mineral y la dinámica microbiana.

Finalmente, se destaca la necesidad de incorporar metodologías avanzadas de fraccionamiento de MOS, caracterización específica de C pirogénico, análisis del microbioma y evaluación de la eficiencia microbiana en futuros estudios. Estas aproximaciones permitirán profundizar en los mecanismos que controlan la estabilización del C en ecosistemas forestales degradados y fortalecerán las bases para diseñar estrategias de restauración y mitigación del cambio climático en bosques degradados de *Nothofagus obliqua*.